

AD-A007 921

**COMPUTATIONAL REPRESENTATION OF  
CONSTITUTIVE RELATIONS FOR POROUS  
MATERIAL**

**Lynn Seaman, et al**

**Stanford Research Institute**

**Prepared for:**

**Defense Nuclear Agency**

**May 1974**

**DISTRIBUTED BY:**

**NTIS**

**National Technical Information Service  
U. S. DEPARTMENT OF COMMERCE**

111128

DNA 3412F

AD A007921

**COMPUTATIONAL REPRESENTATION  
OF CONSTITUTIVE RELATIONS  
FOR POROUS MATERIAL (U)**

Stanford Research Institute  
333 Ravenswood Avenue  
Menlo Park, California 94025

SRI Project PYU-2407

May 1974

Final Report for Period 24 January 1973 to 31 March 1974

CONTRACT DNA001-73-C-0119

Approved for public release;  
distribution unlimited.

THIS WORK WAS SPONSORED BY THE DEFENSE  
NUCLEAR AGENCY UNDER SUBTASK  
NWED N99QAXAC306-03.

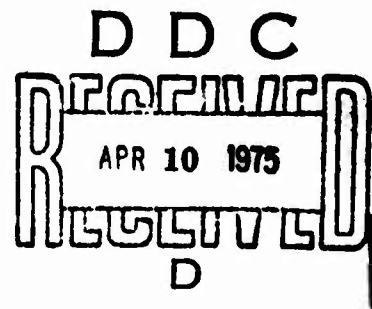
Review of this material does not imply Department of Defense endorsement of factual  
accuracy or opinion.

Prepared for  
Director  
DEFENSE NUCLEAR AGENCY  
Washington, D.C. 20305



**STANFORD RESEARCH INSTITUTE**  
Menlo Park, California 94025 • U.S.A.

Reproduced by  
**NATIONAL TECHNICAL  
INFORMATION SERVICE**  
U.S. Department of Commerce  
Springfield, VA. 22151



UNCLASSIFIED

SECURITY CLASSIFICATION OF THIS PAGE (When Data Entered)

REPORT DOCUMENTATION PAGE		READ INSTRUCTIONS BEFORE COMPLETING FORM	
1. REPORT NUMBER DNA 3412F	2. GOVT ACCESSION NO.	3. RECIPIENT'S CATALOG NUMBER	
4. TITLE (and Subtitle) COMPUTATIONAL REPRESENTATION OF CONSTITUTIVE RELATIONS FOR POROUS MATERIAL (U)		5. TYPE OF REPORT & PERIOD COVERED Final Report 24 January 1973 through 31 March 1974	
7. AUTHOR(s) Lynn Seaman Robert E. Tokheim Donald R. Curran		6. PERFORMING ORG. REPORT NUMBER SRI Project PYU-2407	
9. PERFORMING ORGANIZATION NAME AND ADDRESS Stanford Research Institute 333 Ravenswood Avenue Menlo Park, California 94025		8. CONTRACT OR GRANT NUMBER(s) DNA001-73-C-0119	
11. CONTROLLING OFFICE NAME AND ADDRESS		10. PROGRAM ELEMENT, PROJECT, TASK AREA & WORK UNIT NUMBERS DNA NWED <del>N99QAXAC</del> 306-03 Task	
14. MONITORING AGENCY NAME & ADDRESS (if diff. from Controlling Office) Defense Nuclear Agency Washington, D.C. 20305		12. REPORT DATE May 1974	13. NO. OF PAGES 170
		15. SECURITY CLASS. (of this report) UNCLASSIFIED	
16. DISTRIBUTION STATEMENT (of this report) Approved for public release; distribution unlimited.		15a. DECLASSIFICATION/DOWNGRADING SCHEDULE	
17. DISTRIBUTION STATEMENT (of the abstract entered in Block 20, if different from report)			
18. SUPPLEMENTARY NOTES This work was sponsored by the Defense Nuclear Agency under Subtask N99QAXAC306-03.			
19. KEY WORDS (Continue on reverse side if necessary and identify by block number)			
20. ABSTRACT (Continue on reverse side if necessary and identify by block number)  Constitutive relations for porous materials were developed for wave propagation calculations to simulate x-radiation loading. The relations were implemented in a FORTRAN IV subroutine.  The constitutive relations feature surfaces in energy-pressure-volume space to describe reversible loading and heating at low stresses and energies, compaction and fracture surfaces, and a multiphase equation-of-state surface for consolidated material. All these surfaces provide unique relations			

DDC  
RECEIVED  
APR 10 1975  
RECEIVED  
D

DD FORM 1473  
1 JAN 73  
EDITION OF 1 NOV 65 IS OBSOLETE

PRICES SUBJECT TO CHANGE

UNCLASSIFIED  
SECURITY CLASSIFICATION OF THIS PAGE (When Data Entered)

## 19. KEY WORDS (Continued)

## 20 ABSTRACT (Continued)

between energy, pressure, and volume. In addition, rate-dependence in compaction and fracture processes and deviator stresses are included.

The constitutive model includes versions of the Holt, Carroll-Holt, Seaman-Linde, Herrman  $P-\alpha$ , and Butcher  $P-\alpha-\gamma$  models. All these models have been augmented and put into a single framework to include elastic behavior, energy dependence, and deviator stress. The nucleation-and-growth (NAG) model for ductile fracture is included with modifications to permit elastic as well as plastic volume change of the pores and an energy-dependent threshold for fracture.

Solid behavior may be treated by the usual PUFF equation of state, the Philco-Ford three-phase equation of state, or a new extended two-phase form, which is convenient for fitting experimental data.

Methods for fitting data to the various models are described, especially procedures for generating compaction surfaces and modulus functions from Hugoniot and unloading data. A minimum set of tests required to characterize a porous material is outlined, including impact and electron beam experiments on both solid and porous samples. The region of the Hugoniot near the initial yield is most critical for x-ray simulations and should therefore be emphasized in both impact and electron beam experiments.

May 1974

**Final Report**

**COMPUTATIONAL REPRESENTATION OF CONSTITUTIVE RELATIONS  
FOR POROUS MATERIAL**

**Authors:** L. Seaman, R. Tokheim, D. Curran

**Contributors:** D. Erlich, D. Shockey, J. T. Rosenberg,  
A. Lutze, R. Trottier, M. Ginsberg

**Project Leader:** M. Ginsberg

**Project Supervisor:** D. R. Curran

**Prepared for:**

**Director**

**DEFENSE NUCLEAR AGENCY**

**Washington, D.C. 20305**

**Attn: Mr. Donald Kohler**

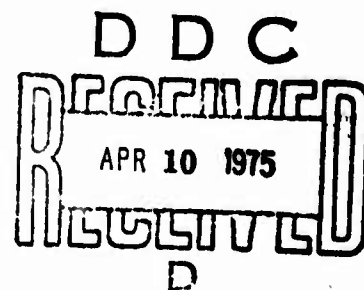
**Contract No. DNA001-73-C-0119**

**SRI Project No. FYU-2407**

**Approved by:**

**G. R. Abrahamson, Director  
Poulter Laboratory**

**C. J. Cook, Executive Director  
Physical Sciences Division**



## PREFACE

This report presents the theoretical results obtained during the first part of a continuing theoretical and experimental effort to understand the response of porous materials to rapid energy deposition. We would like to acknowledge the assistance and support of the following individuals:

D. Kohler - Contracting Officers Representative (DNA)  
R. Elsberry - Project Monitor (AFWL)  
K. Smith - Project Monitor (AFWL)  
R. Fisher (SAI)  
J. Picarelli (SAI)  
R. Stoddard (LASL)  
R. Skaggs (LASL)  
The late J. Rosenthal (LASL)  
H. Read (SSS)  
L. Hearn (LMSC)  
O. Burford (LMSC)  
W. Isbell (LLL)  
J. Shea (PI)  
S. Heurlin and the crew of the Pulserad 738 (PI)

Important technical contributions to the program were also made by the following SRI personnel: L. Hall, J. Busma, J. Hannigan, A. Urweider, J. Dempster, P. De Carli, K. Mahrer, J. Yost, W. Wilkinson, C. Benson, D. Walters, A. Bartlett, C. H. Anderson.

Professor George Duvall of Washington State University acted as our consultant during the formative stages of the program and during the construction of the PEST model.

# CONTENTS

	<u>Page No.</u>
LIST OF ILLUSTRATIONS	3
I INTRODUCTION	9
Background	11
Current State of Knowledge of the Model	19
Measurements Required to Specify the Model for any Material	20
II CONSTITUTIVE RELATIONS FOR POROUS MATERIALS	24
Approach	25
Features of the Model	27
Pressure in the Porous Material	32
Intermediate Surfaces	33
Rate-Independent Yield or Compaction Surface	43
Compaction Curve of Holt's Model	44
Compaction Curve of POREQST	48
Compaction Curve of Carroll-Holt Model	51
Compaction Curve of Hermann's $P-\alpha$ Model	53
Rate-Dependent Compaction	55
Butcher's $P-\alpha-\tau$ Model	56
Holt's Model for Rate-Dependent Compaction	59
Linear Viscous Void Compaction	61
Discussion of Rate-Dependent Models	63
Rate-Independent Fracture Surface	64
Rate-Dependent Fracture	64
Summary of Model Changes	66
III EQUATION OF STATE FOR SOLID MATERIALS	68
Extended Two-Phase Equation of State: ESA	69
Philco-Ford Equation of State	75
IV METHODS FOR DERIVING POROUS MODEL PARAMETERS FROM DATA	80
Data Sources	80
Construction of the Constitutive Relations	82
Thermal Expansion Functions	84
Thermal Strength Effect	84
Bulk Modulus	86
Compaction Curve	86
Rate Effects	89
Deviator Stress	91
Minimum Data Required for Characterizing Porous Materials	91

**APPENDICES**

<b>A</b>	<b>USER INFORMATION FOR PEST SUBROUTINE</b>	<b>95</b>
<b>B</b>	<b>INVERSE SOLUTION OF THE MIE-GRÜNEISEN EQUATION OF STATE</b>	<b>139</b>
<b>C</b>	<b>PHILCO-FORD EQUATION OF STATE</b>	<b>143</b>
<b>D</b>	<b>EXTENDED TWO-PHASE EQUATION OF STATE:ESA</b>	<b>161</b>

<b>REFERENCES</b>	<b>166</b>
-------------------	------------

<b>DISTRIBUTION LIST</b>	<b>169</b>
--------------------------	------------



# LIST OF ILLUSTRATIONS

<u>Figure</u>		<u>Page No.</u>
1	Radiation Response of Porous Material	12
2	Depiction of Energy-Pressure-Volume Space of the Constitutive Relations for a Porous Material	14
3	Depiction in Energy-Pressure-Volume Space of the Constitutive Relations for a Porous Material with Representative Heating, Loading, and Unloading Paths	15
4	Idealized Stress-Volume Paths Followed by a Porous Material	17
5	Equation of State Surface for Uranium in Pressure-Volume-Energy for Several Initial Porosities	18
6	Locus of States Caused by Heating Porous Material Without Expansion	21
7	Assumed Form of Actual Isoenergetic Loading Curves Compared with Idealized Form for the Model	26
8	Pressure-Volume Paths for a Porous Material	28
9	Pressure-Volume Path Computed in PEST for Loading with POREQST and Butcher P- $\alpha$ - $\gamma$ Models, Elastic Unloading, Constant Strength in Tension, Fragmentation, and Recompression with POREQST and Butcher's Model. Data are for Porous Tungsten.	30
10	Pressure-Volume Path Computed in PEST for Loading with PORHOLT Model, Elastic Unloading, Carroll-Holt Model in Tension, and Recompression with PORHOLT Model to Consolidation. Data are for Porous Tungsten.	31
11	Constitutive Relations of a Porous Material, Emphasizing the Intermediate Surface for Reversible Loading and Heating	35
12	Thermal Strength Reduction Function for Effective Moduli	37
13	Compaction Curve of POREQST Model Divided into Three Parabolic Segments	49
14	Pressure-Volume Diagram for Porous Material Showing Static Elastic, Dynamic Compression Paths	58

15	Pressure-Volume Diagram Showing Phases and Phase Boundaries of the Philco-Ford Equation of State	76
16	Variation of Strength with Temperature for 1100 Aluminum: Examples of Thermal Strength Reduction Functions	85
17	Variation of Bulk Modulus with Porosity and Internal Energy	87
18	Hugoniot Data Plotted on the Zero-Energy Reference Plane	88
19	Rate-Dependent Pressure-Volume Paths Generated with the Holt Model at Several Loading Rates	90
A-1	Flow Chart of HSTRESS, Stress-Switching Routine	96
A-2	Sample Input for PEST Subroutine	104
A-3	Flow Chart for PEST Subroutine	111
A-4	Input Deck for Test Case: Distended Tungsten Impact	118
A-5	Initial Layout of Finite Difference Grid for Distended Tungsten Impact Calculation	119
A-6	Stresses, Locations, and Densities at each Finite Difference Cell After 120 Time Increments	121
A-7	Portion of the Historical Listing of Stress at the Impact Interface (S23) and at Cells 34, 37, 41, 45, 50, and 56	122
A-8	Computed Stress Histories at Several Locations in the Distended Tungsten of the Test Case	123
C-1	Simplified Flow Chart for EQSTPF Subroutine	146

# NOMENCLATURE LIST

The quantities listed here appear in the body of the report.  
Separate nomenclature lists appear in the Appendices.

A	$U - \theta S$ , Helmholtz function, erg/g
$A_0, \dots, A_3$	Constants given in Eq. 103, units of $A_0$ are erg/g, others are dyn/cm <sup>2</sup>
a	Constant in the series expansion for $\alpha$ in Holt's model
$a_0, \dots, a_3$	Constants in Eqs. 104, 105, dyn/cm <sup>2</sup> (cm <sup>3</sup> /g) <sup>4</sup>
b	Constant in the series expansion for $\alpha$ in Holt's model, cm <sup>3</sup> /g
$b_0, \dots, b_3$	Constants in an equation of state for expanded material, erg/g (cm <sup>3</sup> /g) <sup>1</sup> for $b_1$
C	Bulk modulus of solid, dyn/cm <sup>2</sup> or sound speed, cm/sec
$C_p$	Specific heat, erg/g/°C
$C_v$	Specific heat at constant volume, erg/g/°C
D	2nd coefficient in series expansion for Hugoniot pressure as a function of strain $\mu$ , dyn/cm <sup>2</sup>
E	Internal energy, erg/g
$E_c$	Internal energy at the critical point, erg/g
$E_H$	Energy on the Hugoniot, erg/g
$E_l$	Internal energy of liquid material, erg/g
$E_{l0}$	Internal energy at the triple point, erg/g
$E_M$	Internal energy at melting, erg/g
$E_{so}$	Internal energy in the solid at the energy of melting and at zero pressure, erg/g
$E_v$	Internal energy of the vapor, erg/g
$E_0$	Internal energy of ideal gas at zero temperature, erg/g
$F_1, F_2$	Coefficients in a series expansion for a nonlinear energy effect
$f(E)$	Thermal strength reduction function
G	Isoenergetic shear modulus of porous material, dyn/cm <sup>2</sup>
$G_I$	Isothermal shear modulus of solid, dyn/cm <sup>2</sup>
$G_{pI}$	Isothermal shear modulus of porous material, dyn/cm <sup>2</sup>
g	Isoenergetic shear modulus at zero energy, dyn/cm <sup>2</sup>
$g_0, g_1$	Constants in an equation of state for expanded material, dimensionless and cm <sup>3</sup> /g

$h_o, h_1$	Constants in an equation of state for expanded material g/erg and $\text{cm}^3/\text{erg}$
$K$	isoenergetic bulk modulus of porous material, $\text{dyn/cm}^2$
$K_I$	Isothermal bulk modulus of solid, $\text{dyn/cm}^2$
$K_i, k_i$	Isoenergetic bulk moduli on the $i^{\text{th}}$ intermediate surface, $\text{dyn/cm}^2$
$K_{PI}$	Isothermal bulk modulus of porous material, $\text{dyn/cm}^2$
$K_s$	Bulk modulus of solid
$K_o$	Initial bulk modulus of porous material, $\text{dyn/cm}^2$
$k$	Bulk modulus of porous material on the zero energy plane, $\text{dyn/cm}^2$
$k_o, k_1, k_2$	Constants in the Philco-Ford equation of state
$L$	$(K/K_o - \alpha)/(\alpha - 1)$ , a constant used in determining the bulk modulus of the porous material
$N$	Number of voids, $\text{number/cm}^3$
$N_g$	Number of voids greater than a given radius, $\text{number/cm}^3$
$\dot{N}_o$	Nucleation rate constant
$P$	Pressure, $\text{dyn/cm}^2$
$\Delta P$	Variation of P-V relation from a straight line at the center of the line for a parabolic segment of the POREQST model
$P_c$	Consolidation pressure at zero energy, $\text{dyn/cm}^2$ , or pressure at critical point, $\text{dyn/cm}^2$
$P_e$	Yield pressure in Holt's model, $\text{dyn/cm}^2$
$P_H$	Pressure on the Hugoniot, $\text{dyn/cm}^2$
$P_{nl}$	Parameter governing sensitivity to nucleation of voids, $\text{dyn/cm}^2$
$P_s$	Pressure in solid material, $\text{dyn/cm}^2$
$P_{st}$	Threshold pressure, $\text{dyn/cm}^2$
$P_{th}$	Threshold pressure in the solid, $\text{dyn/cm}^2$
$P_y$	Yield pressure in Herrmann's model, $\text{dyn/cm}^2$
$P_z$	Pressure at zero energy, $\text{dyn/cm}^2$
$Q$	Acceleration term in the analysis of Carroll, $\text{dyn/cm}^2$

R	Void radius, cm or factor given in Eq. 100, $\text{dyn/cm}^2$ , or the gas constant, $\text{erg/g}^\circ\text{K}$
$R_n$	Nucleation void size distribution parameter, cm
S	3rd coefficient in series expansion for Hugoniot pressure as a function of strain $\mu$ , $\text{dyn/cm}^2$ , or, entropy, $\text{erg/g}^\circ\text{C}$
T	Temperature $^\circ\text{K}$
$T_c$	Temperature at the critical point, $^\circ\text{K}$
$T_F$	$1 + \Gamma_{so} E/K_s$ , temperature factor
$T_M$	Temperature of melting, $^\circ\text{K}$
t	Time
U	Internal energy, $\text{erg/g}$
V	Specific volume, $\text{cm}^3/\text{g}$
$V_c$	Specific volume at critical point, $\text{cm}^3/\text{g}$
$V_l$	Specific volume of liquid material, $\text{cm}^3/\text{g}$
$V_s$	Specific volume of solid material, $\text{cm}^3/\text{g}$
$V_{so}$	Initial specific volume of solid
$V_v$	Specific volume of void, $\text{cm}^3/\text{g}$ , or specific volume of vapor, $\text{cm}^3/\text{g}$
$dV_{ve}$	Elastic change in void volume
$dV_{vp}$	Plastic change in void volume
$v_v$	$V_v/V$ , relative void volume
$\Delta v_n$	Nucleated void volume
$Z_c$	$P V_c / RT_c$ , nonideal compressibility factor at the critical point

$\alpha$	Distension ratio
$\alpha'$	$\rho_{so}/\rho$ , an approximation to the distension ratio
$\alpha_a, \alpha_b$	Material constants used in the Philco-Ford equation of state
$\alpha'_c$	$\rho_{so}/\rho_c$ , value of $\alpha'$ at consolidation
$\alpha_e$	Distension ratio at yield in Holt's model
$\alpha_i$	Distension ratio on $i^{th}$ intermediate surface
$\alpha_{st}$	Distension ratio of the threshold pressure
$\alpha_t$	Volumetric thermal expansion coefficient, $1/^\circ C$
$\alpha_y$	Distension at the yield point in Herrmann's model
$\alpha_o$	Initial distension ratio
$\Gamma$	Grüneisen ratio
$\Gamma_o, \Gamma_1$	Coefficients in a series expansion for Grüneisen's ratio
$\delta$	$2Y/(3K_s)$ , yield parameter of the Carroll-Holt model
$\epsilon$	Small factor used in Carroll-Holt model to permit consolidation at a finite pressure
$\eta$	Coefficient of viscosity, $\text{dyn-sec/cm}^2$
$\theta$	Temperature, $^\circ C$
$\mu$	$\rho_s/\rho_{so} - 1$ , strain
$\rho$	Density, $\text{g/cm}^3$
$\rho'$	Density at a zero energy state in Holt's model, $\text{g/cm}^3$
$\rho_c$	Consolidation density at zero energy, $\text{g/cm}^3$ , or density at the critical point, $\text{g/cm}^3$
$\rho_e$	Density at initial yield, $\text{g/cm}^3$
$\rho_l$	Density of the liquid phase, $\text{g/cm}^3$
$\rho_s$	Density of solid material, $\text{g/cm}^3$
$\rho_{so}$	Initial density of solid, $\text{g/cm}^3$
$\rho_{se}$	Density of solid at initial yield in the porous material, $\text{g/cm}^3$
$\rho_{sy}$	Solid density at the yield point in Herrmann's model, $\text{g/cm}^3$
$\rho_y$	Density at yielding in Herrmann's model, $\text{g/cm}^3$
$\rho_{o1}$	Initial density of porous material, $\text{g/cm}^3$
$\rho_o$	Reference density at zero energy and pressure on the $i^{th}$ intermediate surface, $\text{g/cm}^3$
$\sigma$	Stress, $\text{dyn/cm}^2$
$\sigma'$	Deviator stress, $\text{dyn/cm}^2$
$\tau$	Time constant of Holt's and Butcher's models, sec

## I INTRODUCTION

Porous materials are used as a protection against x-radiation because of their ability to minimize the stress generated by the radiation and to attenuate that stress as it propagates. For accurate design of this protection, wave propagation calculations are made to simulate the radiation deposition, stress generation, propagation, and spallation caused by stress waves. For such a calculation it is necessary to have a constitutive relation (stress-strain-energy relation, or equation of state) that describes the material's response to heating and to compressive and tensile loading.

The objective of this report is to document a set of constitutive relations that provide for:

- Elastic and plastic compaction loading with rate dependence
- Heating or cooling that can occur simultaneously with loading
- Unloading and rate-dependent fracture
- Melting and vaporization, with explicit treatment of solid, liquid, vapor, and mixed phases.

Accompanying these relations is a user's manual that includes a derivation of the equations for the model and procedures for using it in Lagrangian wave propagation computer programs.

For calculations, the computational model must be fitted to data available on the material of interest. A description is given of the methods used for performing this fit, especially the judgmental factors involved.

The model or set of constitutive relations derived here are developed from the same physical basis as that derived earlier by Seaman and Linde.<sup>1</sup> The material response is determined both by the solid material behavior and by the behavior associated with its porosity. Onto this basic framework of the Seaman and Linde model has been added a family of compaction curves suggested by other investigators, rate-dependent compaction, ductile

fracture (rate-dependent), a multiphase equation of state for the continuous material, and several deviator stress models. Specifically the following models are included:

Compaction surface

POREQST (Seaman and Linde)<sup>1</sup>

Holt et al.<sup>2</sup>

Carroll-Holt<sup>3,4</sup>

Herrmann's  $P-\alpha$ <sup>5,6</sup>

Rate-dependent compaction

Holt et al.<sup>2</sup>

Butcher  $p-\alpha-\tau$ <sup>7</sup>

Linear viscous

Fracture

Constant strength

NAG ductile fracture<sup>8</sup>

Solid equation of state

Mie-Grüneisen and PUFF expansion<sup>9</sup>

Philco-Ford<sup>10</sup>

ESA extended two-phase equation of state

Deviator stress

Beryllium rate-dependent, Bauchinger model of Read<sup>11</sup>

Bauchinger model<sup>12</sup>

Standard anelastic model<sup>13</sup>

The constitutive relations for porous material are derived in Chapter II and incorporated into subroutines in Appendices A and B. Chapter III describes the multiphase equations of state for continuous material; the new subroutines are given in Appendices C and D. The needed background for deciding which data to select and for fitting that data to the model is given in Chapter IV.

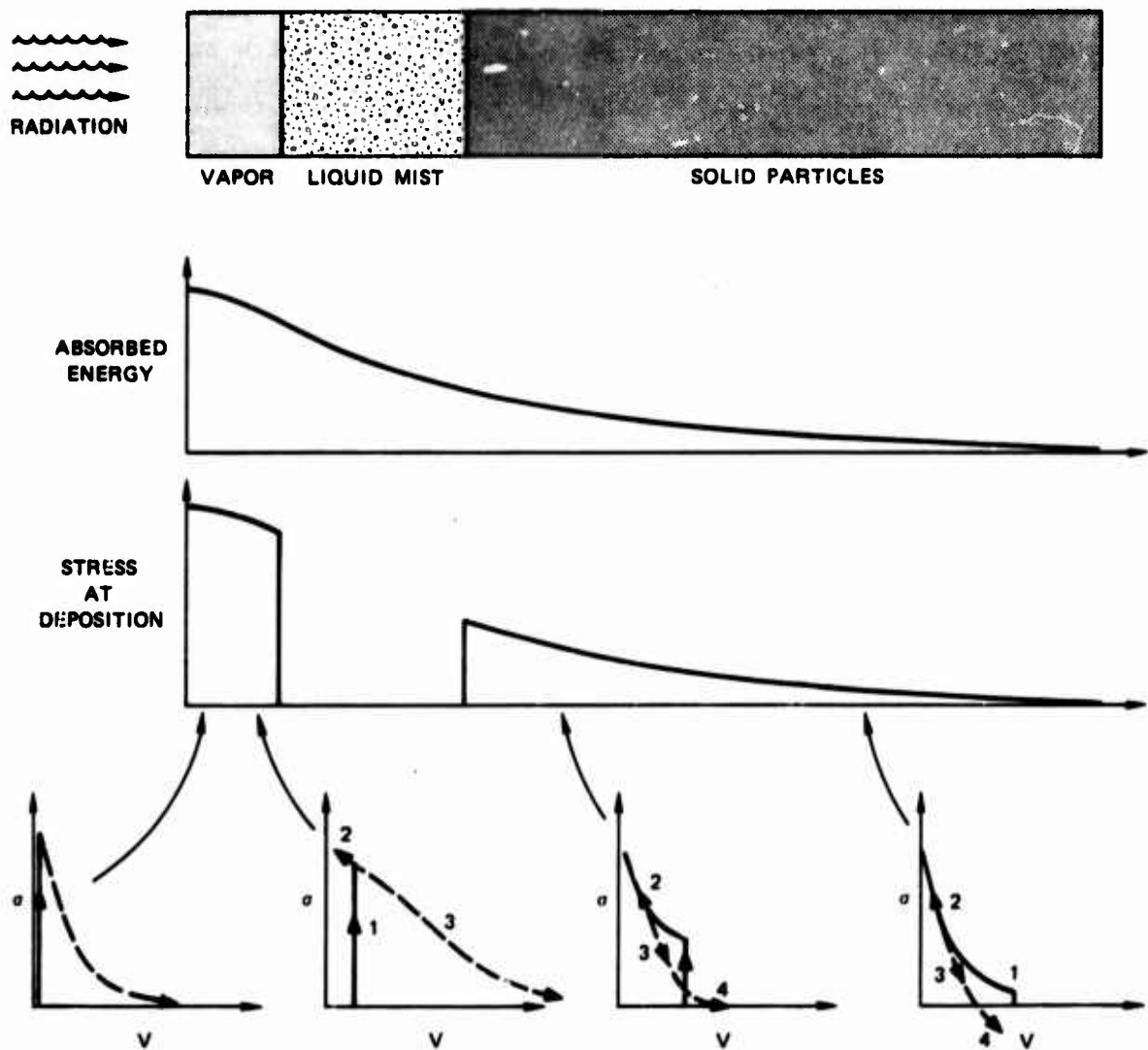


## Background

To be adequate, the porous material model must describe behavior under radiation loading. Therefore we examine first the range of behavior expected.

Radiation heating of porous materials can cause melting and vaporization, shock wave propagation, and spallation. Some of these phenomena are illustrated in Figure 1. Radiation from the left falls on a plate (a thin slice of which is shown). Following deposition the front surface material is in a compressed but expanding vapor state, deeper material is molten, and at greater depths the particles are only warmed. The "absorbed energy" plot shows in a conceptual way the diminution of absorbed radiant energy with depth. Corresponding to this energy, stress arises throughout the plate. In the "vapor" portion the material is heated rapidly during deposition, expands and fills the pores. Continued heating following elimination of the pores causes high thermal stresses to occur, which may reach the megabar region. In the molten region the thermal expansion is smaller, so following deposition the stress is nearly zero. Small thermal stresses are reached by the end of deposition in the region that consists of solid particles.

Wave propagation becomes the dominant feature as the stresses in the high-stress areas are relieved. The vapor expands rapidly, compressing the molten mist and transmitting a compressive wave, which propagates to the right through the mist and into the region of solid particles. The expansion of the left (free) boundary of the vapor causes a rarefaction wave to travel through the vapor to the right, following the compressive wave. As the rarefaction wave traverses the liquid, it produces tensile stresses, spalls the liquid, and continues into the solid particles, usually causing hot spall to some depth. This rarefaction continues moving to the right at reduced amplitude. Meanwhile the compressive wave reaches the rear surface of the plate and reflects as a rarefaction wave, which propagates to the left. At some point near the rear surface, this second rarefaction meets the rarefaction moving to the right, and the tension produced may cause fracture damage in the plate (cold spall).



GA-314582-10

FIGURE 1 RADIATION RESPONSE OF POROUS MATERIAL

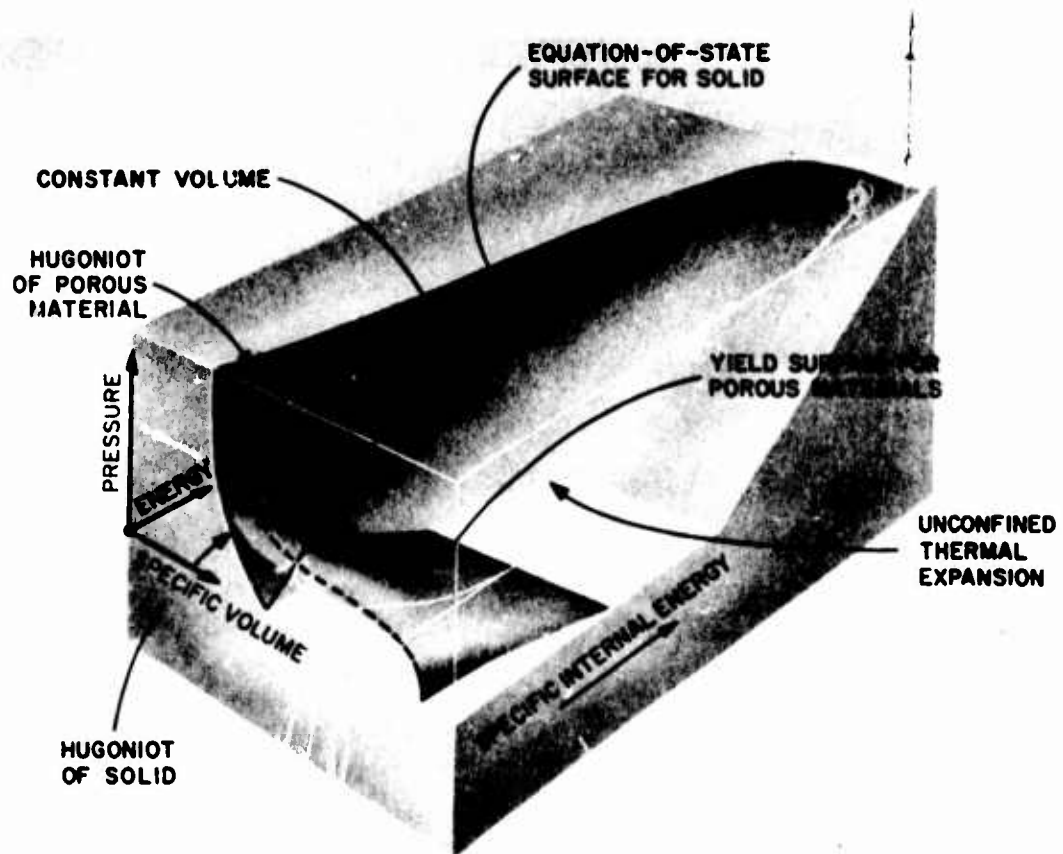
In Figure 1 the inserted stress-volume plots show the behavior at selected points in the target. The material at the surface is heated at constant volume and expands isentropically. The material somewhat below the surface is heated and then compressed further by a compressive wave until the ensuing rarefaction unloads it isentropically. At greater depths, the initial heating is small and the compressive wave dominates. The rarefactions then take the material into tension.

To examine in more detail the processes involved in these heating and loading processes we divide the model into three parts:

- (1) A pressure-volume-energy relation for solid material under thermodynamic equilibrium conditions, called the "equation-of-state surface for solid" in Figure 2.
- (2) A pressure-volume-energy relation for porous material under equilibrium conditions, termed the "yield surface for porous materials" in Figure 2.
- (3) Elastic-plastic behavior, viscous behavior, fracturing, Some of these processes are rate-dependent.

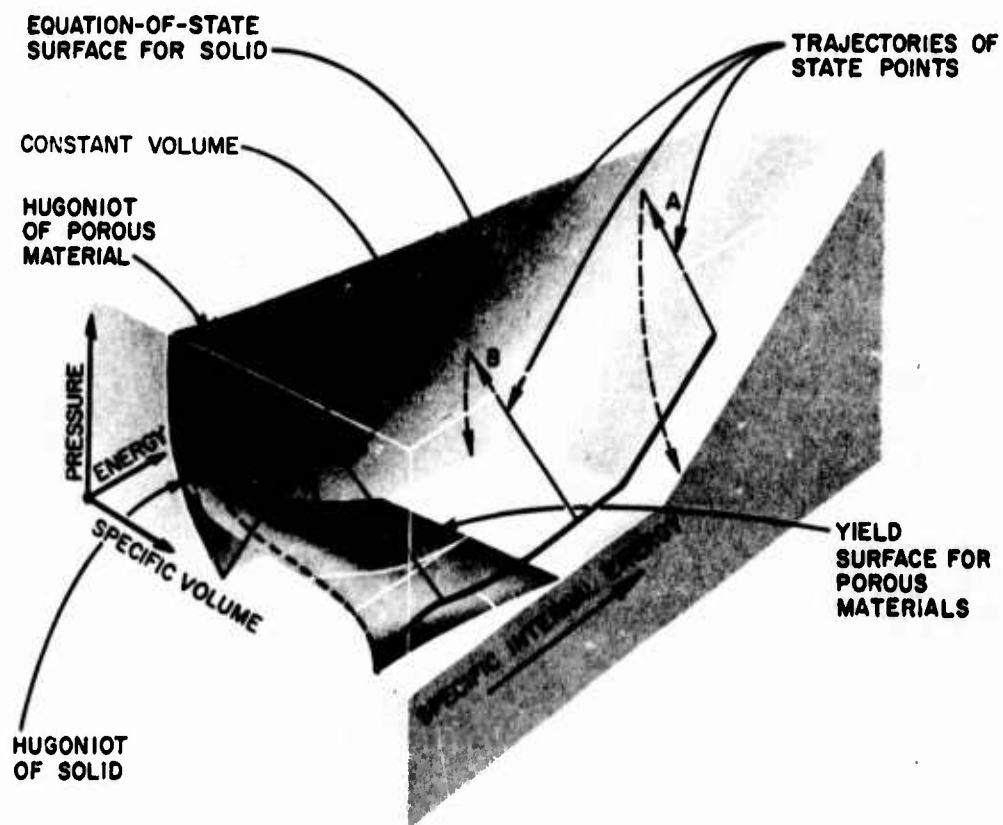
All three aspects of the constitutive model are exercised to follow the behavior shown in Figure 1. To indicate how the first two portions of the model participate, we have shown the paths followed by the material at several depths on the energy-pressure-volume surface of Figure 3.

Near the front (irradiated) surface (Path A), a large amount of energy is deposited at nearly constant volume causing the state point to traverse the yield surface, then through porous liquid and dense vapor states. Finally a compression wave drives the pressure to the peak volume. The unloading occurs along an isentrope. In the figure the isentrope shows a rapid unloading characteristic of a solid or molten material. With a more intense radiation, the state point trajectory would go far to the right before reaching low pressures, and the final state of the material would be a vapor. At a greater depth (Path C) there is slight initial heating at constant volume as the state point travels over the yield surface, followed by a further loading from the compressive wave coming back from the front surface (this wave is caused by the high stresses at the front surface). Unloading then follows an isentrope.



GP-6586-28D

FIGURE 2 DEPICTION OF ENERGY-PRESSURE-VOLUME SPACE OF THE CONSTITUTIVE RELATIONS FOR A POROUS MATERIAL

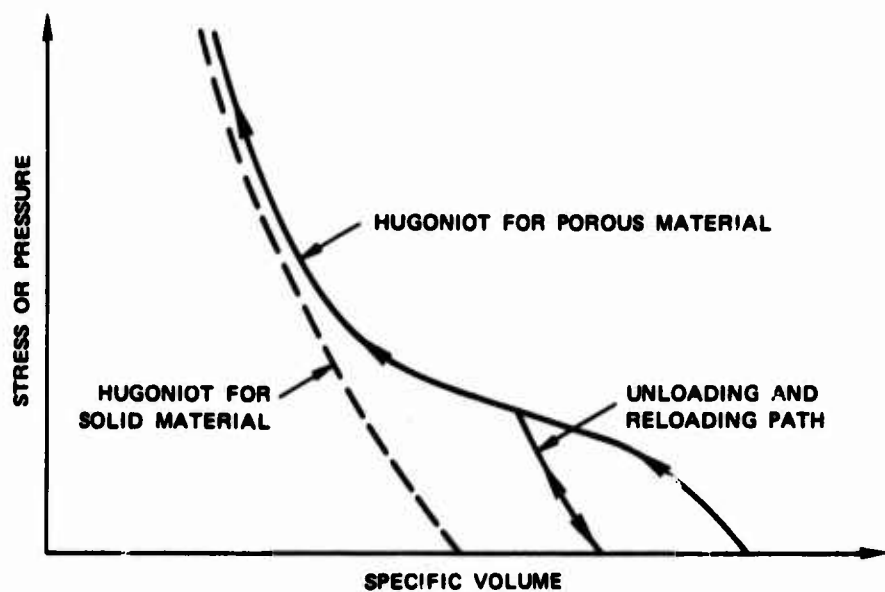


GP-6586-28E

FIGURE 3 DEPICTION IN ENERGY-PRESSURE-VOLUME SPACE OF THE CONSTITUTIVE RELATIONS FOR A POROUS MATERIAL WITH REPRESENTATIVE HEATING, LOADING, AND UNLOADING PATHS

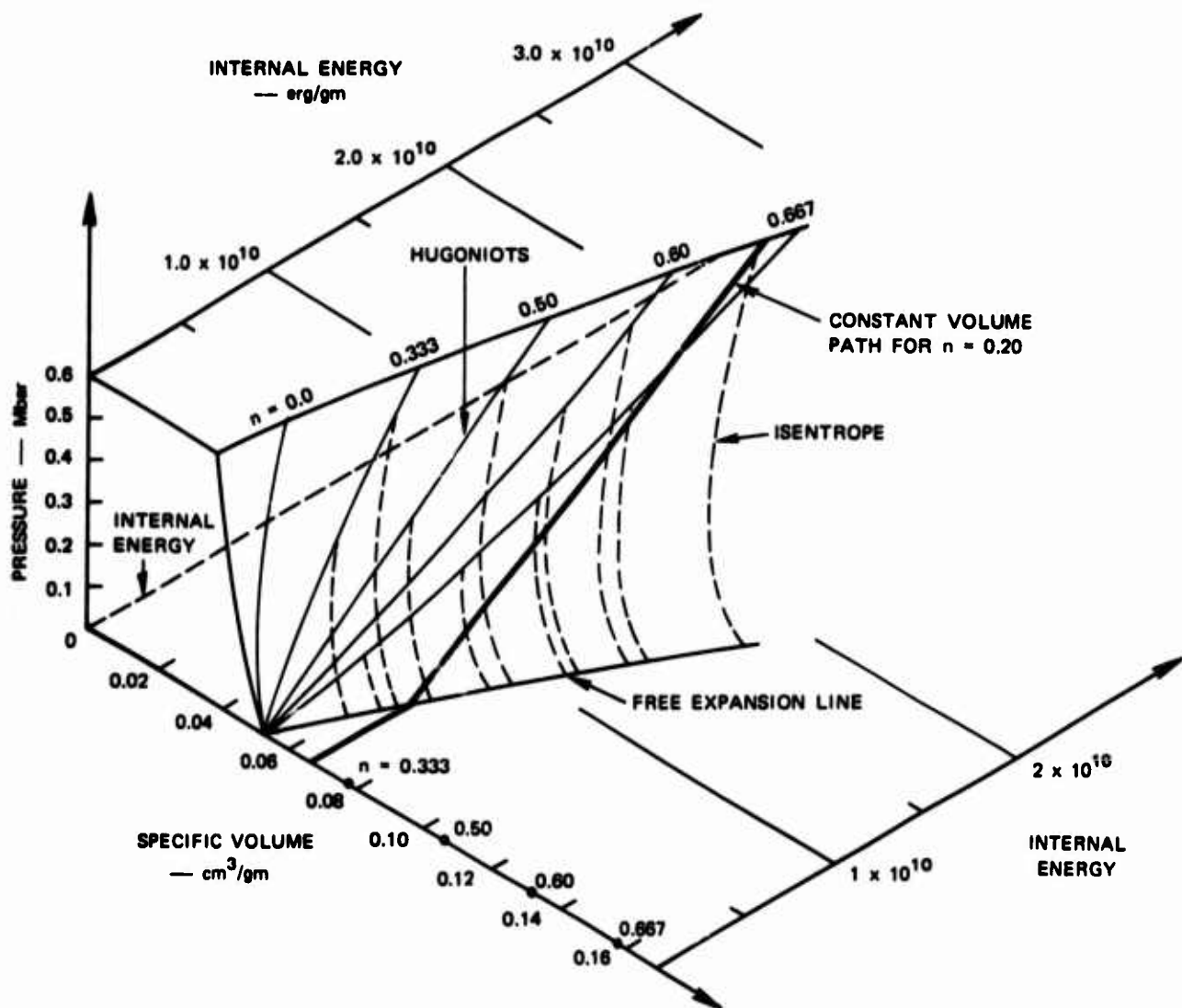
Thus the response of material at all depths is described by the constitutive relations. The slopes of the constant-volume loading lines in the P-E plane are given by the Grüneisen function. Attenuation and hysteresis are given by the stress-volume-energy paths projected onto the P-V plane. The final states reached indicate the expected phase of the material.

In contrast to radiation deposition, impact in porous materials is solely a wave propagation process, although significant heating may occur during compression. For low stresses the compaction and unloading paths resemble those shown in Figure 4. On loading the behavior is initially elastic. At higher stresses, gross yielding and irrecoverable compaction occur. At stresses of several times the initial yield, the voids are eliminated and the behavior is like that of a solid. Initial unloading usually follows essentially elastic paths, so the original specific volume is not recovered. The Hugoniot for the porous material is also shown in Figure 4. The Hugoniot of the porous material is to the right of the Hugoniot for solid material, illustrating that shock waves in porous material induce more heating than the same shocks in solids. This heating effect is explored quantitatively in Figure 5, which was constructed from uranium equation-of-state data.<sup>14</sup> In Figure 5, the low stress region has been completely omitted; the calculations were made on the assumption of zero yield strength. The figure shows Hugoniots for several initial porosities ( $n = 0.0$  to  $0.667$ ) and for impacts up to 600 kbar. Several isentropes are also shown (all the Hugoniots and isentropes are approximated to lie on a single surface). For uranium the melt energy is about  $2.3 \times 10^9$  erg/g and sublimation is at  $2.0 \times 10^{10}$  erg/g. Hence, internal energies equivalent to the sublimation energy can be reached by impacting very porous samples. Similar results can be expected for many other porous materials.



GA-6586-27

FIGURE 4 IDEALIZED STRESS-VOLUME PATHS FOLLOWED BY A POROUS MATERIAL



NOTE:  $n$  = porosity.

GA-314582-11

FIGURE 5 EQUATION OF STATE SURFACE FOR URANIUM IN PRESSURE-VOLUME-ENERGY SPACE WITH HUGONIOTS AND ISENTROPES FOR SEVERAL INITIAL POROSITIES



The third part of the constitutive model for porous materials contains all the nonhydrostatic and nonequilibrium parts. Here are the elastic-plastic or yield phenomena, the rate-dependence associated with yielding, the rate-dependence associated with pore collapse, and time-dependent ductile and brittle fracture. The rate-dependence associated with phase changes would also be included here.

#### Current State of Knowledge of the Model

The pressure-volume-energy relation for solids is well-known mainly from impacts. Thus the known states lie near the Hugoniot curve shown in Figure 2. Recent progress has been made in developing three-phase (solid, liquid, and gas) equations of state for metals through the work of Royce,<sup>15</sup> Thompson,<sup>16</sup> Goodwin et al.,<sup>10</sup> and Naumann.<sup>17</sup> Since all of these are now based on static thermodynamic data, no effort is made to handle the rate effects associated with changing phases. Zel'dovich<sup>18</sup> states that the equilibrium surface (such as that described by these four equations of state) is not followed in a shock or rarefaction wave because there is no time for the phase change to occur. Goodwin et al.,<sup>10</sup> make it plain that there is no satisfactory data in the liquid range, even for metals. Thus we conclude that:

- The solid behavior near the Hugoniot is well known for many materials and can be derived from impact data. The common equation-of-state relations adequately describe this solid behavior.
- The liquid states are essentially unexplored experimentally.
- The vapor and mixed liquid-vapor states for metals have been studied experimentally and theoretically under static conditions. The results give some guidance toward constructing dynamic models, but cannot be relied on without dynamic experimental verification.

The second portion of the constitutive model, the pressure relation for porous material, is probably better understood than the first portion.

The framework described in our model several years ago has gradually been verified experimentally and theoretically. With the recent results of Read,<sup>19</sup> we now know that the Grüneisen ratio for ductile porous material containing voids is related to the Grüneisen ratio for solid material in the manner given in our porous model. Many experiments have confirmed that the pressure-energy relation for a porous material has the form given by our model (shown as the line V2-A-B-C-D in Figure 6). However, some experimental evidence suggests that a lower Grüneisen ratio should be used for some materials. We suspect this discrepancy is caused by pore shape and inclusions. Some experimental work has been done to determine the variation of yield strength and modulus as a function of internal energy. Unfortunately only a few materials have been studied so general conclusions cannot yet be reached. These variations are important features of the model.

Considerable effort has been expended in understanding the third portion of the constitutive model: nonhydrostatic and nonequilibrium phenomena. We are now aware of rate-dependent yield phenomena, Bauschinger effects, phase changes, rates of pore collapse, and the rate phenomena associated with fracture. Many of these studies have led to an understanding of these phenomena in a large class of materials, although specific data are available for very few materials. Thus, we now realize that we must expect those effects in all materials and have analytical models for these effects.

In a recent parameter study Buxton<sup>20</sup> confirmed the above conclusions for porous beryllium. He found that each portion of the constitutive model discussed above may have a dominant effect on the stress and impulse generation.

#### Measurements Required to Specify the Model for any Material

With so much information required to determine the model parameters for each material, it is clear that a fairly large number of experiments

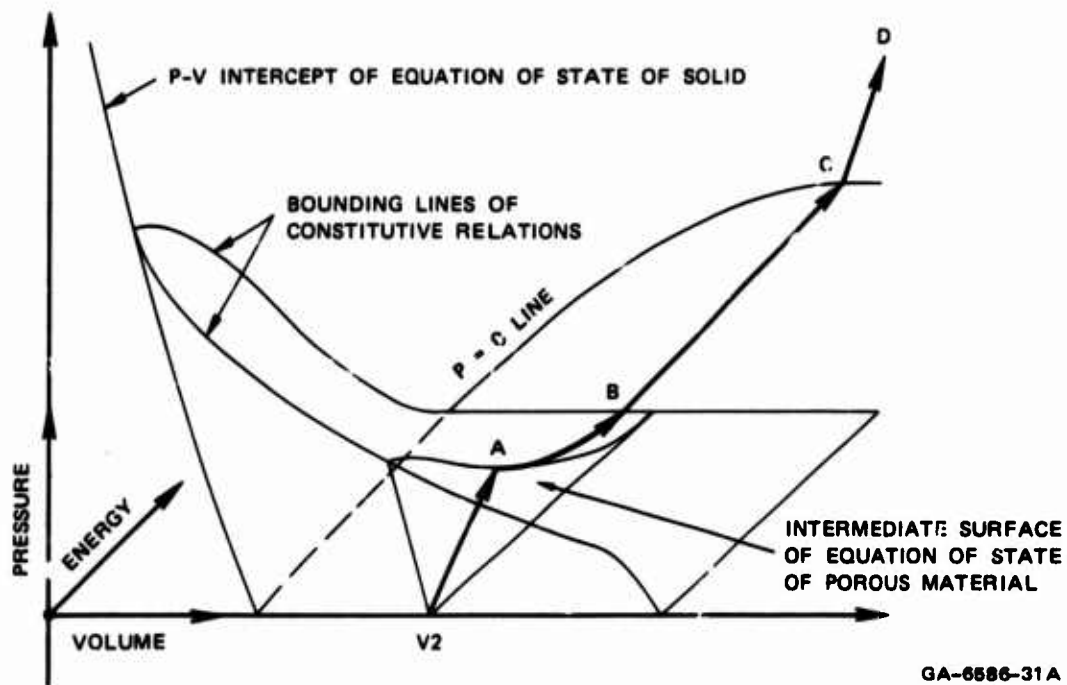


FIGURE 6 LOCUS OF STATES CAUSED BY HEATING POROUS MATERIAL WITHOUT EXPANSION

are required. Where possible, each parameter should be derived from experimental results that depend uniquely on that parameter. From plate impact experiments, for example, the impedance, wave velocity, and unloading moduli can be derived directly. But in electron beam experiments, Grüneisen's ratio, modulus, and attenuation all have some influence so that none is determined uniquely.

The behavior of the solid is determined by impact and electron beam experiments on the solid and also on porous material. The impacts provide loading and unloading data on and near the Hugoniot and also at higher energy states as shown in Figures 3 and 5. Because the Lagrangian<sup>\*</sup> analysis can be used to reduce the data, much of the pressure-volume-energy surface near solid density can be explored with impacts. The impacts determine the moduli and give some indication of Grüneisen's ratio. Electron beam experiments are performed to define states of larger specific volume than those reached in impacts and to determine the Grüneisen's ratio throughout the range of interest. Because of the more complex loading path (such as paths A, B, or C in Figure 3) taken in the electron beam experiments, the equation-of-state surface must be known fairly well before the e-beam data can be reduced. With a combination of impacts and e-beam experiments in the same region of the surface, we feel that a valid reduction of the data can be made.

Porous material is studied in a manner similar to that used for solids. Impacts at several peak stress levels and initial internal energies are used to map the "yield surface" of Figure 2 and the unloading behavior. Then e-beam experiments are conducted at low energies so that little of the material melts. The e-beam data are reduced with the aid of the constitutive relations based on the impacts. In this way, the e-beam

---

\* Lagrangian analysis is a method for transforming stress or particle velocity records from impact experiments to obtain stress-volume-energy paths followed by the material during the impact.

measurements are used to provide an effective Grüneisen's ratio and need not explain the wave propagation phenomena. These experiments in the porous material lead to determinations of the baushinger effect, the rate-dependence of yielding, the pore collapse process, fracturing, and the variation of yield and moduli with internal energy. Because of the variety of effects, special experiments must be conducted with different target thicknesses, different initial temperatures, and different instrumentation. Some targets must be sectioned to examine internal effects.

The foregoing experiments are all dynamic. However, some auxiliary data may be obtained from other kinds of experiments. A crush-up curve and unloading moduli may also be obtained statically, although these may not be appropriate for dynamic conditions. It is necessary to verify static data by comparison with wave propagation data before using them in dynamic calculations.

## II CONSTITUTIVE RELATIONS FOR POROUS MATERIALS

This study is directed toward deriving a thermodynamic description of the stress, energy, and volume states reached by porous material during shock wave loading. Such a description is usually termed the constitutive relations. For convenience the constitutive relations are separated into components by dividing the stress into pressure and deviatoric stress.

$$P = P(E, V) \quad (1)$$

$$\sigma' = \sigma'(E, V) = \sigma - P \quad (2)$$

where

$\sigma$  is the stress in the direction of wave propagation

$P, \sigma'$  are pressure and deviator stress

$E, V$  are internal energy and specific volume.

The deviatoric component is associated with yielding and mechanical rate effects; it is important only while the material is solid. The pressure portion provides the major part of the stress for solid behavior and all the stress for liquid and vapor states. As an aid in visualizing the  $P(E, V)$  function, it is often depicted as a surface, as shown in Figure 2. Solid behavior is given by points near  $E = 0$  on the left in the figure; vaporized states are on the right.

If the material is initially porous, a combination of compressive loading and heating will cause the pressure to lie on the "yield surface for porous material," shown in Figure 2. Thus the thermodynamic behavior of the porous material is an augmentation of the behavior of the solid. In porous materials the states reached in shock wave experiments depend on the loading history and rate of loading and not simply on the thermodynamic state variables.

This chapter describes our approach to constructing a model: our view of how porous material actually behaves. We outline the features included in the present computational model and give detailed derivation of the constitutive relations included in the model.

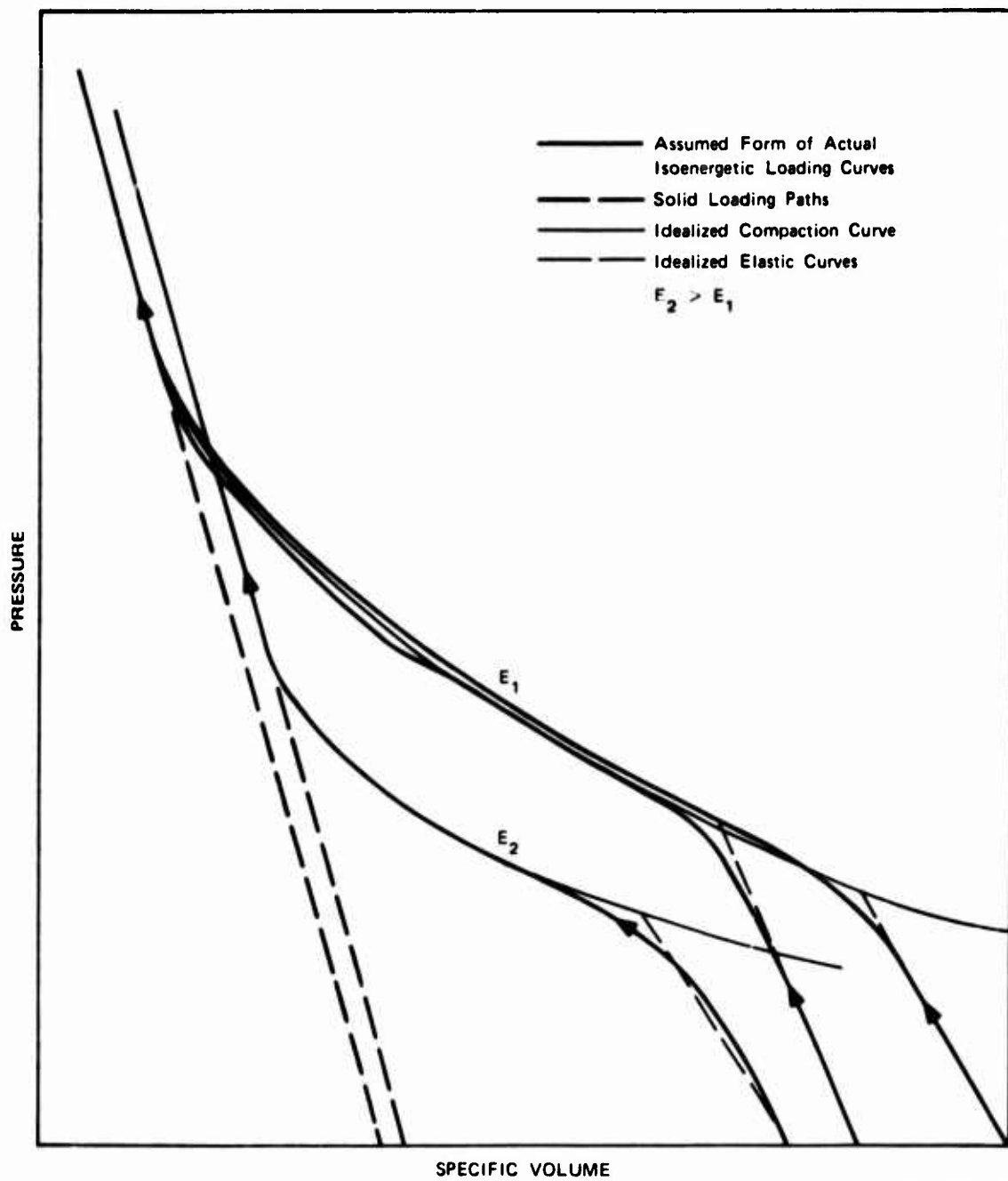
### Approach

The energy-absorbing and stress-generating mechanisms in porous materials are assumed here to be related to the behavior of the solid particles. The computational model is constructed by combining the behavior of the solid material with the effects associated with the structure of the porous material. No special treatment is required to handle stress-generation under rapid heating. At low stresses the porous material responds elastically but with a lower modulus than the solid particles. At higher stresses the structure yields, allowing the collapse of some pores. This structural yield is associated with the yield strength of the solid material and of the interparticle bondstrengths.

A family of assumed isoenergetic loading curves are shown in Figure 7 together with idealizations of this path. There is assumed to be a variation of yield and bulk modulus with energy, and a gradual transition from elastic to fully plastic behavior. These curves are represented in the model by paths with a linear elastic loading up to a sharp yield. After yielding, all paths at the same energy coincide in the model.

Deviator stresses are always present in quasi-static, one-dimensional strain experiments on porous materials (that is, stresses are not equal in three orthogonal directions). Such measurements usually show very complex relations between deviator stress and strain, relations indicative of work-hardening, rate-dependence, and Bauschinger effects.

Fracture in porous material has been studied very little, but it is assumed that fracture occurs, as in solids, by the growth of cracks or voids. The strength of porous materials is smaller than the corresponding



MA-2407-25

FIGURE 7 ASSUMED FORM OF ACTUAL ISOENERGETIC LOADING CURVES COMPARED WITH IDEALIZED FORM FOR THE MODEL



solids because there are so many large inherent flaws. Under sustained tensile loading, the porous material should come apart and produce some fragments. On recompaction the fragments will not necessarily follow the same loading path they did on initial compression.

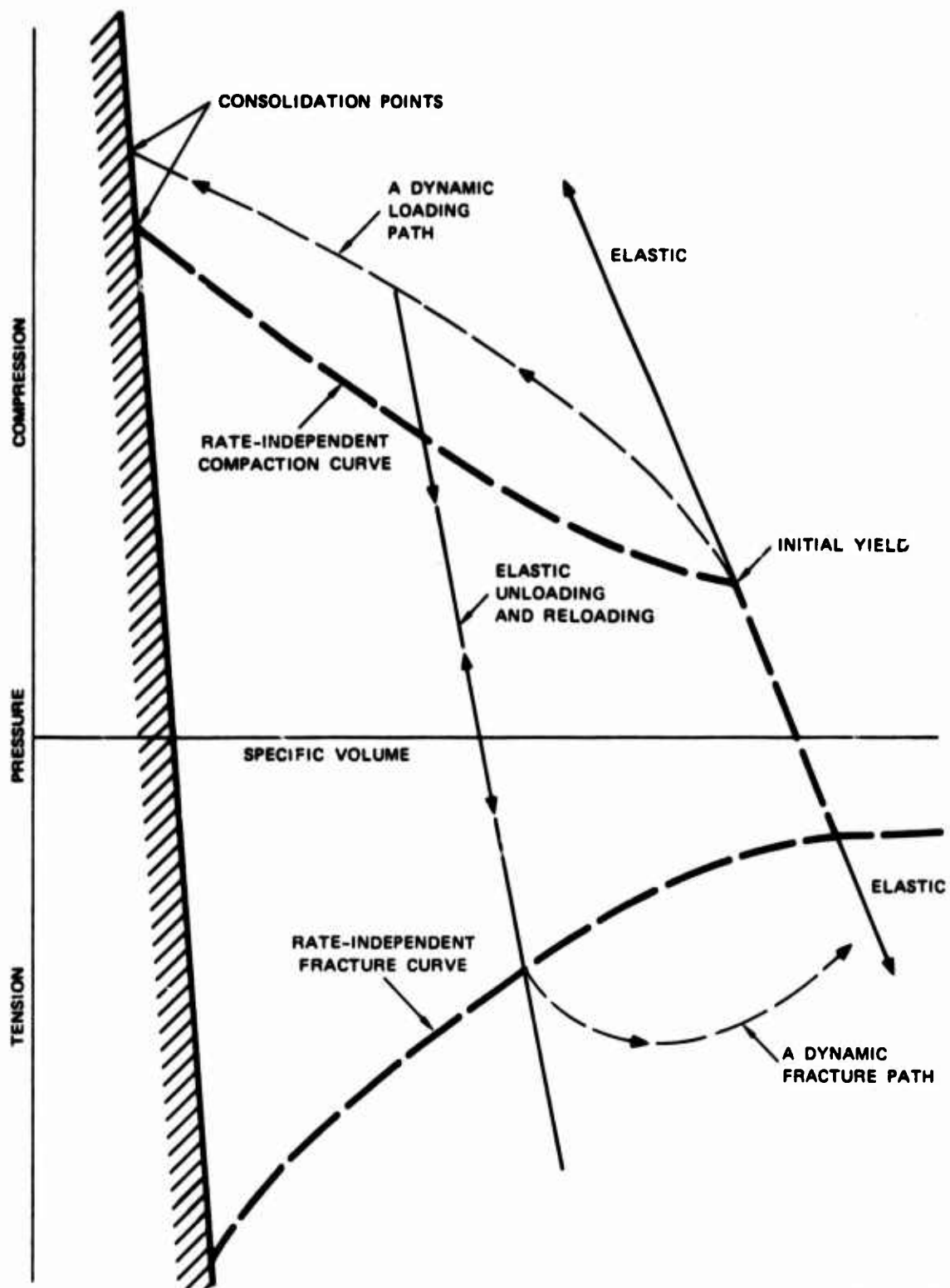
#### Features of the Model

The model developed is intended to describe the thermodynamic behavior of porous ceramics, metals, and plastics. It should also be applicable to geologic materials. It is intended to readily fit data available in various forms so that little recasting of data is required. The flexibility required to treat many kinds of material with data in many forms is obtained by providing several options for each of the following portions of the model:

- Solid constitutive relations
- Yield surface for porous material
- Rate effects in the porous material
- Deviator stress.

The solid behavior is treated by a combination of the Mie-Grüneisen and PUFF expansion equations of state, the ESA extended equation of state, or the Philco-Ford three-phase equation of state. The yield surface for the porous material is provided by versions of the P- $\alpha$  model,<sup>5,6</sup> the Carroll-Holt model,<sup>3,4</sup> the POREQST model,<sup>1</sup> and the Holt model.<sup>2</sup> Rate-dependent effects are treated by Butcher's<sup>7</sup> or Holt's<sup>2</sup> models or by the SRI void growth model.<sup>8</sup> Deviator stress is handled by the usual elastic, plastic, or work-hardening models, by several rate-dependent models, a Bauschinger model,<sup>12</sup> or by a special model for S200 beryllium.<sup>11</sup>

The logic used for joining the components of the model is illustrated in Figure 8. Here, possible loading and unloading paths are given for a porous material. Initially, the loading is elastic; above the "initial



MA-2407-10

FIGURE 8 PRESSURE-VOLUME PATHS FOR A POROUS MATERIAL

yield" point, the loading continues elastically only for very rapid loading. For quasi-static loading, the path follows the line on the yield surface. For wave propagation, the path will depend on the loading rate and will lie somewhere between the elastic and the static curves (for example, the "dynamic" path). If unloading occurs, the path will be on an "intermediate" surface and the behavior will be elastic. Continued unloading will cause tension stresses. In tension there are also three paths: elastic for instantaneous loading, static fracture threshold, and between these, a dynamic path. During the compression phase, the path may reach the solid curve, that is, the material may consolidate. The foregoing paths concern only the pressure; the deviator stress follows a similar set of paths.

The procedure used to perform the calculations and the switching between options is illustrated in Figure 8. For porous material, the calculations are first made on the assumption that the response is elastic, that is, that the path lies on the "intermediate surface" defining reversible loading and heating. Then the rate-independent compaction (or fracture) pressure is calculated. If the elastic pressure exceeds the static, the dynamic pressure is computed. In this way, the very complex model is isolated into small, independent portions.

A sample of some capabilities of the model is shown in the computed loading paths in Figures 9 and 10. The paths were constructed by computing pressure with the subroutine for a sequence of increasing densities, followed by a decreasing sequence and another increasing sequence. The computed paths show rate-independent and rate-dependent loading, unloading, rate-independent fracture, complete separation (in Figure 9) and recompression to consolidation. Other possible paths would show various combinations of heating and loading.

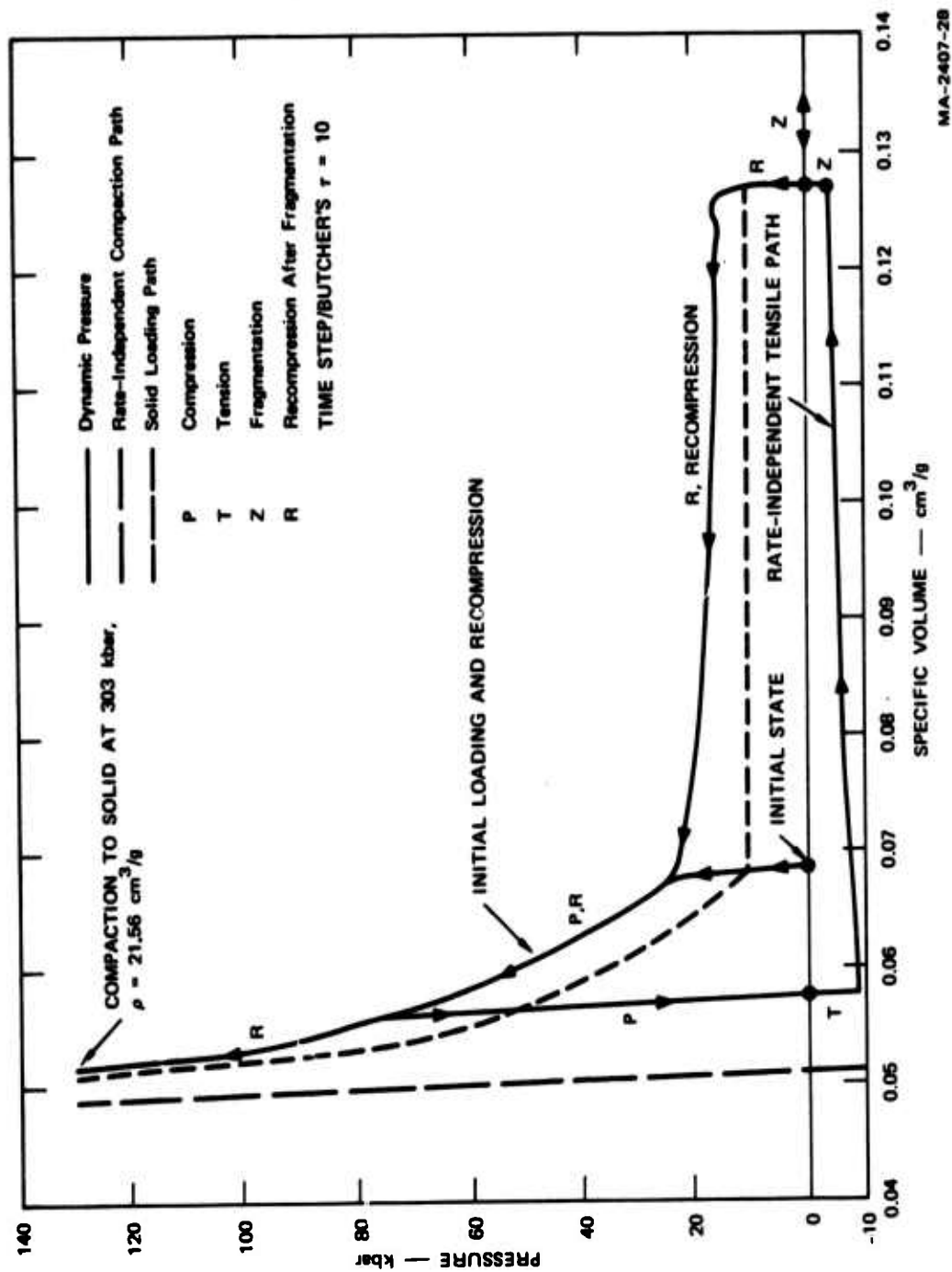
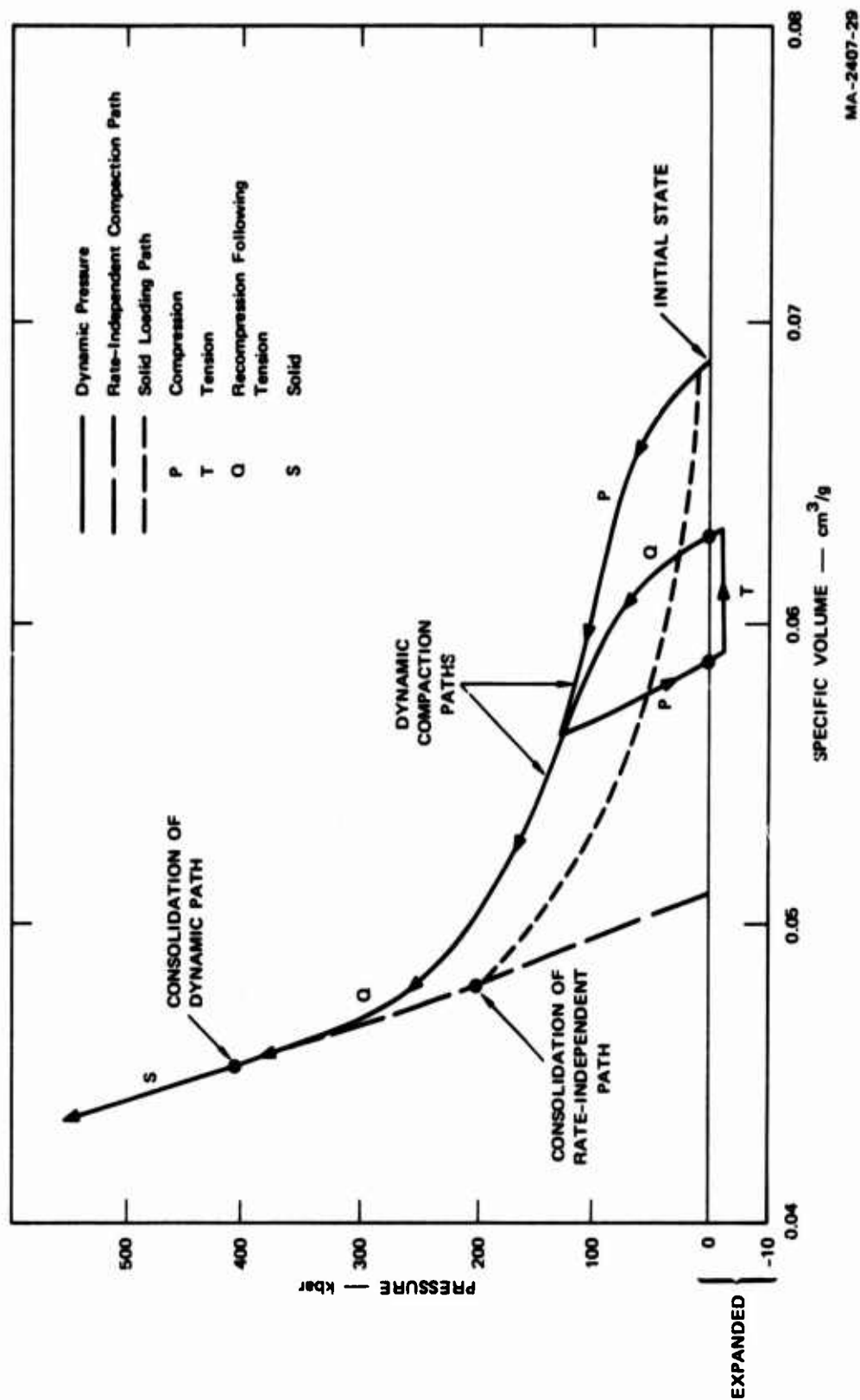


FIGURE 9 PRESSURE-VOLUME PATH COMPUTED IN PEST FOR LOADING WITH POREOST AND BUTCHER P- $\alpha$ - $\tau$  MODELS, ELASTIC UNLOADING, CONSTANT STRENGTH IN TENSION, FRAGMENTATION, AND RECOMPRESSION WITH POREOST AND BUTCHER'S MODEL

Data are for Porous Tungsten.



MA-2407-29

FIGURE 10 PRESSURE-VOLUME PATH COMPUTED IN PEST FOR LOADING WITH PORHOLT MODEL, ELASTIC UNLOADING, CARROLL-HOLT MODEL IN TENSION, AND RECOMPRESSION WITH PORHOLT MODEL TO CONSOLIDATION  
Data are for porous tungsten.

### Pressure in the Porous Material

The stress in the solid particles of the porous material must vary from zero at free surfaces to large values at contact points. For pressure calculations we consider, however, only an average stress over all the solid matter. If a cross section is cut through the porous material, some of the cross section is void. The average stress or pressure on this section is a function of the average stress in the solid and of the void volume. Carroll and Holt<sup>21</sup> have shown that

$$P_s = \alpha P \quad (3)$$

where  $P$  is the average of three orthogonal stresses on the porous material

$P_s$  is the average pressure in the solid particles

$\alpha = V/V_s$ , the distension ratio

$V$  is the gross specific volume

$V_s$  is the average specific volume of the solid particles.

In the discussion of analytical models for porous materials, some investigators have used the relative void volume,  $v_v$ , and others have used the distension ratio,  $\alpha$ . The relative void volume or porosity is defined as

$$v_v = \frac{V - V_s}{V} = \frac{V - V_s}{V} \quad (4)$$

where  $V_v$ ,  $V_s$ , and  $V$  are the specific volumes of void and solid, and the gross specific volume. The distension ratio is defined as

$$\alpha = \frac{V}{V_s} = \frac{\rho_s}{\rho} \quad (5)$$

where  $\rho$  and  $\rho_s$  are gross density and average density of the solid particles. Through Eqs. (4) and (5), relations can be found between  $v_v$  and  $\alpha$

$$v_v = 1 - \frac{1}{\alpha} \quad (6)$$

and

$$\alpha = \frac{1}{1 - v_v} \quad (7)$$

The pressure in the solid material below melting,  $\rho_s$ , is assumed to be given by the Mie-Grüneisen equation of state with the Hugoniot as the reference function.

$$\begin{aligned} P_S &= P_H + \Gamma p (E - E_H) \\ &= C\mu + D\mu^2 + S\mu^3 + \Gamma p (E - E_H) \end{aligned} \quad (8)$$

where  $\mu = \rho_s / \rho_{so} - 1$

$P_H$  and  $E_H$  are pressure and internal energy at the density  $\rho$  on the Hugoniot

$\Gamma$  is the Grüneisen ratio

$C, D, S$  are constants.

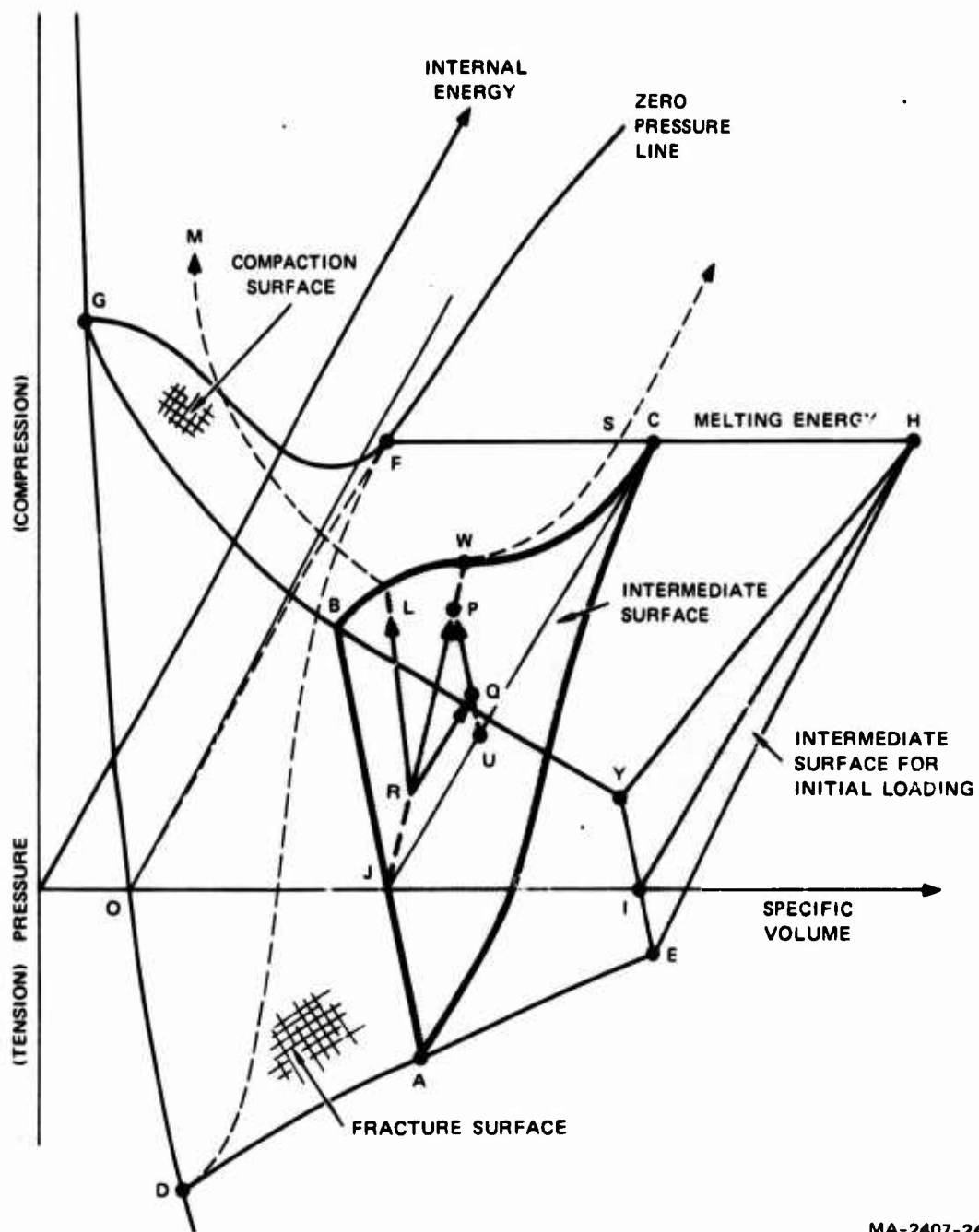
### Intermediate Surfaces

The model must provide for elastically loading, unloading, or heating material with arbitrary porosity. For this purpose we define an "intermediate surface" in pressure-energy-volume space. This warped surface contains the locus of points that can be reached from a given point by an elastic (reversible) loading or heating process. If yielding occurs, the state point leaves the first intermediate surface and proceeds to another. This behavior is analogous to the usual elastic-plastic response in which unloading after yielding determines a new elastic path. When energy must be considered, as in our case, a new surface instead of a path is determined. Thus there are an infinite number of nonintersecting intermediate surfaces that can be defined between the initial porous density and the solid density.

The intermediate surface concept is introduced here from a physical point of view, and derived mathematically, and then the thermodynamic requirements for it are discussed.

One intermediate surface ABC is shown in Figure 11 together with a compaction surface YBGFCH, fracture surface DFHE, and consolidation lines GF and DF. To explore the nature of the intermediate surface, consider a series of processes that must be represented on the surface. For example, a zero-pressure expansion under heating must define a line on the surface. Along this zero-pressure-expansion line, shown as JC on Figure 11, the specific volume must increase in proportion to the change in energy. An elastic loading or unloading process defines a line such as RL on the intermediate surface in Figure 11. The slope of this line in the pressure-volume plane is a bulk modulus. If radiant energy is deposited rapidly in the material such that no volume change can occur, pressure rises immediately because of the restraint of the surrounding material. Such a line is RP. If the energy increase is small enough so that only elastic response occurs, the response can be decomposed into thermal expansion at zero stress (RQ) and a recompression at constant energy to the initial density (QP). Both expansion and recompression paths must lie on the intermediate surface and so must the resultant path, which occurs at constant volume. Together these three paths must define the nature of the intermediate surface. Slopes such as the adiabatic loading path RL in Figure 11 are represented by an effective bulk modulus, while constant-volume slopes such as RP provide the effective Grüneisen ratio. Since the bulk moduli of the material vary with internal energy, the surface is not plane, but warped. In the following paragraphs the bulk moduli for loading processes and the thermal expansion behavior are derived. Then these two processes are combined to form an expression for pressure associated with any loading or heating process on an intermediate surface.





MA-2407-24

FIGURE 11 CONSTITUTIVE RELATIONS OF A POROUS MATERIAL, EMPHASIZING THE INTERMEDIATE SURFACE FOR REVERSIBLE LOADING AND HEATING

An isoenergetic bulk modulus is derived for use in our calculations. Along an isoenergetic path, the pressure is

$$P = K \left( \frac{\rho}{\rho_0} - 1 \right) \quad (9)$$

where  $K$  is the isoenergetic modulus

$\rho_0$  is the density at zero pressure on this path.

It is assumed that  $K$  is a function only of density and energy and that these functional dependencies are separable.

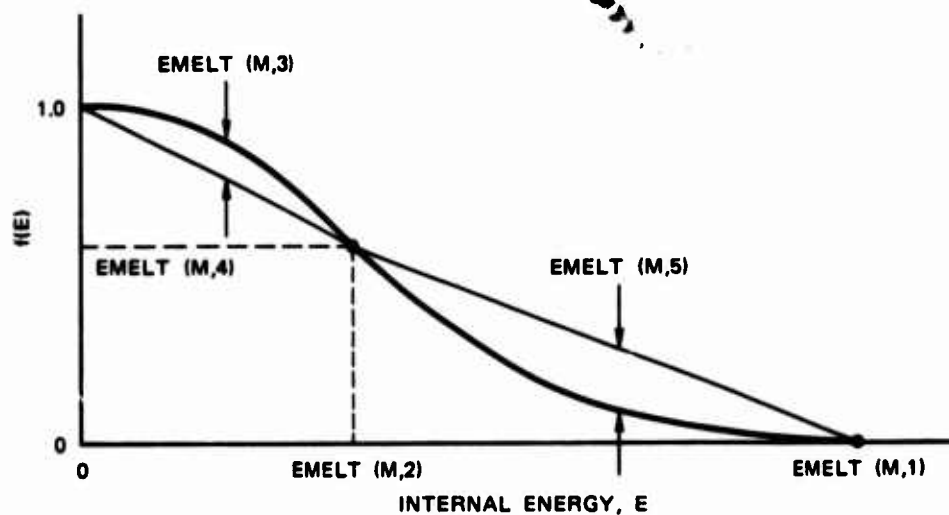
$$K = k(\rho)f(E) \quad (10)$$

The functions of  $k(\rho)$  and  $f(E)$  are derived separately. The energy dependence  $f(E)$  of the effective modulus is described by two parabolas for the model. The form of  $f(E)$  is shown in Figure 12. The parabolas usually provide enough flexibility to fit the meager data available.

The form of  $k(\rho)$ , the porosity dependence of bulk modulus, is derived to meet three criteria:

- The modulus variation should be like that obtained from the elastic analysis of porous material.
- The value of the modulus at the initial density must fit data on the material, and the modulus at consolidation should approximate the isoenergetic modulus of the solid.
- The bulk sound speed should never exceed the bulk sound speed of the solid. Thus, because  $k/\rho$  is an approximation to the square of the bulk sound speed,  $K/\rho$  should always be less than  $K_s/\rho_{so}$ .

The theoretical variation of modulus with porosity is obtained from the works of MacKenzie<sup>22</sup> and Warren<sup>23</sup> on material with noninteracting spherical pores. For linear elastic loading with small deformations, they



GA-6586-34

$$f(E) = 1 - (1 - E_4) \frac{E}{E_2} \left[ 1 + \frac{4E_3}{E_2} \cdot \frac{E - E_2}{1 - E_4} \right] \quad E \leq E_2$$

$$= E_4 \left[ 1 - \frac{E - E_2}{E_1 - E_2} \left( 1 + \frac{4E_5}{E_4} \cdot \frac{E - E_1}{E_1 - E_2} \right) \right] \quad E_2 < E < E_1$$

Where  $E$  = current internal energy

$E_1, E_2 \dots = \text{EMELT}(M,1), \dots$

FIGURE 12 THERMAL STRENGTH REDUCTION FUNCTION  
FOR EFFECTIVE MODULI

derived the following relations for the effective isothermal bulk moduli from small-deflection theory.

$$K_{pI} = \frac{K_I}{\alpha_1 + \frac{3K_I}{4G_I} (\alpha_1 - 1)} \quad (11)$$

where  $K_I$  and  $G_I$  are the isothermal bulk and shear moduli of the solid

$\alpha_1$  is the distension ratio on the  $i$ th intermediate surface.

Equation (11) may greatly overestimate the effective stiffness if the pores are nonspherical or there is intergranular sliding. Therefore the theoretical form is modified to permit the specification of an initial bulk modulus  $K_0$ . Then the dependence of bulk modulus on distension ratio is

$$k(\rho) = \frac{K_s}{\alpha_1 + \left( \frac{K_s}{K_0} - \alpha_0 \right) \frac{\alpha_1 - 1}{\alpha_0 - 1}} = \frac{K_s}{\alpha_1 + L(\alpha_1 - 1)} \quad (12)$$

where  $\alpha_0 = \rho_{so}/\rho_0$  is the initial distension ratio of the unheated material

$K_s$  is the adiabatic bulk modulus of the solid at initial density

$$L = \frac{K_s/K_0 - \alpha_0}{\alpha_0 - 1}, \text{ a constant.}$$

Here we have used the adiabatic modulus  $K_s$  instead of the isoenergetic modulus because it corresponds to the  $C$  in the Hugoniot relation in Eq. (8) for the solid.

To keep the bulk sound speed from exceeding that of the solid, we also require that

$$K_0 \leq K_s/\alpha_0 \quad (13)$$

Thus the behavior of  $k(\rho)$  as determined by Eqs. (12) and (13) is similar to that determined by Eq. (11), but now  $k(\rho)$  also depends on the ratio of the

initial modulus of the porous material to the modulus of the solid material.

During elastic loading there will be a small change in distension, a change not noticed in MacKenzie's small-deflection analysis. If the current distension were used in Eq. (12), a nonlinear loading would occur. This nonlinearity is eliminated by defining  $\alpha_1$  as the distension at zero pressure and energy on the  $i$ th intermediate surface, that is

$$\alpha_1 = \rho_{so} / \rho_o^1 \quad (14)$$

where  $\rho_{so}$  is the solid density and  $\rho_o^1$  is the porous density, both defined at zero pressure and energy.

$\alpha_1$  is equal to  $\alpha_o$  on the intermediate surface passing through the initial state of the porous material.

The isoenergetic shear modulus also is reduced for porosity and internal energy. As for the bulk modulus, the effective shear modulus is presumed to be a product of functions of  $\rho$  and  $E$ .

$$G = g(\rho)f(E) \quad (15)$$

The same thermal strength reduction function is used as for the bulk modulus. According to MacKenzie's analysis, the isothermal shear modulus varies linearly with density

$$G_{pI} = G_I \left[ 1 - 5 \left( 1 - \frac{1}{\alpha_1} \right) \frac{3K_I + 4G_I}{9K_I + 8G_I} \right] \quad (16)$$

As with the bulk modulus, we may wish to define an initial shear modulus,  $G_o$ . This is achieved by writing an expression for  $g(\rho)$  that is linear in density as is  $G_{pI}$  but permits an arbitrary specification of  $G_o$ . Then

$$g(\rho) = G_s \left[ 1 - \left( 1 - \frac{G_o}{G_s} \right) \frac{1 - 1/\alpha_1}{1 - 1/\alpha_o} \right] \quad (17)$$

where  $G_I$  has been replaced by the adiabatic modulus  $G_s$ .

The intermediate surface also represents state points reachable by heating or cooling. When a solid is heated at zero pressure, the material expands uniformly in all directions. The specific volume increases by an amount proportional to the initial specific volume, the thermal expansion coefficient, and the temperature change. A porous material expands under heating in much the same way; even the voids retain their shape and simply enlarge. For a porous material at an arbitrary point at zero pressure, such as point J in Figure 11, the expansion path is along the curve JC defined by

$$P = 0$$

$$V = V_J (1 + \alpha_t \Delta\theta) \quad (18)$$

where  $\alpha_t$  is the volumetric thermal expansion coefficient, a constant  
 $\Delta\theta$  is the change in temperature  
 $V_J$  is the specific volume at point J.

This expression is valid for  $V_J = V_o$ , the initial specific volume, and also for  $V_J = V_{so}$ , the initial solid volume.

The temperature is eliminated from Eq. (18) by introducing a constant specific heat,  $C_p$ , and the Grüneisen ratio,  $\Gamma = K_s \alpha_t / (\rho_{so} C_p)$ . Then the volumetric expansion along the zero pressure line JC in the intermediate surface of Figure 11 is

$$\frac{1}{\rho_U} = \frac{1}{\rho_o} \left( 1 + \frac{\Gamma \rho_{so} E}{K_s} \right) = \frac{T_F}{\rho_o} \quad (19)$$

where  $\rho_o^i$  is the reference density at J on the  $i$ th intermediate surface  
 $\rho_U^i$  is the density at point U on the line JC.  
 $T_F$  is a thermal expansion factor.

When the equation for the zero pressure line is solved from the Mie-Grüneisen Eq. (8), the following expansion is obtained:

$$\frac{1}{\rho} = \frac{1}{\rho_{so}} \left[ 1 + \frac{\Gamma \rho_{so} E}{C} - \frac{1}{2} \left( \frac{\Gamma \rho_{so} E}{C} \right)^2 \dots \right] \quad (20)$$

Thus, to a first approximation in  $\Gamma \rho_{so} E/C$  (and with  $K_s = C$ ), the zero pressure line follows the same expression in the solid and porous materials.

The pressure at an arbitrary point P on the intermediate surface in Figure 11 is obtained by expanding from J to U using Eq. (19) and then loading on an isoenergetic path to P using Eq. (9). The isoenergetic loading follows the relation:

$$P = K_1 \left[ \frac{\rho}{\rho_U} - 1 \right] = k_1 f(E) \left[ \frac{\rho}{\rho_U} - 1 \right] \quad (21)$$

By inserting Eq. (19) into Eq. (21), we obtain the complete expression for pressure:

$$P = k_1 f(E) \left[ \frac{\rho}{\rho_o} \left( 1 + \frac{\Gamma \rho_{so} E}{K_s} \right) - 1 \right] \quad (22)$$

Eq. (22) provides a unique expression for  $P(\rho, E)$ , independent of loading path or direction.

The foregoing intermediate surface expressions provide a unique relationship between energy, pressure and volume. This uniqueness (path-independence) is one requirement of equilibrium thermodynamics. The expressions above impose no requirements on temperature and entropy and hence they may not meet all the thermodynamic requirements: this question is examined below.

For thermodynamic completeness, an equation of state must provide a unique relationship between energy, volume, and entropy

$$E = E(V, S) \quad (23)$$

Then, with the aid of the energy balance relation

$$dE = TdS - PdV = \left( \frac{\partial E}{\partial S} \right)_V dS + \left( \frac{\partial E}{\partial V} \right)_S dV, \quad (24)$$

the other basic thermodynamic quantities can be determined, that is

$$T = \left( \frac{\partial E}{\partial S} \right)_V \quad (25)$$

$$P = - \left( \frac{\partial E}{\partial V} \right)_S \quad (26)$$

Thus the uniqueness requirement is that all five quantities - E, P, S, T, V - be uniquely given at each point on the equation-of-state surface.

While the present results uniquely define E, P, and V, the temperature and entropy are path-dependent. This path-dependence can be illustrated with the aid of the following equations for temperature and entropy

$$dT = \frac{1}{C_P} (dE + PdV + T\alpha_t dP) \quad (27)$$

$$\text{and} \quad TdS = dE + PdV \quad (28)$$

For example, examine alternate paths such as heating and then loading (path RQP in Figure 11), or loading followed by heating (RLP in Figure 11). Different temperatures and entropies are obtained at the final point (point P).

We expect to examine this problem of thermodynamic consistency further and to propose a solution if the discrepancies are significant.

In preparation for each elastic calculation with Eq. (22), it is necessary to locate the appropriate intermediate surface. Since surface is related to a particular value of  $\rho_0^1$ , it is necessary to solve Eq. (22) only for  $\rho_0^1$ , using the values of P, E,  $\rho$  from the previous state point



calculation. The inversion of Eq. (22) with Eq. (12) substituted for  $k_1$  leads to a linear result for  $\rho_o^1$ .

$$\rho_o^1 = \frac{K_s f(E) \rho_f \Gamma_f - P \rho_{so} (1 + L)}{K_s f(E) - PL} \quad (29)$$

#### Rate-Independent Yield or Compaction Surface

When loading or heating occurs in a porous material, the initial response is elastic. But eventually the stress reaches a level that causes a general yielding of the assemblage and a consequent collapse of the voids. This yielding may occur for many combinations of density and internal energy so that the yield points form a surface in P-V-E space. If loading or heating continues, it is assumed that the state point moves across this surface. Thus, we assume that the yield surface is unique and can be reached by arbitrary combinations of heating and loading (cooling and unloading cannot be included). This uniqueness has been verified for static loadings but has never been tested by heating.

The compaction surface is an upper bound on the static pressure obtainable at a given density and internal energy. It also serves as a threshold level for rapid collapse of voids under dynamic loading. As shown in Figure 11, the compaction surface joins the solid equation-of-state surface along a consolidation line (FG) and ends at a zero pressure line at the melt energy for the material (FCH). The compaction surface also passes through zero along a line corresponding to the free expansion of the material from its original density (line IH). The joint between the compaction surface and any intermediate surface is represented by BC in Figure 11.

A rate-independent compaction surface occurs in all the porous models considered. In some cases one model may fit the material behavior better than another. Usually several models are equally appropriate, but the

data may have already been fitted to one of the models; in that case, the model that matches the data should be used if it is available.

The compaction surfaces are defined by functions of the form  $P_{com}(\rho, E)$  or  $P_{com}(\alpha, E)$ .

To simplify the form of the surface, we assume that it is formed by two independent processes: (1) isoenergetic compaction and thermal expansion and (2) thermal strength reduction. The  $P_{com}(\rho, E)$  becomes a product of two functions, each representing one of the processes:

$$P_{com} = p_{com}(\rho_{ref})f(E) \quad (30)$$

where  $p_{com}(\rho_{ref})$  is the crush curve defined in the  $E = 0$  plane. The variable  $\rho_{ref}$  is computed from the current values of  $\rho$  and  $E$  with the aid of Eq. (19), thus accounting for the thermal expansion effect.

The same function of energy  $f(E)$  is used here as in the modulus function, but this equivalence is not a requirement.

In the following subsections, several forms for  $p(\rho_{ref})$ , the compaction curve, are given that are in common use and appear to represent the experimental data, at least for some materials.

#### Compaction Curve of Holt's Model

The static compaction curve at  $E = 0$  is defined by providing an analytic relation between any two of the following three variables: the distension ration  $\alpha$ , specific volume, and pressure. Various functional forms have been given by Herrmann,<sup>5,6</sup> Butcher,<sup>7</sup> and Holt.<sup>2</sup> Holt's formulation has the advantage that  $\alpha$  is given as a function of specific volume, a known quantity; therefore no iteration is required. (Herrmann's and Butcher's  $\alpha$ 's are functions of pressure.) However, in using a function of volume, care must be taken to assume a reasonable form. The following restrictions are suggested.

- $\alpha$  must go to 1.0 at consolidation,  $\rho = \rho_c$ .
- $\alpha$  should be initially equal to  $\rho_{so}/\rho_o$ , the ratio of solid density to initial density.
- The pressure should increase monotonically with density.
- The initial slope of the P-V curve past the initial yield value should be modeled.
- The consolidation should occur with the porous P-V curve tangent to the solid curve (no discontinuity in sound speed).

First, the expression of Holt was examined, but it did not meet the third requirement--monotonically increasing pressure. After several attempts, it was decided to use a second-order expansion in density and to meet only the first four requirements. The expansion is written

$$\rho' \alpha = \rho_{se} + a(\rho' - \rho_e) + b(\rho' - \rho_e)^2 \quad (31)$$

$$= \rho_s \quad (32)$$

where  $\rho_e$  is the density at initial yield

$\rho_{se}$  is the density of the solid particles at initial yield

$\rho'$  is the density for a state of zero internal energy.

The constant  $a$  is derived from the slope of the static compaction curve at the left of the point  $\rho' = \rho_e$ .

$$\rho_e \left. \frac{dP}{d\rho} \right|_e = \rho_e \left( \left. \frac{d \left( \frac{P_s}{\alpha} \right)}{d\rho} \right|_e \right) = \rho_e K_s \frac{d \left( \frac{\rho_s - \rho_{so}}{\alpha \rho_{so}} \right)}{d\rho} = \rho_e K_s \frac{d \left( \frac{\rho' - \rho_{so}}{\rho_{so} \rho_s} \right)}{d\rho} \quad (33)$$

Here Eqs. (3) and (5) have been used to replace  $\alpha$  and  $P$ , and the pressure in the solid has been written as a function of density:

$$P_s = K_s \left( \frac{\rho_s}{\rho_{so}} - 1 \right) \quad (34)$$

where  $K_s$  is the bulk modulus. When  $\rho_s$  is replaced by its value from Eq. (32), the differentiation is performed, and  $\rho'$  is set to  $\rho_e$ , the following is obtained

$$\begin{aligned} \rho_e \frac{dP}{d\rho} \bigg|_e &= K_s \left[ \frac{\rho_e}{\rho_{se}} \frac{\rho_{se} - \rho_{so}}{\rho_{so}} + \frac{\rho_e^2}{\rho_{se}^2} a \right] \\ &= P_e + \frac{a K_s}{\alpha_e^2} \end{aligned} \quad (35)$$

since

$$P_e = \frac{K_s}{\alpha_e} \frac{\rho_{se} - \rho_{so}}{\rho_{so}} \quad (36)$$

and

$$\alpha_e = \frac{\rho_{se}}{\rho_e} \quad (37)$$

where  $P_e$  is the pressure in the porous material at  $\rho = \rho_e$

$\rho_{se}$  is the solid density at the same point.

Then the parameter  $a$  can be determined for prescribed values of the slope at yield.

$$a = \frac{\alpha_e^2}{K_s} \left[ \rho_e \frac{dP}{d\rho} \bigg|_e - P_e \right] \quad (38)$$

the constant  $b$  in Eq. 31 is determined by requiring that  $\rho_s = \rho' = \rho_c$  at consolidation.

$$b = \frac{1}{\rho_c - \rho_e} \left( \frac{\rho_c - \rho_{se}}{\rho_c - \rho_e} - a \right) \quad (39)$$

The function thus defined for the static distension ratio has no extremum between  $\rho_o$  and  $\rho_c$  unless  $(dP/d\rho_e)$  is negative (downward initial slope of the P-V curve) or the initial slope greatly exceeds that required for a linear P- $\rho'$  curve. The value of an "a" for an approximately linear P- $\rho'$  curve is

$$a = \frac{\alpha_e}{\rho_c - \rho_e} (\rho_c - \rho_{se}) \quad (40)$$

This value of a is the largest value that would be used normally to fit data.

The densities  $\rho_e$  and  $\rho_{se}$  are computed from the elastic relation on the intermediate surface, Eq. (9), and the corresponding relation for the solid:

$$P_e = K_o \left( \frac{\rho_e - \rho_o}{\rho_o} \right) \quad (41)$$

$$P_{se} = K_s \left( \frac{\rho_{se}}{\rho_{so}} - 1 \right) = \alpha_e P_e \quad (42)$$

where  $P_e$  and  $P_{se}$  are pressures at the elastic limit, and  $K_o$  is the stiffness on the intermediate surface through the point  $\rho = \rho_o$ . Eq. (41) can immediately be solved for  $\rho_e$

$$\rho_e = \rho_o \left( \frac{P_e}{K_o} + 1 \right) \quad (43)$$

From Eq. (3) the densities can be related to  $\alpha_e$

$$\rho_{se} = \alpha_e \rho_e \quad (44)$$

Now Eqs. (42) and (43) can be solved simultaneously for  $\rho_{se}$ .

$$\rho_{se} = \frac{\rho_{so}}{1 - \frac{P_e \rho_{so}}{K_s \rho_e}} \quad (45)$$

#### Compaction Curve of POREQST

The rate-independent compaction curve of Seaman and Linde<sup>1</sup> was constructed to be convenient for fitting experimental data. The compaction curve is divided into a series of parabolic segments as shown in Figure 13. The segments are specified by a series of densities:  $\rho_1$ ,  $\rho_2$ , ...  $\rho_5$ , where  $\rho_1 = \rho_0$  and  $\rho_5$  is at the point of consolidation. Up to four segments are permitted. Within each segment, the curve is defined by the pressures at each end of the segment ( $P_1$  and  $P_2$  for the third segment of Figure 13) and by the variation  $\Delta P$ . As shown in Figure 13,  $\Delta P$  is measured midway between the specific volumes at each end of the segment and is the vertical distance from the straight line to the parabola. With this definition, the value of  $\Delta P$  is negative in the third segment shown. These quantities--densities and pressures--are readily determined from a measured or estimated P-V curve: these are the input data for the model.

For the wave propagation calculations, the input data that define the measured compaction curve are transformed to coefficients of a quadratic series in specific volume. In terms of the input variables the parabolic form is

$$P = P_1 + (P_2 - P_1) \left( \frac{V - V_1}{V_{i+1} - V_1} \right) - 4\Delta P \frac{(V - V_1)(V - V_{i+1})}{(V_{i+1} - V_1)^2} \quad (46)$$

where  $V_1$  and  $V_{i+1}$  are specific volumes at either end of the  $i$ th segment and correspond to  $\rho_1$  and  $\rho_{i+1}$ . By gathering terms in  $V$  and  $V^2$ , we can rewrite Eq. (46) as

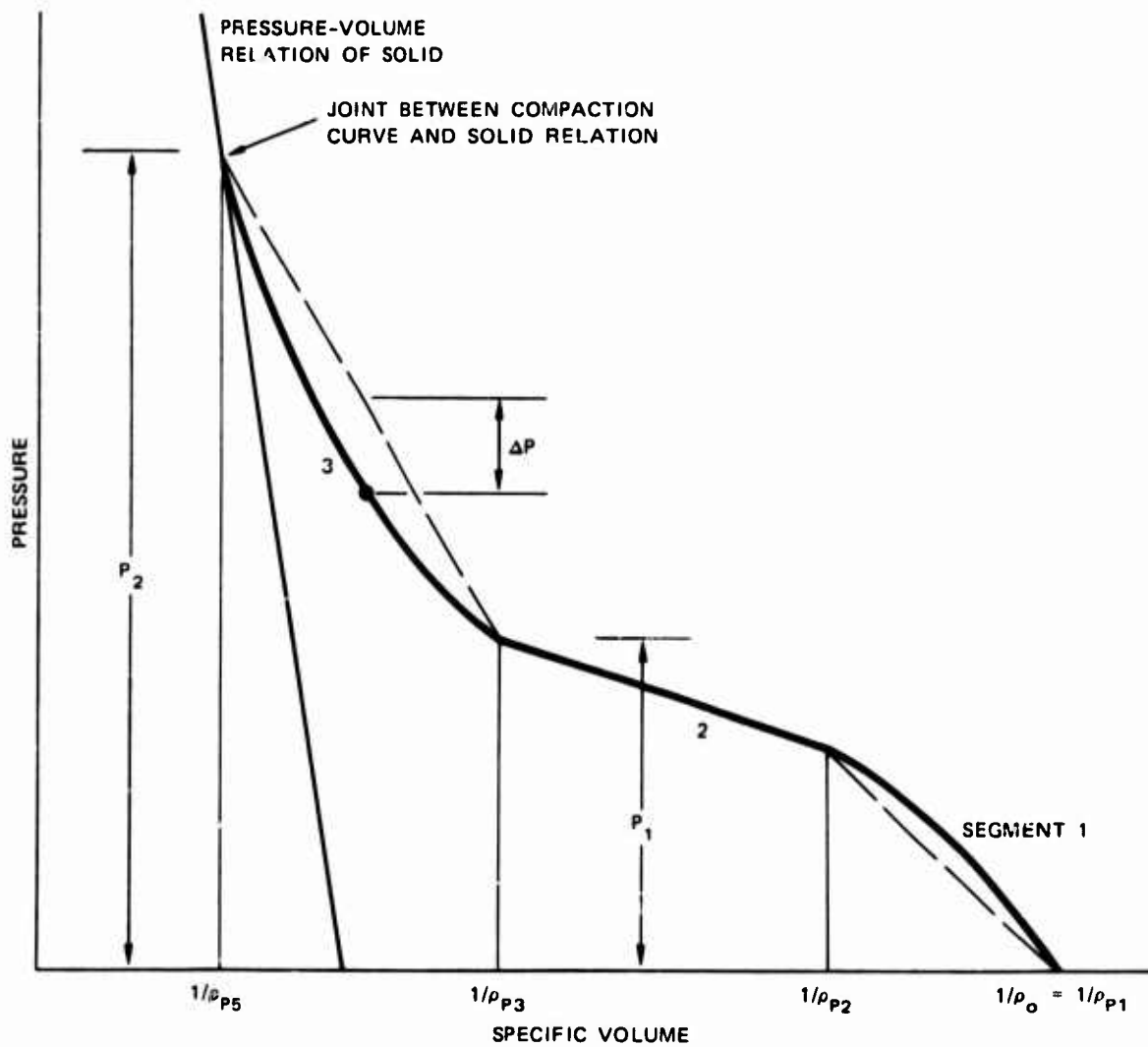


FIGURE 13    COMPACTION CURVE OF POREQST MODEL DIVIDED INTO THREE PARABOLIC SEGMENTS

$$P = P_{ai} + P_{bi} V + P_{ci} V^2 \quad (47)$$

$$\text{where } P_{ai} = P_1 + \frac{\rho_{i+1}}{\rho_{i+1} - \rho_i} \left[ P_2 - P_1 - \frac{4\Delta P \rho_i}{\rho_{i+1} - \rho_i} \right]$$

$$P_{bi} = \frac{-\rho_{i+1} \cdot \rho_i}{\rho_{i+1} - \rho_i} \left[ P_2 - P_1 - 4\Delta P \frac{(\rho_i + \rho_{i+1})}{\rho_{i+1} - \rho_i} \right]$$

$$P_{ci} = - \frac{4\Delta P \cdot \frac{1}{2} \rho_{i+1} \cdot \rho_i}{(\rho_{i+1} - \rho_i)^2}$$

The quantities  $P_{ai}$ ,  $P_{bi}$ , and  $P_{ci}$  are computed in the code and stored for use during the wave propagation computations.

With only three points to define each segment, the slopes of the data may be poorly represented. The slopes of the parabolic segments can be determined from Eq. (47).

$$\left. \frac{dP}{dV} \right|_{V=V_i} = \frac{P_2 - P_1 - 4\Delta P}{V_{i+1} - V_i}$$

$$\left. \frac{dP}{dV} \right|_{V=\bar{V}} = \frac{P_2 - P_1}{V_{i+1} - V_i} \quad (48)$$

$$\left. \frac{dP}{dV} \right|_{V=V_{i+1}} = \frac{P_2 - P_1 - 4\Delta P}{V_{i+1} - V_i}$$

where  $\bar{V} = (V_{i+1} + V_i)/2$

These equations should be used to verify that slopes of the data are being fairly modeled by the parabolas. If necessary the slope representation can be improved by using more segments or by repositioning the segment boundaries.



The point of consolidation may be more readily specified as a pressure  $P_c$  than a density. Therefore, the consolidation density may be given as zero in the input. Then the  $P_2$  value for the last segment is interpreted as  $P_c$  and used with the equation of state of the solid to determine the consolidation density. The solid equation of state is usually given in the Mie-Grüneisen form

$$P = (C\mu + D\mu^2 + S\mu^3)(1 - \frac{\Gamma\mu}{2}) + \rho\Gamma E \quad (49)$$

where  $C, D, S$  are coefficients of the Hugoniot

$\Gamma$  is Grüneisen's ratio

$E$  is internal energy

$$\mu = \rho/\rho_{so} - 1.$$

Eq. (49) is solved for  $\rho = \rho_5$ , the consolidation density, with  $P = P_c$  and  $E = 0$ . The solution for  $\rho_5$  is described in Appendix B.

#### Compaction Curve of Carroll-Holt Model

The Carroll-Holt<sup>3</sup> model is based on an analysis of the spherically symmetric compaction of a single spherical void in rigid-plastic material. The analysis led to the following relation between pressure and distension ratio:

$$\alpha = \frac{1}{1 - e^{-|3P/2Y|}} \quad (50)$$

Carroll and Holt suggested that this result could be extended to elastic-plastic material behavior through the use of Eqs. (3) and (5) and the stress-strain relation for a solid. Then

$$P = \frac{P_s}{\alpha} = \frac{K_s \left( \frac{\rho_s}{\rho_{so}} - 1 \right)}{\alpha} = K_s \left( \frac{1}{\alpha'} - \frac{1}{\alpha} \right) \quad (51)$$

where  $\alpha' = \rho_{so}/\rho$ .

By eliminating  $\alpha$  between Eqs. (50) and (51) Carroll and Holt derived an expression relating  $P$  to  $\rho$  for elastic-plastic behavior.

Here Eqs. (50) and (51) are used to find an expression relating  $\alpha$  to the density (represented by  $\alpha' = \rho_{so} / \rho$ ). The result is

$$\frac{1}{\alpha} = \frac{1}{\alpha'} + \delta \ln \left(1 - \frac{1}{\alpha}\right) \quad (52)$$

where  $\delta = \frac{2Y}{3K_s}$

The absolute value sign in Eq. (50) is accounted for by letting  $\delta$  be positive for compression and negative in tension. With Eq. (52) complete consolidation cannot occur although  $\alpha$  approaches arbitrarily close to 1.0. To permit consolidation, we introduce a small parameter  $\epsilon$  into Eq. (52) in such a way that  $\alpha = 1.0$  for a finite consolidation pressure  $P_c$ . The new form is then

$$\frac{1}{\alpha} = \frac{1}{\alpha'} + \delta \ln \left(1 + \epsilon - \frac{1}{\alpha}\right) \quad (53)$$

With  $\alpha = 1.0$ , Eq. (53) can be solved for the consolidation density  $\rho_c$  and for the value of  $\alpha'$  at consolidation.

$$\frac{\rho_c}{\rho_{so}} = \frac{1}{\alpha'_c} = 1 - \delta \ln \epsilon \quad (54)$$

Under the assumption of a constant bulk modulus, an expression for the consolidation pressure  $P_c$  can be derived from Eqs. (54) and (34).

$$P_c \cong \frac{2Y}{3} \ln \epsilon \quad (55)$$

For example, with  $\epsilon = 0.0001$ ,  $P_c/Y = 6.15$ .

Equation (53) is solved for  $\alpha$  by an iteration procedure. The starting estimate for the iterations is based on  $\alpha'$  because  $\alpha \approx \alpha'$  except very near consolidation. To avoid an estimate of  $\alpha$  less than 1.0, the following estimate is used

$$\alpha_1 = \alpha' \text{ for } \frac{1}{\alpha'} \leq 2 - \frac{1}{\alpha'_c}$$

$$\alpha_1 = \frac{1}{1 - (1/\alpha'_c - 1/\alpha')/2} \text{ for } \frac{1}{\alpha'} > 2 - \frac{1}{\alpha'_c}$$

From this first estimate a Newton-Raphson method is used to compute  $\alpha$ .

#### Compaction Curve of Herrmann's P- $\alpha$ Model

The most popular models for the compaction curve are those known generally as the P- $\alpha$  model.<sup>5</sup> Here we use a quadratic relation between P and  $\alpha$ , which is available in WONDY IV<sup>6</sup> as:

$$\alpha = 1 + (\alpha_y - 1) \left( \frac{P_c - P}{P_c - P_y} \right)^2 \quad (56)$$

where  $P_y$ ,  $\alpha_y$  are the pressure and distension at the yield point

$P_c$  is the consolidation pressure.

In Eq. (56)  $\alpha$  goes smoothly from  $\alpha_y$  at the initial yield to 1.0 at consolidation, as required. Also the derivative  $d\alpha/dP$  is zero at consolidation so there is a smooth transition from porous to solid.

The only parameters to specify are therefore  $P_c$  and  $P_y$ , quantities with clear physical significance.

This model is treated somewhat differently from the preceding three. To preserve the continuity at consolidation, we presume that Eq. (56) is valid for all energy values up to melting. The yield and consolidation pressures are interpreted as  $P_y f(E)$  and  $P_c f(E)$ , that is,

to reduced values appropriate to the current internal energy. To eliminate the iteration procedure normally required to solve Eq. (56), we substitute densities for pressures in Eq. (56). This substitution in fact follows from Eq. (56) under the approximations

$$P_s = K_s \left( \frac{\rho_s}{\rho_{so}} - 1 \right) + \Gamma \rho_{so} E \quad (57)$$

$$P_s = P \quad (58)$$

The omission of  $\alpha$  in Eq. (58) [compared with Eq. (14)] is the usual assumption of the P- $\alpha$  model. Then Eq. (56) becomes

$$\alpha = 1 + (\alpha_y - 1) \left( \frac{\rho_c - \rho_s}{\rho_c - \rho_{sy}} \right)^2 \quad (59)$$

where  $\rho_c$  is the consolidation density at the current energy E,

$\rho_{sy}$  is the solid density at yield and the current energy.

Both densities are functions of internal energy. The first step in solving Eq. (59) for  $\alpha$  is to compute  $\rho_c$  and  $\rho_{sy} = \alpha_y \rho_y$ . The yield point, given by the coordinates  $(\rho_y, P_y f(E), E)$  is on the intermediate surface that passes through the initial density  $\rho_o$ . It is computed from Eq. (21), which is simplified because  $\rho_o = \rho_o^1$ . The density  $\rho_u^1$ , the zero-pressure density defined at the current E, is related to  $\rho_o$  through Eq. (19)

$$\rho_u^1 = \rho_o / T_f \quad (60)$$

Then Eq. (21) is

$$P_y \cdot f(E) = k_o f(E) \left( \frac{\rho_y T_f}{\rho_o} - 1 \right) \quad (61)$$

Hence the density at the yield point is

$$\rho_y = \frac{\rho_o}{T_f} \left( 1 + \frac{P_y}{k_o} \right) \quad (62)$$

The distension ratio  $\alpha_y = \rho_{sy}/\rho_y$  is solved from the Mie-Grüneisen equation by neglecting the Hugoniot energy and the D and S terms.

$$P_{sy} = K_s \left( \frac{\rho_{sy}}{\rho_{so}} - 1 \right) + \Gamma \rho_{sy} E = \alpha_y P_y \quad (63)$$

Inserting  $\alpha_y \rho_y = \rho_{sy}$  into Eq. (63) yields

$$\alpha_y = \frac{K_s}{K_s \frac{\rho_y}{\rho_{so}} + \Gamma \rho_y E - P_y} \quad (64)$$

The consolidation density  $\rho_c$  is found from an iterative solution of the Mie-Grüneisen equation with known E and  $P = P_c f(E)$ . Then, with  $\rho_s = \alpha \rho$ , Eq. (59) is a quadratic equation in  $\alpha$  and can be readily solved. With  $\alpha$  known,  $\rho_s = \alpha \rho$  is obtained, and  $P_s$  is found from the equation of state of the solid. The required pressure on the compaction surface is then  $P_s/\alpha$ , where we have now used Eq. (3) to define the average pressure in the porous material.

#### Rate-Dependent Compaction

The process of void compaction requires some time to occur. This time of compaction will appear as a rate-dependence in the constitutive relations. Several models have been proposed to represent this rate-dependence: three are incorporated here as options. Each model requires one additional parameter, a time constant.

All three have been constructed here in a common form, the one suggested by Herrmann.<sup>24</sup> The volume change is separated into three components as follows

$$\frac{dV}{dt} = \frac{dV_s}{dt} + \frac{dV_{ve}}{dt} + \frac{dV_{vp}}{dt} \quad (65)$$

where  $dV_s$  is the change in solid volume

$dV_{ve}$  is the elastic change in pore volume

$dV_{vp}$  is the plastic change in pore volume.

The plastic change in pore volume is rate dependent and not elastically recoverable on unloading. For instantaneous loads, only elastic changes occur. For low rate loads, a large amount of volume change may be taken plastically. For intermediate loads, the volume change is partly elastic and partly plastic. The foregoing process matches exactly the behavior usually assumed for rate-dependent shear deformation.

#### Butcher's $P$ - $\alpha$ - $\tau$ Model

To account for the rate-dependent effects that Butcher<sup>7</sup> observed in the compaction of polyurethane foam, he proposed a rate-dependent model in which the dynamic pressure could exceed the static for short duration loads. He proposed the following relation between the dynamic overpressure  $P - P_{st}$  and the rate of change of distension  $d\alpha/dt$ .

$$\frac{d\alpha}{dt} = \frac{d\alpha_e}{dt} + \frac{d\alpha_e}{dP} \left( \frac{P - P_{st}}{\tau} \right) \quad (66)$$

where  $\alpha_e$  is the value of  $\alpha$  for purely elastic compaction

$P_{st}$  is the pressure on the rate-independent compaction surface

$\tau$  is a time constant and  $\partial\alpha_e/\partial P$  is taken along a loading path.

Rate-dependent effects can occur whenever the pressure computed on an elastic basis exceeds the pressure on the compaction surface,  $P_{st}$ . The pressures involved in the compaction process are shown on the  $P$ - $V$  diagram

of Figure 14. The dynamic pressure  $P$  can be approximated as the following function of  $\alpha$ .

$$P = P_{st} + \frac{\alpha - \alpha_{st2}}{\alpha_e - \alpha_{st2}} (P_e - P_{st2}) \quad (67)$$

where  $\alpha_e$  and  $\alpha_{st2}$  are distension ratios corresponding to  $P_e$ , the pressure at the current density based on elastic behavior, and  $P_{st2}$ , the value of  $P_{st}$  at the current density. The derivative  $d\alpha_e/dt$  in Eq. (66) is taken as a constant for each time step  $\Delta t$ .

$$\frac{d\alpha_e}{dt} = \frac{\alpha_e - \alpha_1}{\Delta t} \quad (68)$$

It can be shown that the derivative  $d\alpha_e/dP$  in Eq. (66) is given approximately by

$$\frac{d\alpha_e}{dP} \approx \frac{\alpha_o}{K_s} \left( \alpha_o - \frac{K_s}{K_o} \right) \equiv \left( \frac{d\alpha_e}{dP} \right)_o \quad (69)$$

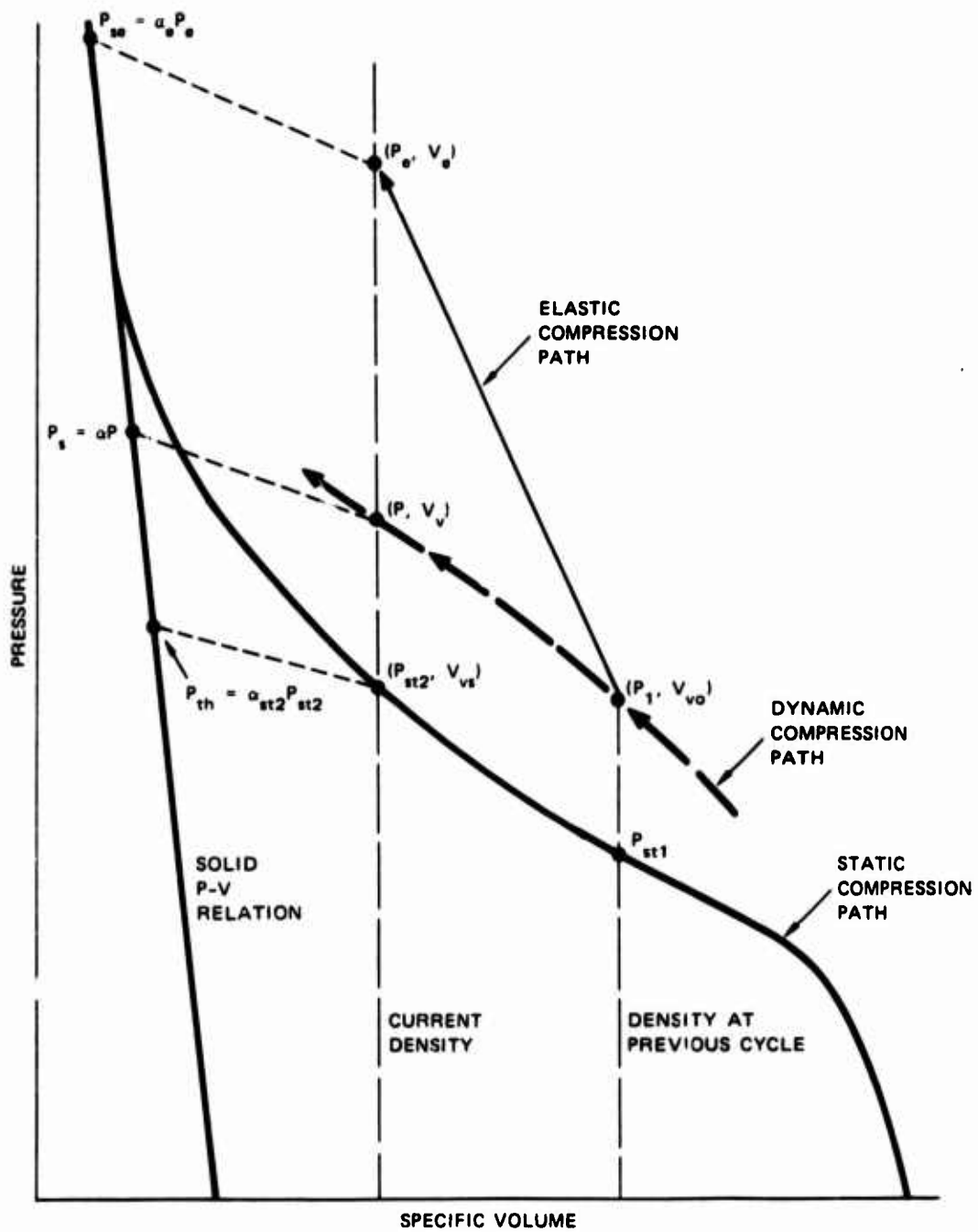
where  $(d\alpha_e/dP)_o$  is taken as a material constant. Equations (67), (68), and (69) are then substituted into Eq. (66).

$$\frac{d\alpha}{dt} = \frac{\alpha_e - \alpha_1}{\Delta t} + \frac{1}{\tau} \left( \frac{d\alpha_e}{dP} \right)_o \left( \frac{\alpha - \alpha_{st2}}{\alpha_e - \alpha_{st2}} \right) (P_e - P_{st2}) \quad (70)$$

The following value of  $\alpha$  is obtained by integrating Eq. (70) and evaluating the result at the current time.

$$\begin{aligned} \alpha = & \left[ \frac{\tau}{\Delta t} \left( \frac{\alpha_e - \alpha_{st2}}{P_e - P_{st2}} \right) \left( \frac{\alpha_e - \alpha_1}{(d\alpha_e/dP)_o} \right) - \alpha_{st2} + \alpha_1 \right] \exp \left[ \frac{\Delta t}{\tau} \left( \frac{d\alpha_e}{dP} \right)_o \left( \frac{P_e - P_{st2}}{\alpha_e - \alpha_{st2}} \right) \right] \\ & + \alpha_{st2} - \frac{\tau(\alpha_e - \alpha_{st2})}{\Delta t(P_e - P_{st2})} \frac{\alpha_e - \alpha_1}{(d\alpha_e/dP)_o} \end{aligned} \quad (71)$$

This result indicates that  $\alpha$  approaches  $\alpha_{st2}$  as  $\tau$  goes to zero, and  $\alpha$  approaches  $\alpha_e$  as  $\tau$  goes to infinity, as required.



MA-2407-12

FIGURE 14 PRESSURE-VOLUME DIAGRAM FOR POROUS MATERIAL SHOWING STATIC, ELASTIC, DYNAMIC COMPRESSION PATHS



### Holt's Model for Rate-Dependent Compaction

Holt<sup>2</sup> introduced a rate-dependence that is a function of the difference between the current distension and the equilibrium distension at the same density:

$$\alpha = \alpha_s - \tau \frac{d\alpha}{dt} \quad (72)$$

where  $\alpha_s$  is the value of  $\alpha$  for the density  $\rho$  on the static compaction surface, and  $\tau$  is a time constant. This form contains the assumption that there is no elastic change in  $\alpha$  associated with changes in density. When this elastic change is included and the equation rearranged, the result is

$$\frac{d\alpha}{dt} = \frac{d\alpha_e}{dt} - \frac{\alpha - \alpha_{st}}{\tau} \quad (73)$$

where  $d\alpha_e/dt$  is the elastic change. Here  $d(\alpha - \alpha_e)/dt$  is the rate of inelastic change in  $\alpha$  and is proportional to the difference between  $\alpha$  and  $\alpha_{st}$ . Thus the rate goes to zero as  $\alpha$  approaches  $\alpha_{st}$ . To integrate Eq. (73), it is assumed that  $d\alpha_e/dt$  is a constant, as in Eq. (68), and that  $\alpha_{st}$  varies linearly with time from  $\alpha_{st1}$  to  $\alpha_{st2}$ . Then Eq. (73) takes the form

$$\frac{d\alpha}{dt} = \frac{\alpha_e - \alpha_1}{\Delta t} - \frac{\alpha}{\tau} + \frac{1}{\tau} \left[ \alpha_{st1} + (\alpha_{st2} - \alpha_{st1}) \frac{t}{\Delta t} \right] \quad (74)$$

The solution to Eq. (74) evaluated at the current time, is

$$\begin{aligned} \alpha = & \frac{\tau}{\Delta t} (\alpha_e - \alpha_1) + \alpha_{st2} - \frac{\tau}{\Delta t} (\alpha_{st2} - \alpha_{st1}) \\ & + \left[ \alpha_1 - \frac{\tau}{\Delta t} (\alpha_e - \alpha_1) - \alpha_{st1} + \frac{\tau}{\Delta t} (\alpha_{st2} - \alpha_{st1}) \right] \exp(-\Delta t/\tau) \end{aligned} \quad (75)$$

For small values of  $\Delta t/\tau$ ,  $\alpha \cong \alpha_e$ , while for large values of  $\Delta t/\tau$ ,  $\alpha \cong \alpha_{st2}$ ; hence the physical requirements are met.

From a comparison of Eqs. (66) and (73), Holt's model appears to have a completely different physical basis from Butcher's. However, similarity in the model can be demonstrated by placing Eq. (69) into Eq. (66) and equating the right hand side to the right hand side of Eq. (73).

$$\frac{d\alpha}{dt} = \frac{d\alpha_e}{dt} + \frac{\alpha_e - \alpha_1}{P_e - P_1} \cdot \frac{P - P_{st}}{\tau_B} = \frac{d\alpha_e}{dt} - \frac{\alpha - \alpha_{st}}{\tau_H} \quad (76)$$

where  $\tau_B$  and  $\tau_H$  are time constants for Butcher's and Holt's models. The time constants of the two models are related as follows

$$\frac{\tau_B}{\tau_H} = - \frac{\alpha_e - \alpha_1}{P_e - P_1} \cdot \frac{P - P_{st}}{\alpha - \alpha_{st}} = \frac{\frac{d\alpha_e}{dP}}{\left(\frac{\partial\alpha}{\partial P}\right)_\rho} \quad (77)$$

which is obtained from Eq. (76). The two derivatives may be evaluated approximately:

$$\frac{d\alpha_e}{dP} \cong \frac{\alpha\rho_{so}}{K_s \rho} - \frac{\alpha\rho_{o1}}{K_1 \rho} \cong \frac{\alpha^2}{K_s} - \frac{\alpha}{K_1} \quad (78a)$$

and

$$\left(\frac{\partial\alpha}{\partial P}\right)_\rho \cong \frac{\alpha\rho_{so}}{K_s \rho} \cong \frac{\alpha^2}{K_s} \quad (78b)$$

With the foregoing values of the derivatives, the relationship between the time constants is

$$\frac{\tau_B}{\tau_H} \cong \frac{K_s}{K_1 \alpha} - 1 \quad (79)$$

If  $K_1 \alpha$  were nearly constant, then the two models would be equivalent. Generally  $\tau_H$  will be much larger than  $\tau_B$  for the same material. We note that for  $K_1 = K_s / \alpha$ , the Butcher model provides no rate dependence.

### Linear Viscous Void Compaction

The linear viscous void compaction model is derived from the work of Berg<sup>25</sup> and Poritsky,<sup>26</sup> and from our observations of void growth. For this model it is presumed that the material surrounding the void follows a linear viscous law with a coefficient of viscosity  $\eta$ . Then, neglecting inertial and surface tension effects, the rate of change of unrecoverable relative void volume is

$$\frac{dv_{vp}}{dt} = - \frac{3(P_s - P_{th})}{4\eta} v_v \quad (80)$$

Thus the rate of plastic void collapse is dependent on the dynamic overpressure,  $P_s - P_{th}$ , acting in the solid material, and on the current void volume. With the presumption that pressures vary linearly during the time increment, Eq. (80) can be integrated to obtain

$$v_{vp} = v_{vo} \exp \left[ - \frac{3\Delta t}{8\eta} (P_s - P_{th} + P_{so} - P_{tho}) \right] \quad (81)$$

where  $v_{vo}$  is the relative void volume at the beginning of the time increment

$P_s, P_{so}$  are pressures in the solid material at the end and beginning of the increment

$P_{th}, P_{tho}$  are the threshold pressures for growth at the end and beginning of the increment.

The elastic void volume change occurs because of a change in pressure from  $P_{so}$  to  $P_s$ . The elastic modulus associated with this change is the one governing the void volume change from  $P_{so}$  to  $P_{se}$ . Therefore, this elastic change in void volume is

$$\Delta V_{ve} = \frac{P_s - P_{so}}{P_{se} - P_{so}} (V_{ve} - V_o v_{vo}) \quad (82)$$

where  $v_e$  and  $v_{vo}$  are the relative void volumes associated with the pressures  $P_{se}$  and  $P_{so}$ , and  $V$  and  $V_o$  are gross specific volumes.

For the model calculations, the pressure is determined by requiring the elastic and plastic void volume change and the solid volume change to match the total volume change as in Eq. (65). The plastic volume change follows Eq. (81).

The solid volume change is presumed to be linearly related to the solid pressures at the current gross density.

$$V_s = V_{sth} + (V_{se} - V_{sth}) \frac{P_s - P_{th}}{P_{se} - P_{th}} \quad (83)$$

where  $V_{sth}$  and  $V_{se}$  are solid specific volumes corresponding to  $P_{th}$  and  $P_{se}$ . When Eqs. (81), (84), and (83) are inserted into Eq. (65), the following results.

$$\begin{aligned} \Delta V = & V_{sth} + (V_{se} - V_{sth}) \frac{P_s - P_{th}}{P_{se} - P_{th}} - V_{so} + \frac{P_s - P_{so}}{P_{se} - P_{so}} (V_e - V_o v_{vo}) \\ & + v_{vo} V \left\{ \exp \left[ \frac{T_1 \Delta t}{2} (P_s - P_{th} + P_{so} - P_{tho}) \right] - 1 \right\} \end{aligned} \quad (84)$$

where  $T_1 = -3/(4\eta)$ , the growth coefficient.

Eq. (84) is then solved by iteration to determine  $P_s$ . The first approximation is obtained by assuming that  $P_s - P_{th}$  are approximately equal to  $P_{so} - P_{tho}$ . The last term in Eq. (84) is then linearized as follows:

$$\begin{aligned} \exp \left[ \frac{T_1 \Delta t}{2} (P_s - P_{th} + P_{so} - P_{tho}) \right] & \approx \exp \left[ T_1 \Delta t (P_{so} - P_{tho}) \right] \times \\ \left[ 1 + \frac{T_1 \Delta t}{2} (P_s - P_{th} - P_{so} + P_{tho}) \right] & \end{aligned} \quad (85)$$

The resulting equation is then solved for  $P_s = P'_s$ , the first approximation. With  $P'_s$  in Eq. (84), a value of  $\Delta V = \Delta V'$  is obtained. The second iteration begins with a linearization as in Eq. (85) based on the assumption that there is a small difference between  $P_s$  and  $P'_s$ .

The foregoing iteration scheme works best for small changes in density. Therefore, a provision is made for subcycling in cases where large changes in density occur in a single time step.

#### Discussion of Rate-Dependent Models

All three of the foregoing models were derived to fit observed pore volume change data, and they were cast in a form like the modified Maxwell element proposed by Zener<sup>13</sup> for shear stress relaxation. But in fact, do any of these models really represent dynamic pore collapse in a solid with a stress relaxation like the Maxwell model? This question can be answered by a recent analysis of Carroll<sup>27</sup> in which he treated spherically symmetric void compaction in such a solid. The equation of motion he obtained for the combination of void and solid material is

$$P = P_{st}(\alpha) + Q(\ddot{\alpha}, \dot{\alpha}, \alpha) - \frac{4\eta\dot{\alpha}}{3\alpha(\alpha - 1)} \quad (86)$$

where  $P$  is the external pressure and  $Q$  is an acceleration term that might be neglected in a macroscopic model. Since the material is treated as rigid-plastic, no elastic term appears. Comparing Eq. (86) with Butcher's model in Eq. (54) and neglecting  $Q$  and the elastic term in (54), we see that the time constant  $\tau$  must be given by

$$\frac{\tau dP}{d\alpha_e} = \frac{4\eta}{3\alpha(\alpha - 1)} \quad (87)$$

Thus  $dP/d\alpha_e$  must be given a special form for  $\tau$  to remain constant.

The usual form for the linear viscous model can be derived from Eq. (86) by replacing  $\alpha$  with  $v_v$  through the aid of Eq. (6). The resulting

expression, neglecting  $Q$ , is

$$P = P_{st} - \frac{4\eta\dot{v}_v}{3v_v} \quad (88)$$

which is equivalent to Eq. (80) for rigid-plastic behavior with the solid pressure equal to the porous pressure. Thus the linear viscous model used here has the correct physical form for describing pore collapse in elastic-plastic material from initial yielding to full compaction.

#### Rate-Independent Fracture Surface

The fracture surface is defined in  $P$ - $V$ - $E$  space in the same way as the compaction surface. The shape is similar to the compaction (yield) surface shown in Figure 2: the ordinate increases in the tensile sense with density, and decreases with increasing internal energy. A curve on the surface is shown in Figure 8. The intercept of the surface with the solid equation of state determines the threshold pressure for fracture of solid material. All other points define thresholds for porous or partially fractured material. The surface is assumed to be unique so, for a given  $(\rho, E)$  state, the behavior is the same whether the porosity results from fracture or from the manufacturing process. Two options are provided for treating this surface. In the constant strength option, the threshold pressure in the solid material ( $P_s$ ) is taken as a function of internal energy only. Then the threshold pressure  $P$  in the porous material decreases with increasing  $\alpha$ , because  $P = P_s/\alpha$ . The second option is the Carroll-Holt<sup>3</sup> model, which is also used in compression. The algebra of this model is handled as described earlier.

#### Rate-Dependent Fracture

Fracture occurs gradually through the nucleation and growth of small voids or cracks. Because these processes require time, a rate-dependent relationship should be used for dynamic calculations. Currently the PEST

subroutine contains the SRI model for ductile fracture.<sup>8</sup>

The ductile fracture model fits naturally into the PEST subroutine because they are both concerned with pressure and not with deviator stress. The ductile fracture model has been described in detail elsewhere<sup>8</sup> and is simply summarized here.

The nucleation rate is given by the expression

$$\dot{N} = \dot{N}_0 \exp\left(\frac{P_s - P_{th}}{P_{nl}}\right) \quad (89)$$

where  $P_{th}$  is the threshold pressure in the solid material required to permit nucleation. The corresponding pressure on the rate-dependent surface is  $P_{st} = P_{th}/\alpha$ .

$P_{nl}$  is a parameter governing the sensitivity of the material to nucleation.

$\dot{N}_0$  is a nucleation rate constant.

The voids are presumed to be nucleated according to a distribution:

$$N_g(R) = \dot{N} \Delta t \exp(-R/R_n) \quad (90)$$

where  $N_g$  is the number of voids per unit volume larger than  $R$

$R_n$  is a nucleation distribution parameter

$\Delta t$  is the time increment.

By integrating with respect to  $R$  over the entire distribution, we obtain a nucleated void volume

$$\begin{aligned} \Delta v_n &= 6 \cdot \frac{4}{3} \pi R_n^3 \dot{N} \Delta t \\ &= 8 \pi R_n^3 \dot{N}_0 \Delta t \exp\left(\frac{P_s - P_{th} + P_{so} - P_{tho}}{2 P_{nl}}\right) \end{aligned} \quad (91)$$

Here  $P_{th}$  and  $P_{tho}$  are threshold pressures at the end and beginning of the time increment.

The void growth rate is given by

$$\dot{v}_v = - \frac{3(P_s - P_{th})}{4\eta} v_v \quad (92)$$

where  $P_{th}$  is the threshold pressure for growth. There is no theoretical justification for using solid pressure rather than gross pressure in Eq. (92). However, use of the solid pressure permits fracture to continue to full separation rather than being quenched when the pressures are low. Thus this form is used until more is learned about the late stages of fracture.

The solution for pressure in the ductile fracture model proceeds as in the linear viscous void model with the addition of nucleated volume as part of the plastic void volume change. The exponential in Eq. (91) is approximated in the same manner as the growth exponential in Eq. (85).

#### Summary of Model Changes

Most of the foregoing models for porous behavior are derived from work of other investigators. The following changes were made in these models to put them into a form suitable for insertion into PEST.

- The Holt model was augmented to include elastic behavior, deviator stresses and the effects of internal energy. Also the static P-V curve was given a different analytical form because Holt's form did not increase monotonically.
- The POREQST<sup>1</sup> was improved to provide a more rigorous treatment of the intermediate surfaces.
- The Carroll-Holt<sup>3</sup> model was expanded to include elastic behavior, deviator stress, and thermal effects.
- Herrmann's<sup>5</sup>  $P - \alpha$  model was recast as a  $\rho_s - \alpha$  model, and changes were made for elastic and thermal behavior.



- Butcher's<sup>7</sup> model was modified to include thermal effects and deviator stresses. Also the treatment of elastic behavior was altered slightly, and the relation between pressure in the solid and porous material was changed from  $P_s = P$  to  $P_s = \alpha P$ .
- The dynamic fracture model was altered to permit elastic behavior of the pore volume. Previously the void volume was allowed to change only by viscous growth and not by elastic expansion.

### III EQUATION OF STATE FOR SOLID MATERIALS

In hydrodynamic calculations, the equation of state provides the pressure as a function of internal energy and specific volume. (In a complete equation of state pressure, energy, volume, temperature, and entropy are determined.) The material may be treated as solid, liquid, or vapor or in a mixed phase. In simple equations of state, such as the one used in the PUFF code,<sup>9</sup> an accurate treatment is given of the equation of state surface only in the vicinity of the Hugoniot. Since it is presumed that the material expands similarly to a perfect gas, a modified gas equation is used for expanded states. Between the Hugoniot and the highly expanded states, a fitting function is used. For computer calculations to follow wave propagation in a material, a choice must be made between the simple and sophisticated types of equation of state. The sophisticated equations of state may require much more data than are available. Even if available, these data are normally procured at static testing rates, and therefore the data and possibly the form of the equation of state are inappropriate at shock loading rates. Although the simple equation of state provides little insight into the detailed behavior of the material, it has the advantage of containing only a few parameters that must be varied to match the experimental data.

In the current SRI PUFF wave propagation code, three equation-of-state options for solids are provided. The first is the usual PUFF equation of state: a combination of the Mie-Grüneisen form for compressed states and the PUFF expansion relation for expanded states. As a second option, an extended version of this PUFF equation of state was constructed and incorporated into a subroutine ESA. This new equation of state adds some flexibility in fitting dynamic and thermal data. The third option is the three-phase equation of state constructed by Philco-Ford and implemented in the subroutine EQSTPF. The ESA and EQSTPF options are described here and listed in more detail in Appendices D and C.

### Extended Two-Phase Equation of State: ESA

The ESA equation-of-state model constructed here is intended to simulate approximately the more complex surfaces of the multiphase equations of state while retaining enough simplicity that its parameters can provide a match to experimental data. Specifically the new model should provide the following three features;

- (1) Variable Grüneisen ratio as a function of energy and density.
- (2) A nonlinear variation of pressure with energy at constant density.
- (3) An approximate simulation of unloading isentropes of the multiphase equations of state.

The ESA equation-of-state model is constructed in the following way. A Mie-Grüneisen form is adopted for compression, and terms are added for varying the Grüneisen ratio and producing the nonlinearity in internal energy. For the expanded states, the forms used are similar to those used in the compression states for varying Grüneisen ratio and internal energy. In addition, a series expansion is made in density. As with the PUFF equation of state, the expansion and compression forms are joined at the initial solid density. At that density the pressure must be equal in the two forms and the derivative  $DP/D\rho$  must be equal from both expressions. Additional constants in the expansion equation of state are evaluated by requiring that the equation of state surface pass through given pressure, density, energy state points. Such state points might be the zero pressure melt point, a boiling point, and a critical point. Or one or two of them might lie on an unloading isentrope obtained from experimental data or from a multiphase equation-of-state calculation.

For compressed states, that is, states where the density is greater than the initial solid density, a modified form of the Mie-Grüneisen equation of state is used. The following form was adopted:

$$P = (C\mu + D\mu^2 + S\mu^3) \left( 1 - \frac{\Gamma_0\mu}{2} - \frac{\Gamma_1\mu^2}{2} \right) + (\Gamma_0 + \Gamma_1\mu)\rho E + (F_1 + F_2\mu) E^2 \quad (93)$$

where C, D, S are usual Hugoniot coefficients

$\mu = \rho/\rho_0 - 1$  is strain

$\rho$  is density

$\rho_0$  is initial density

$\Gamma_0, \Gamma_1$  are Grüneisen coefficients

$F_1, F_2$  are constants for nonlinear energy effect

E is internal energy.

In Equation (93),  $\Gamma_0$  is the usual Grüneisen ratio,  $\Gamma_1$  describes the variations of Grüneisen ratio with density. For example, to make the factor  $\Gamma\rho$  approximately constant, let  $\Gamma_1 = -\Gamma_0$ . The derivatives of the pressure from Equation (93) are used to assure continuity with the expansion equation and to determine the sound speed. These derivatives are

$$\begin{aligned} \left( \frac{\partial P}{\partial \rho} \right)_E &= (C + 2D\mu + 3S\mu^2) \left( 1 - \frac{\Gamma_0\mu}{2} - \frac{\Gamma_1\mu^2}{2} \right) \frac{1}{\rho_0} \\ &+ (C\mu + D\mu^2 + S\mu^3) \left( -\frac{\Gamma_0}{2} - \Gamma_1\mu \right) \frac{1}{\rho_0} \\ &+ (\Gamma_0 + \Gamma_1 + 2\Gamma_1\mu) E + \frac{F_2 E^2}{\rho_0} \end{aligned} \quad (94)$$

$$\left(\frac{\partial P}{\partial E}\right)_\rho = (\Gamma_0 + \Gamma_1 \mu) \rho + 2(F_1 + F_2 \mu) E \quad (95)$$

The equation of state for expanded material, that is, for  $\rho$  less than  $\rho_0$  is:

$$P = \rho(g_0 + g_1 \rho)E + \rho(h_0 + \rho h_1)E^2 + (\rho - \rho_0)(b_0 + b_1 \rho + b_2 \rho^2 + b_3 \rho^3) \quad (96)$$

where  $g_0, g_1, h_0, h_1, b_0 \dots b_3$  are constants.

In equation (96) all the terms are written as functions of  $\rho$  rather than  $\mu$  as in the compression equation of state. The  $\rho$  form is used so that as  $\rho$  approaches 0, the nonlinear terms in  $\rho$  will disappear and the equation approaches the perfect gas form  $P = \rho \Gamma E$ .

For use in the sound speed calculations which are given later, the two derivatives of Equation (96) are listed:

$$\begin{aligned} \left(\frac{\partial P}{\partial \rho}\right)_E &= (g_0 + 2g_1 \rho)E + (h_0 + 2h_1 \rho)E^2 \\ &+ (b_0 + b_1 \rho + b_2 \rho^2 + b_3 \rho^3) + (\rho - \rho_0)(b_1 + 2b_2 \rho + 3b_3 \rho^2) \end{aligned} \quad (97)$$

$$\left(\frac{\partial P}{\partial E}\right)_\rho = \rho(g_0 + g_1 \rho) + 2\rho(h_0 + \rho h_1)E \quad (98)$$

A smooth joint at  $\rho = \rho_0$  is produced between the compression and expansion equations of state by requiring that the pressures and the derivative of pressure with respect to density are equal at  $\rho = \rho_0$ . For making this joint calculation it is presumed that all the parameters of the compression equation of state are known and that the joint requirements serve to evaluate some of the expansion parameters. With this

approach and the use of Eqs. (93), (94), (96), and (97), we obtain the following conditions:

$$\begin{aligned}
 g_0 &= \Gamma_0 - \Gamma_1 \\
 g_1 &= \frac{\Gamma_1}{\rho_0} \\
 h_0 &= \frac{1}{\rho_0} (2F_1 - F_2) \\
 h_1 &= \frac{1}{2\rho_0} (F_2 - F_1) \\
 (b_0 + b_1\rho_0 + b_2\rho_0^2 + b_3\rho_0^3) &= \frac{C}{\rho_0}
 \end{aligned} \tag{99}$$

Evidently three more conditions can be imposed to evaluate the  $b$  terms in the expansion equation of state. The conditions we wish to impose are that the expansion equation of state surface pass through three state points identified as follows:

$$(P_1, \rho_1, E_1), (P_2, \rho_2, E_2), \text{ and } (P_3, \rho_3, E_3)$$

For convenience in evaluating the  $b$  terms in the expansion equation of state, we introduce a new variable  $R$ , which is simply the contribution of the  $b$  terms to the pressure in Eq. (96).

$$\begin{aligned}
 R &= P - \rho(g_0 + g_1\rho)E - \rho(h_0 + \rho h_1)E^2 \\
 &= (\rho - \rho_0)(b_0 + b_1\rho + b_2\rho^2 + b_3\rho^3)
 \end{aligned} \tag{100}$$

The solution for the b coefficients can now be obtained by inspection by rewriting R in the following expanded form:

$$\begin{aligned}
 R = & \frac{A_0 (\rho - \rho_0)(\rho - \rho_1)(\rho - \rho_2)(\rho - \rho_3)}{(\rho_0 - \rho_1)(\rho_0 - \rho_2)(\rho_0 - \rho_3)} \\
 & + \frac{A_1 (\rho - \rho_0)^2 (\rho - \rho_2)(\rho - \rho_3)}{(\rho_1 - \rho_0)^2 (\rho_1 - \rho_2)(\rho_1 - \rho_3)} \\
 & + \frac{A_2 (\rho - \rho_0)^2 (\rho - \rho_1)(\rho - \rho_3)}{(\rho_2 - \rho_0)^2 (\rho_2 - \rho_1)(\rho_2 - \rho_3)} \\
 & + \frac{A_3 (\rho - \rho_0)^2 (\rho - \rho_1)(\rho - \rho_2)}{(\rho_3 - \rho_0)^2 (\rho_3 - \rho_1)(\rho_3 - \rho_2)}
 \end{aligned} \tag{101}$$

where the  $A_i$  are constants to be determined. The constants are evaluated from the following observations:

$$R = 0 \quad \text{at} \quad \rho = \rho_0$$

$$R = A_i \quad \text{at} \quad \rho = \rho_i \quad \text{for} \quad i = 1, 2, 3$$

$$\frac{dR}{d\rho} = A_0 \quad \text{at} \quad \rho = \rho_0 \tag{102}$$

By comparing the conditions in Eqs. (102) with Eq. (100) we can evaluate the constants as follows:

$$A_0 = \frac{C}{\rho_0} \tag{103}$$

$$A_i = P_i - \rho_i (g_0 + g_1 \rho_i) E_i - \rho_i (h_0 + h_1 \rho_i) E_i^2 \quad i = 1, 2, 3$$

Thus a complete solution is now available for all the constants in the expansion equation of state. However, for the computer calculations it will be expedient to evaluate the  $b$  terms from the  $A_i$  terms. This evaluation is performed in two steps: first, multiply all the factors in the numerators of Eq. (101) to obtain series expressions in  $\rho$ . For convenience the following definitions are made:

$$a_0 = \frac{A_0}{(\rho_0 - \rho_1)(\rho_0 - \rho_2)(\rho_0 - \rho_3)}$$

$$a_i = \frac{A_i}{(\rho_i - \rho_0)^2(\rho_i - \rho_j)(\rho_i - \rho_k)} \quad \begin{array}{l} i = 1, 2, 3 \\ i \neq j \neq k \end{array} \quad (104)$$

Now when the expanded terms are collected into a single series in  $\rho$ , the  $b$  terms can be evaluated as follows:

$$b_0 = -a_0\rho_1\rho_2\rho_3 - a_1\rho_0\rho_2\rho_3 - a_2\rho_0\rho_1\rho_3 - a_3\rho_0\rho_1\rho_2$$

$$b_1 = \rho_0\rho_1(a_2 + a_3) + \rho_0\rho_2(a_1 + a_3) + \rho_0\rho_3(a_1 + a_2) \\ + \rho_1\rho_2(a_0 + a_3) + \rho_1\rho_3(a_0 + a_2) + \rho_2\rho_3(a_0 + a_1)$$

$$b_2 = -\rho_0(a_1 + a_2 + a_3) - \rho_1(a_0 + a_2 + a_3) \\ - \rho_2(a_0 + a_1 + a_3) + \rho_3(a_0 + a_1 + a_2)$$

$$b_3 = a_0 + a_1 + a_2 + a_3 \quad (105)$$



Besides computing pressure, the equation-of-state subroutine in a wave propagation computer code is often required to compute sound speed. For the present calculations the sound speed referred to is the bulk sound speed, dependent only on the pressure term. The square of the sound speed is given as the derivative of pressure with density along an isentrope and has the following form:

$$c^2 = \left( \frac{\partial P}{\partial \rho} \right)_s = \left( \frac{\partial P}{\partial \rho} \right)_E + \frac{P}{\rho^2} \left( \frac{\partial P}{\partial E} \right)_\rho \quad (106)$$

Since the present equation-of-state model does not include entropy, the first form for the sound speed cannot be evaluated. However, the sound speed can be determined from the other two derivatives; these are given in Eqs. (94), (95), (97), and (98).

#### Philco-Ford Equation of State

The Philco-Ford model<sup>10</sup> is a three-phase equation of state for metals. It was selected for the present project because it appeared to provide enough flexibility that it could be applied to ceramics and other nonmetals. This equation of state was incorporated into a subroutine described by Goodwin, et al. Our subroutine is organized very differently from Goodwin's, but the equation of state is not modified. This equation of state is described in some detail here because of the unavailability of Goodwin's report.

This model treats specifically the solid, liquid, and vapor phases, mixed liquid-vapor and solid-liquid phases, and the phase boundaries. These regions are shown in Figure 15. The solid phase is handled by a Mie-Grüneisen equation of state. The pressure-volume-temperature relation for the solid-liquid mixed phase is the Clapeyron equation. In addition it is assumed that the following ratio is independent of temperature.

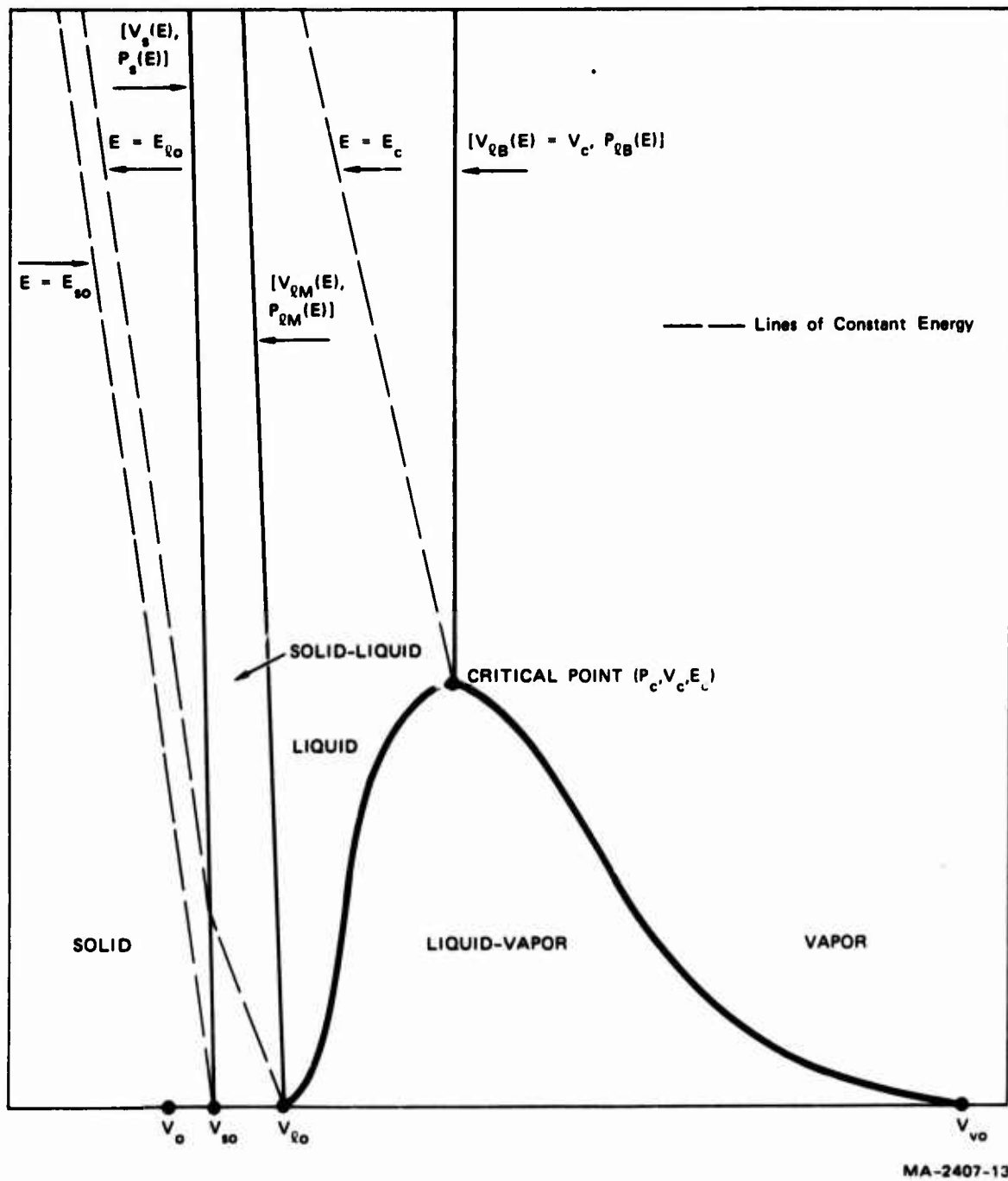


FIGURE 15 PRESSURE-VOLUME DIAGRAM SHOWING PHASES AND PHASE BOUNDARIES OF THE PHILCO-FORD EQUATION OF STATE

$$\frac{E_{\ell}(T) - E_s(T)}{V_{\ell}(T) - V_s(T)} = \frac{\Delta E_o}{\Delta V_o} \quad (107)$$

Here  $E_{\ell}$  and  $E_s$  are internal energies in liquid and solid.

$V_{\ell}$  and  $V_s$  are specific volume of liquid and solid, all defined at the same temperature.

$\Delta E_o$  is approximately equal to the heat of fusion at zero pressure.

$\Delta V_o$  is the volume change from solid to liquid at zero pressure.

Then the Clapeyron equation takes the form

$$P(T) = \frac{\Delta E_o}{\Delta V_o} \left( \frac{T}{T_M} - 1 \right) \quad (108)$$

where  $T$  and  $T_M$  are temperature and temperature of melting. The internal energies  $E_{\ell}$  and  $E_s$  in the liquid and solid phases in the mixed phase region are computed from the following relations

$$E_{\ell} = E_{\ell o} + \bar{C} T_M (T/T_M - 1) - \frac{\Delta C T_M}{2} (T_M/T - 1) \quad (109)$$

$$E_s = E_{s o} + \bar{C} T_M (T/T_M - 1) + \frac{\Delta C T_M}{2} (T_M/T - 1) \quad (110)$$

where  $E_{\ell o}$  and  $E_{s o}$  are internal energies at zero pressure on the phase lines on either side of the solid-liquid region.

$\bar{C}$  is the average specific heat at constant pressure in solid and liquid phases.

$\Delta C$  is the difference between liquid and solid specific heats.

The phase line between solid and mixed solid-liquid phases is obtained by equating pressures in the two regions at the same density and internal energy. The phase line between the liquid and the mixed solid-liquid phases is determined by computing the point where the solid fraction of material just reaches zero.

The liquid phase equation of state is simply an interpolation function between the phase lines on either side. The interpolation is a combined linear and logarithmic function of density along lines of constant internal energy.

The phase line between liquid and more expanded states is given by the Hirschfelder relation up to the critical point.

$$\frac{\rho_l}{\rho_c} = 1 + c_1 \left(1 - \frac{T}{T_M}\right)^{1/3} + d_1 \left(1 - \frac{T}{T_M}\right) \quad (111)$$

where  $\rho_l$  is the density in the liquid phase

$\rho_c$  is the density at the critical point

$T$  and  $T_M$  are variable temperature and melting temperature

$c_1$  and  $d_1$  are material constants.

Above the critical point the phases are divided arbitrarily by the specific volume at the critical point. The pressure in the mixed liquid-vapor phase is given by a modification of the Clapeyron equation.

$$\ln \frac{P}{P_c} = (\alpha_a - \alpha_b) \left(1 - \frac{T}{T_M}\right) + \alpha_b \ln \frac{T}{T_M} \quad (112)$$

where  $P$  and  $P_c$  are pressure and pressure at the critical point

$\alpha_a$  and  $\alpha_b$  are material constants.

The internal energies  $E_v$  and  $E_l$  in vapor and liquid states in the mixed-phase region are given by

$$E_v = E_o + C_v T - Z_c R T_c \left[ (k_o + 2k_1 T_c/T) \frac{\rho_v}{\rho_c} - \frac{k_2 T_c}{T} \left(\frac{\rho_v}{\rho_c}\right)^2 \right] \quad (113)$$

$$E_l = E_v - Z_c R T_c \rho_c (V_v - V_l) \frac{P}{P_c} \left[ \frac{(\alpha_a - \alpha_b) T_c}{T} + \alpha_b - 1 \right] \quad (114)$$

where  $E_0$  is the internal energy of ideal gas at zero temperature

$C_v$  is specific heat of vapor of constant volume

$Z_c = P_c V_c / RT_c$ , nonideal gas compressibility factor at critical point.

$T_c, P_c, V_c, \rho_c$  are temperature, pressure, volume, and density at critical point.

$\rho_v, V_v$  are density and specific volume of vapor

$V_\ell$  is specific volume of liquid

$k_0, k_1, k_2, \alpha_a, \alpha_b$  are constants

$R$  is the gas constant.

The pressure in the vapor state is given by a relation due to Hirschfelder, a generalization of the van der Waals equation of state.

$$P = \frac{\rho RT}{1 - b \frac{\rho}{\rho_c} + b' \left( \frac{\rho}{\rho_c} \right)^2} - a \left( \frac{\rho}{\rho_c} \right)^2 - a' \left( \frac{\rho}{\rho_c} \right)^3 \quad (115)$$

$b$  and  $b'$  are material constants

$a$  and  $a'$  are functions of  $T/T_M$ .

The phase line between vapor and mixed liquid-vapor phases is found by equating pressures in the two regions at the same internal energy and density.

The SRI subroutine incorporating the Philco-Ford model is given in Appendix C together with a description of the nomenclature and sample input data for aluminum, beryllium, and titanium.

#### IV METHODS FOR DERIVING POROUS MODEL PARAMETERS FROM DATA

To derive a set of constitutive relations for porous material it is necessary to have a quantity of material data available. The cost of data acquisition can be reduced by performing only those experiments that will provide the most important data. Several of the common sources for data and the types of data that may be obtained from them are described here. Duplicate sets of information may be obtained in many categories, but this is often necessary because of the uncertainty in the data from each source. In addition, some data may be obtained at static testing rates and room temperature, whereas the information desired would pertain to impact testing rates and near melting. In the absence of better data, however, the static, low-temperature data can be useful in guiding estimates.

With the available set of data summarized, the methods used for constructing the material model are developed. This construction proceeds in two steps. First the data are used to construct graphic forms for such functions as the compaction curve and the thermal strength reduction factor. When all the necessary functions have been constructed, a set of mathematical models describing each aspect of the constitutive relations for porous materials is selected, and the parameters for these models are chosen by fitting them to the appropriate functions.

##### Data Sources

For most materials, some handbook data are available for solid and possibly for porous material. The thermal expansion coefficient for the solid material aids in constructing the intermediate surface for the porous material and guides the selection of the Grüneisen ratio for solid and porous material. The bulk modulus aids in constructing the intermediate surface and also in reducing Hugoniot data into separate pressure and deviator stress components. The Grüneisen ratio and Hugoniot parameters for the solid are indispensable in constructing the equation of state for the

porous and solid material. Sound speeds and the Poisson ratio can be helpful in determining shear and bulk moduli from Hugoniot data. The shear modulus is also helpful in interpreting Hugoniot data. Thermal strength reduction information is usually available from slow testing-rate experiments and can give a lower bound on the true thermal strength reduction factor for dynamic experiments. The yield strength can aid in interpreting Hugoniot data and in providing fracture parameters for porous and solid materials.

Quasi-static one-dimensional compression experiments are often conducted on porous materials to obtain the crush curve, that is, a loading line across the compaction surface in energy-pressure-volume space. If intermediate unloading and reloading occur during the compression experiment, bulk moduli may be obtained to aid in determining the intermediate surfaces for the porous material. If lateral stresses are measured as well as axial stresses, an indication of the magnitude of the deviator stress is obtained.

Impact experiments can provide loading and unloading paths and the equation-of-state surface for the solid and the constitutive relations for the porous material at the appropriate testing rates and temperatures. If multiple embedded gages are used and a Lagrangian analysis is performed on the resulting stress or velocity records, unloading moduli may be obtained for construction of the intermediate surfaces of the porous material. If a Lagrangian analysis is not performed, it will be necessary to construct a possible set of constitutive relations and then simulate the experiment with a wave propagation computer program. If the computed stress or velocity histories match the experimental results closely enough, it is assumed that the constitutive relations are correct.

Electron beam and x-ray sources provide a means for nearly constant volume heating of the material; this condition allows for a study of the constitutive relations in a direction unobtainable by other means. Usually stress or velocity gages provide records at several points in the target. Impulse may also be measured. Although the measured results do not give any equation-of-state information directly, important data can be obtained by estimating the complete set of constitutive relations for the porous material and then attempting to simulate the entire experiment with a wave propagation computer program. Modifying the constitutive relations until the computed histories match the gage measurements provides evidence about the crush curve in the energy direction, the Grüneisen ratio for porous material, the moduli in the porous material, and the vapor equation of state. To guarantee that the resulting set of constitutive relations will be applicable to a wide range of behavior, the radiation data base must include experiments in which the radiation depth is both shallow and deep, and the fluence levels must range from those that cause only yielding up to those that cause significant vaporization.

#### Construction of the Constitutive Relations

Constitutive relations for a porous material are developed in two stages. First all the data are gathered, and all the necessary functions and parameters are estimated. However, much of the data, such as attenuation data and electron-beam and x-ray measurements, cannot be used directly to construct the constitutive relations. Therefore, the next stage is to use the estimated relations to simulate some of the experiments with wave propagation calculations. In this stage the initial constitutive relations are modified to provide a satisfactory match between the recorded stresses or velocities and the computed values. In the following discussion the functions required for the constitutive relations are listed and methods for making initial estimates are described.



Construction of the constitutive relations for a porous material begins with the determination of the equation of state of the corresponding solid. Hugoniot data, including the bulk modulus, solid density, and Grüneisen ratio must be available. The yield strength and shear modulus, melt energy, and sublimation energies are also necessary to give even a minimal definition to the equation of state. If experimental data are not available on the solid, estimates of some of these quantities can be made. The solid density can be estimated from the theoretical density. For example the density of  $\text{HfTiO}_4$  could be estimated by the method of mixtures from the densities of  $\text{HfO}_2$  and  $\text{TiO}_2$ . Moduli, melting, and vaporization parameters of the unknown solid may be obtained from measurements on substances from the same family. Such estimated values should not be regarded as accurate but may be sufficient for treating material that remains porous throughout the calculations.

The Grüneisen ratio should be taken from energy deposition experiments if possible. It should provide the relation between internal energy and pressure for specific volumes near the initial specific volume. Impacts may give some circumstantial evidence of Grüneisen's ratio, but only for densities and pressures that are not critical for simulating x-ray depositions. Thermal expansion and specific heat data may be combined to form a Grüneisen ratio as follows

$$\Gamma = \frac{K_s \alpha_t}{\rho_{so} C_p} \quad (116)$$

where  $C_p$  is the specific heat at constant pressure. However, this method of computing  $\Gamma$  is usually unreliable. To have any meaning, the four quantities must be known at the same pressure and temperature. If possible, Eq. (116) should be based on average values over the range of temperature of interest. Thus we recognize that  $\Gamma$ ,  $\alpha_t$ ,  $K_s$ , and  $C_p$  are not constants and that average values obtained in the temperature, pressure, and density ranges of interest must be used.

The development of constitutive relations for the porous material begins with the construction of a series of functions: a thermal expansion function, thermal strength effect, compaction curve, fracture curve (fracture strength as a function of porosity), bulk moduli as a function of porosity and energy, rate functions for pore collapse, and a deviator stress function. These functions cannot be treated independently. Normally one attempts an initial construction of each function and then modifies them slightly so that they do not conflict in their representation of a porous material. These functions are presented here in an arbitrary but possible order that might be followed in constructing the functions.

#### Thermal Expansion Functions

The thermal expansion effect, referred to in Eqs. (18) and (19) governs part of the intermediate surface construction. Usually  $\alpha_t$ , the volumetric thermal expansion coefficient, can be obtained from room temperature measurements. If possible, it is important to obtain an average value that is valid from room temperature to melting. Such a value aids in determining the Grüneisen ratio. If the energy and density at incipient melt,  $E_M$  and  $\rho_M^1$ , are available for an initial density  $\rho_O^1$ , then Eq. (20) provides the approximate result

$$\Gamma = \frac{K_s}{\rho_O^1 E_M} \left( \frac{\rho_M^1}{\rho_O^1} - 1 \right) \quad (117)$$

If this Grüneisen ratio conflicts with that in the solid equation of state, adjustments must be made based on the relative certainty of the two ratios.

#### Thermal Strength Effect

As a material is heated, its strength is usually reduced. Handbook data such as that shown in Figure 16 are often available to guide in constructing this function. The analytical function representing the strength effect is constructed from two parabolas as shown in Figure 12. The five parameters shown in the figure are two abscissas, an ordinate at the joint between the parabolas, and the midpoint distances from straight lines. These values can all be easily selected from a strength-energy curve.

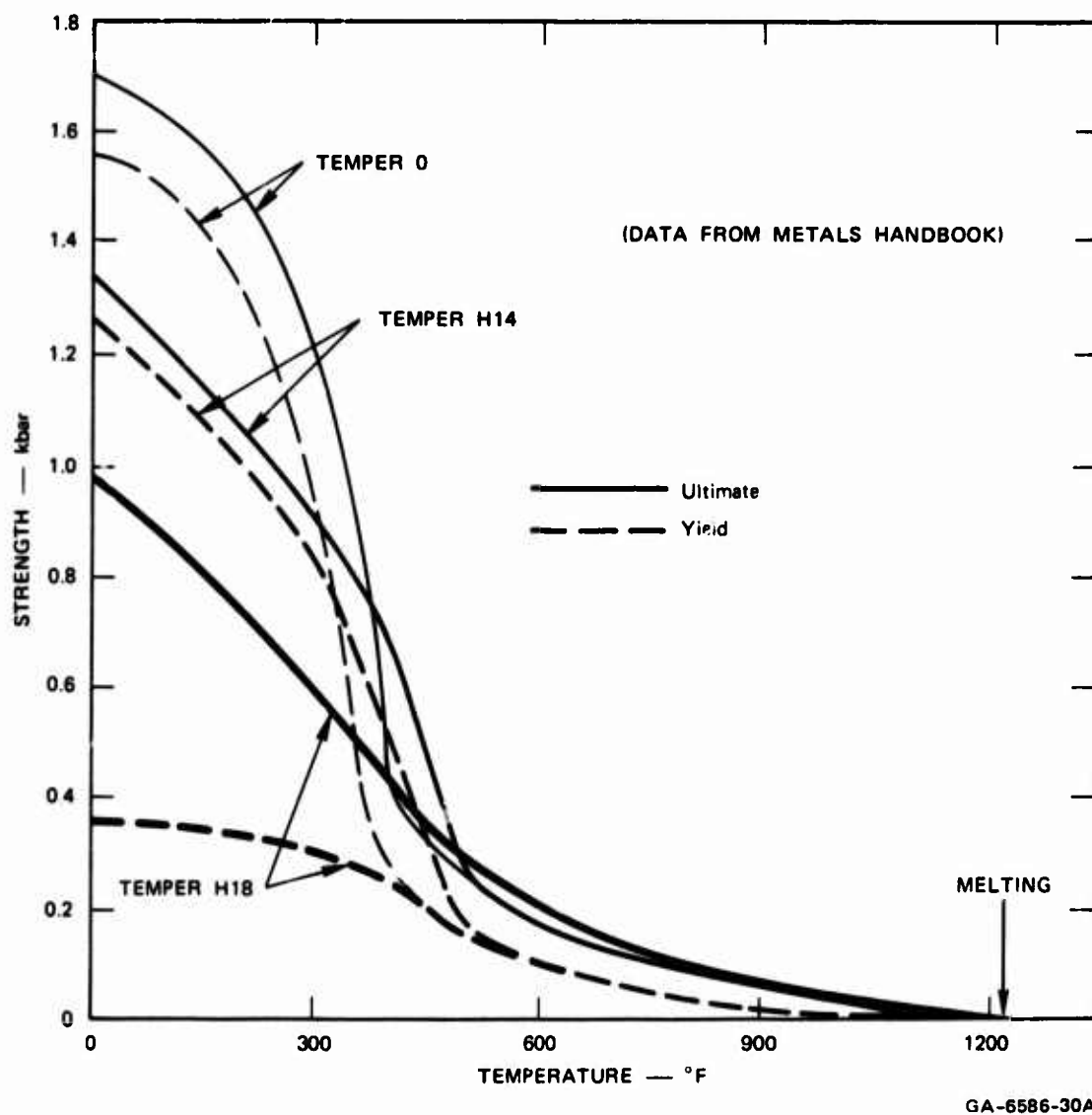


FIGURE 16 VARIATION OF STRENGTH WITH TEMPERATURE FOR 1100 ALUMINUM: EXAMPLES OF THERMAL STRENGTH REDUCTION FUNCTIONS

If a set of electron-beam data, such as that of Shea et al.<sup>28</sup> on copper, is available, it should be used. These data have the advantage of representing the heating rate and loading durations of most interest.

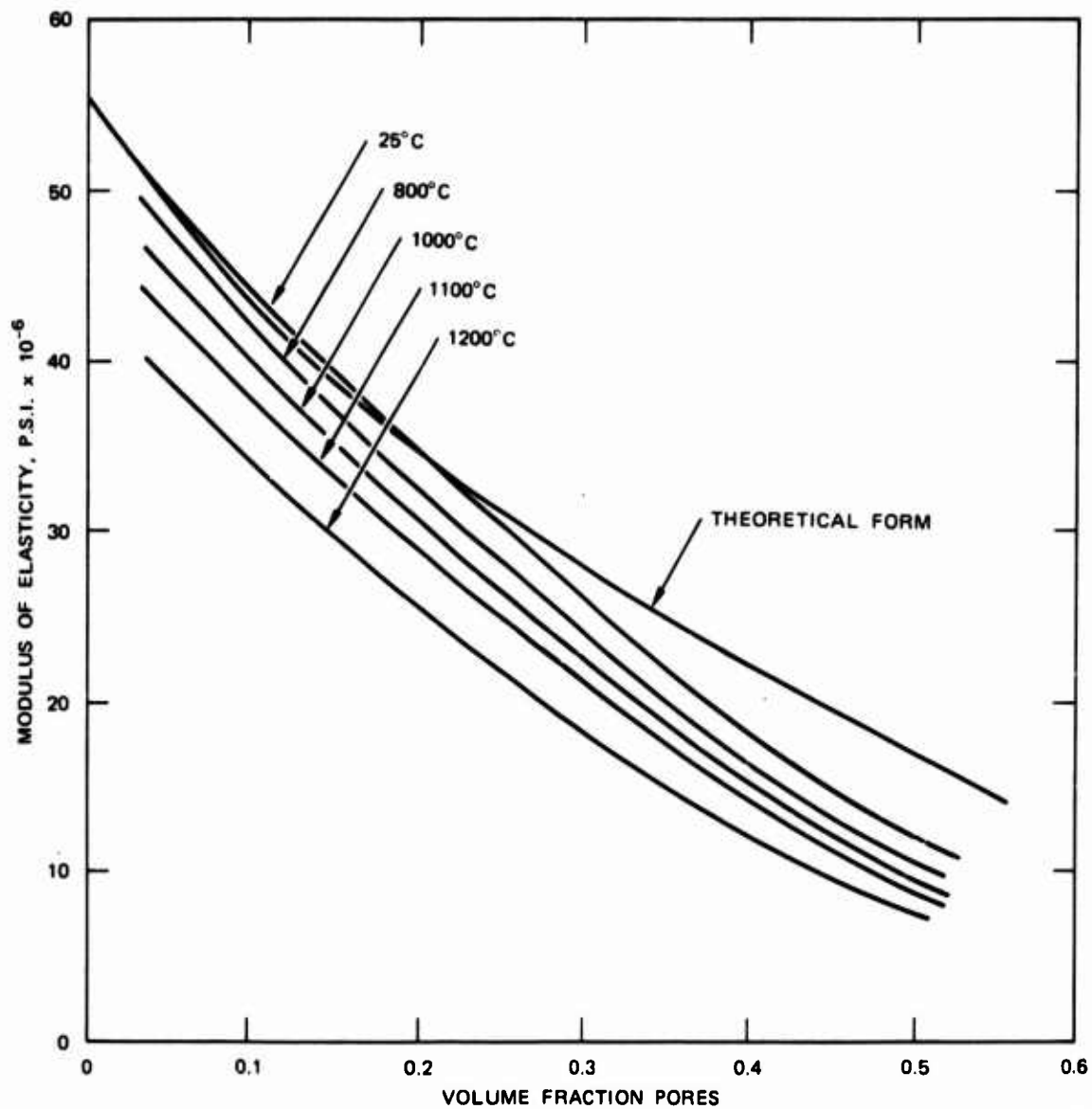
#### Bulk Modulus

The bulk modulus varies as a function of both porosity and internal energy. In the model we have presumed that the thermal strength effect also governs the reduction of the modulus. If this is not true, an additional function should be used. Data may be assembled in the form shown in Figure 17, which also shows the theoretical variation of modulus with porosity from Eq. (11). The static data are from reference 29. All the data may be plotted on a single curve by using  $k_1 = K_1/f(E)$  as the ordinate and  $\rho_0^1 = \rho^1 (1 + \Gamma \rho_{s0} E/K_s)$  as the abscissa. From the fit of the  $k_1, \rho_0^1$  data to the model curve, an appropriate value of  $K_0$  can be chosen. This value of  $K_0$  may disagree with that from ultrasonic data. In case of conflict, a choice must be made based on the relative reliability of the data and on the importance of the effects attributable to each measurement (attenuation would depend on the unloading modulus; precursor arrival would follow sonic velocity).

#### Compaction Curve

The compaction curve at zero internal energy is constructed from a combination of static compaction data and Hugoniot data on porous materials. The Hugoniot data should be modified before plotting, as shown in Figure 18. Here Eq. (22), the expression for pressure on the intermediate surface has been used to eliminate the effect of internal energy in reducing the pressure and  $\rho_0^1$ . The zero-energy pressure and density are then

$$P_Z = P/f(E) \quad (118)$$



MA-2407-26

FIGURE 17 VARIATION OF BULK MODULUS WITH POROSITY AND INTERNAL ENERGY

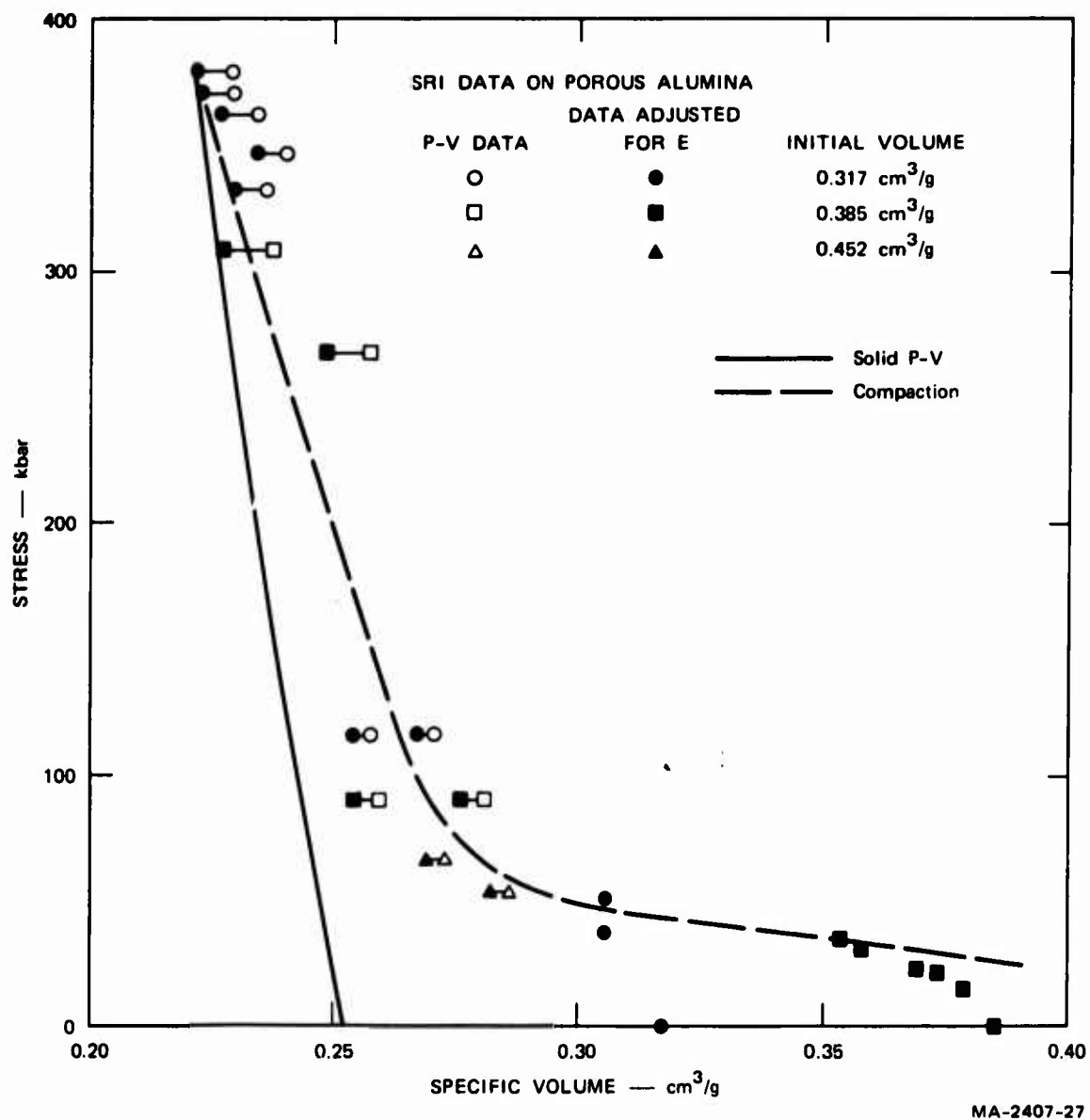


FIGURE 18 HUGONIOT DATA PLOTTED ON THE ZERO-ENERGY REFERENCE PLANE

$$\rho_z = \rho \left( 1 + \frac{\Gamma \rho_{so} E}{K_s} \right) \quad (119)$$

The pressures in Figure 18 were not modified because  $f(E) \cong 1.0$  for the impacts up to 120 kbar, and the higher pressure points were assumed to lie on the solid equation of state, not on a compaction surface. With the data shifted according to Eqs. (118) and (119), there should be a unique, zero-energy compaction curve generated. This compaction curve can be fitted to any of the four models included in PEST. With the data in pressure-volume or pressure-density form, the POREQST model is the easiest to use because it requires the input of a selected set of coordinates along the compaction curve. The Holt, Carroll-Holt, and Herrmann  $P-\alpha$  model parameters can also be easily selected from the plot, but there is no guarantee that the entire analytical function will fit the data. Therefore if one of these  $P-\alpha$  formulations is chosen, it is advisable to make a  $P-\alpha$  plot of the data and the compaction curve of the model to assure that the fit is satisfactory.

#### Rate Effects

Loading rate or load duration has some effect at all testing speeds. However, the effect may not be important in comparing data from tests that differ only by an order of magnitude in loading rate. In these cases it is often possible to use a rate-independent model to describe rate processes. If the data strongly indicate the presence of rate effects, then these effects may be fitted to one of the rate-dependent models.

For rate-dependent compaction, each of the three models has only one free parameter. That parameter can best be selected by constructing a series of loading curves as a function of the parameter, as shown in Figure 19, and comparing the curves to the data. Alternatively, it may be desirable to select the appropriate time constant or viscosity coefficient based on known shock-front thickness, void growth information, or other auxiliary data. The loading curve prescribed by this choice of the time parameters should be checked by comparing it with the data.

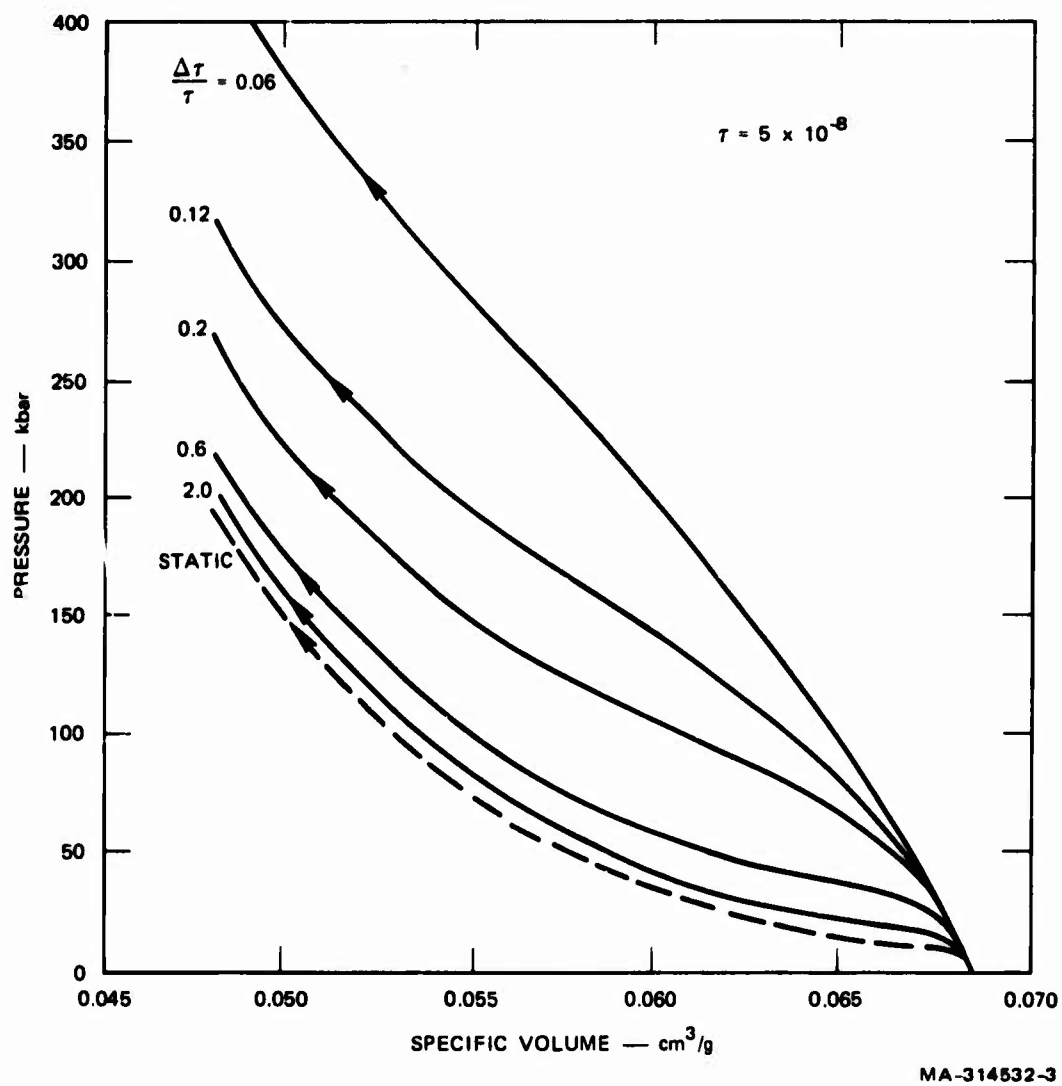


FIGURE 19 RATE-DEPENDENT PRESSURE-VOLUME PATHS GENERATED WITH THE HOLT MODEL AT SEVERAL LOADING RATES



### Deviator Stress

Even weak porous materials sustain some shear or deviator stress. However, this stress is not available from dynamic one-dimensional planar experiments and is usually not obtained in static experiments. The measured stress is a sum of the pressure and deviator stress in the direction of propagation. With no experimental constraints on the magnitude of the deviator stress, the analyst often presumes that there is none: this choice has prevailed among users of  $P-\alpha$  models. If it is desirable to postulate the presence of a deviator stress, some circumstantial evidence may be available to guide the prescription:

- Strength of the material in static tensile or compressive measurements.
- An initially large unloading modulus corresponding to  $K + 4G/3$  followed by a gradual reduction to the expected bulk modulus.
- The shear strength of the solid material.
- The difference between the stress compaction surface resulting from impacts and compaction surface from electron beam experiments (which represents only pressure).

Together these data can be used to prescribe a shear modulus and initial yield strength, plus a work-hardening modulus that will allow the yield strength to reach the solid value at consolidation.

### Minimum Data Required for Characterizing Porous Materials

Often it is necessary to construct constitutive relations for a material for which there are few data. A minimum number of experiments must be planned to provide the needed data. To discuss this problem we have divided the constitutive relations into three groups: solid equation of state, compaction and intermediate surfaces, and fracture behavior.

The determination of the solid equation of state requires several well-instrumented Hugoniot and attenuation experiments plus some electron beam or x-ray measurements. At least three Hugoniot flyer-plate impact

experiments should be planned at three stress levels spanning the expected range of interest. Each impact should have multiple, embedded gages. These experiments yield three Hugoniot points and three unloading paths, providing the Hugoniot function, bulk modulus, and estimates of yield strength and shear modulus. These Hugoniot impacts should be supplemented with at least two attenuation experiments to verify the unloading behavior.

To explore the high energy states of the solid it is necessary to conduct some electron beam or x-ray experiments. For electron beam experiments a choice must be made between voltage levels (which determine depth of deposition and uniformity of the radiant energy through the material) and total fluence levels. A pressure-energy relation is needed that spans from low energies to the highest values of interest in the x-ray simulations. A low-voltage beam gives a range of internal energies in a single test and is therefore well-adapted for a rapid survey of material over a wide range of internal energies. Two or three tests covering the range of energies of interest are probably enough if accurate depth-dose profiles and stress records are obtained. Because of the usual variability of electron-beam data, each experiment should be replicated three or more times. The electron-beam records are used to compare with stress or velocity histories computed in a wave propagation simulation. In preparation for this simulation the impact data must have been used to generate a complete equation of state. Then the electron-beam data provide a basis for altering the Grüneisen ratio, sublimation energy, and other vapor-state parameters.

The compaction-surface and intermediate surfaces are also obtained from a combination of electron-beam and impact data. There is considerable material variability and a large change in unloading modulus as a function of porosity in porous materials. Therefore, at least five Hugoniot impacts with multiple embedded gages should be performed to obtain Hugoniot points on the compaction surface and unloading moduli to define the intermediate surface. For x-ray simulations the most important information is the initial yield point on the crush curve; therefore, this region should be emphasized

in the impact experiments. At least two attenuation experiments (thin flyer impacts) should be performed to verify the unloading moduli that govern attenuation.

A complete pressure-energy curve to melting should be obtained from electron-beam or x-ray data. This curve is essentially that given by JRPWS in Figure 11. One good record with a depth-dose profile that provides the required range in energy would be sufficient, but two or three tests are usually required to give sufficient accuracy in deposited energy over the entire range. The low-energy portions of the pressure energy profile (JRPW in Figure 11) determine the pressure-energy relation on the intermediate surface, while the higher energy portions determine the compaction surface. The most important information is the peak pressure on the pressure-energy curve (point W in Figure 11) because this pressure generally governs the peak recorded stress in x-ray experiments. The electron-beam experiments should be performed with the shortest deposition time possible. During a large deposition time, wave propagation reduces the peak pressures, smooths out the features of the wave, and generally causes a loss of detail. The depth-dose profile, total fluence, and flux history should be measured and used in the computational simulation of the electron beam experiments.

Fracture in porous materials requires more of the same type of data needed for solids because fracture may begin at many porosities. For solids, impact experiments are performed in which rarefaction waves interact and produce tension for a brief period. Since the fracture process is time-and-stress-dependent, tests must be performed at a range of stress levels and stress durations. The stress and time ranges must span those of interest, and the stress range should include one point below the damage threshold and one just above to ensure accurate definition of the threshold stress. The number of fracture experiments may be minimized by using tapered-flyer impacts that provide a range of tensile

stress durations in each impact. At least three tapered-flyer experiments with a range of damage are required to determine a fracture model at a single initial porosity. This requirement is valid for the SRI ductile and brittle fracture models,<sup>8</sup> the Tuler-Butcher<sup>30</sup> model, and any other model that recognizes both stress- and time-dependence of fracture.

Electron-beam experiments can aid in determining the fracture parameters under radiation or at high internal energies. The data from the electron beam experiments should be viewed as an aid in adjusting the model for energy effects and not for the initial construction of the model. Fracture, even in ductile materials, is strongly dependent on stress level; hence a test technique in which stress can be controlled to a few percent and measured even more accurately is necessary for model construction.

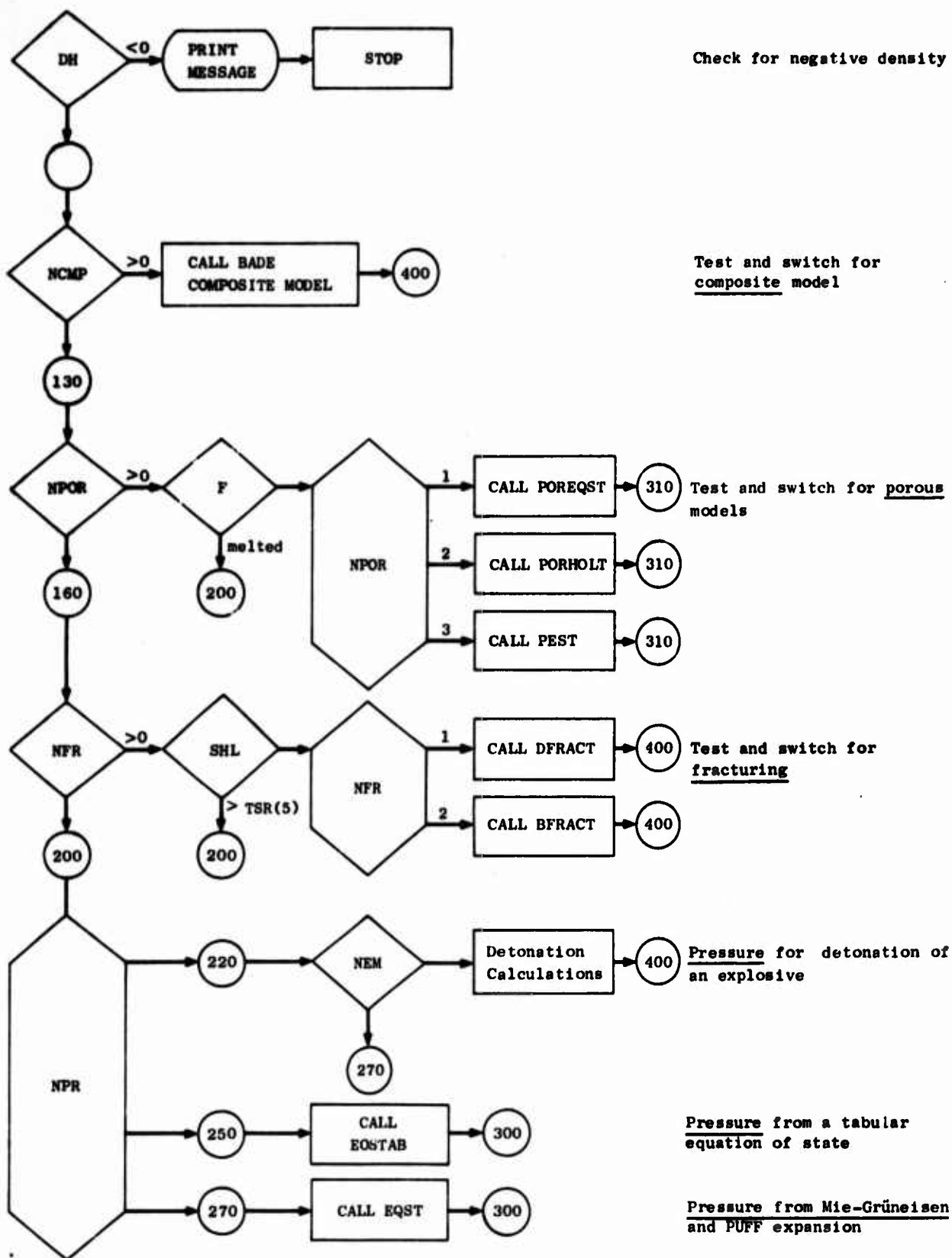
## APPENDIX A

### USER INFORMATION FOR PEST SUBROUTINE

This appendix contains instructions for using PEST, the generalized porous equation-of-state model, in a wave propagation calculation. Flow charts, nomenclature, and listing of PEST are presented. The function TSQE utilized by PEST is described in Appendix B.

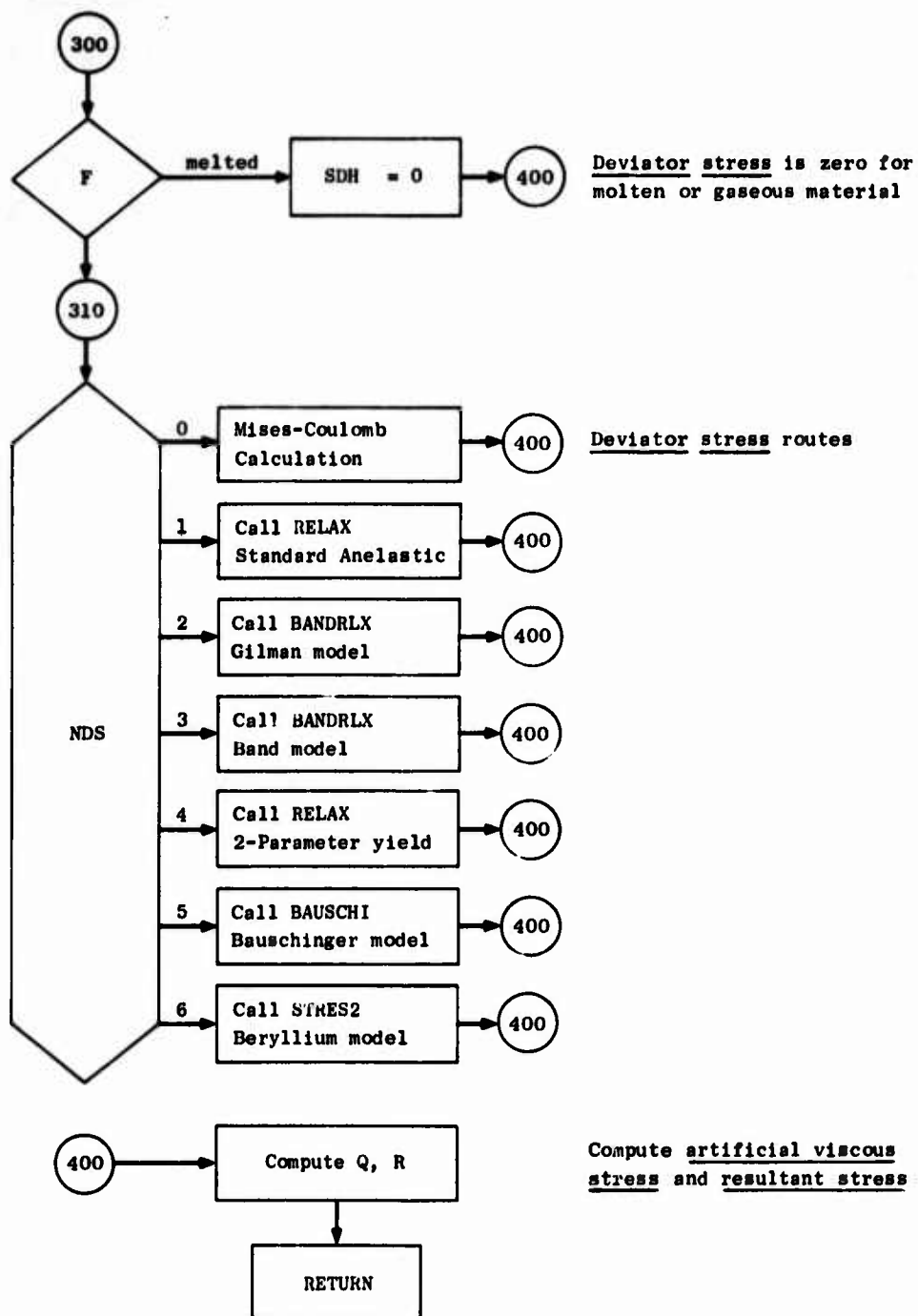
Although pressure and deviator stress are computed for all porous materials, the PEST subroutine calculates only pressure. Then an auxiliary subroutine is called to handle the deviator stress. In SRI PUFF the stress calculations are controlled in a subroutine called HSTRESS. This subroutine acts as a switch to determine which solid equation of state, which porous pressure model, and which deviator stress model are used for each material. The flow chart for the subroutine is shown in Figure A-1. All of the stress calculating subroutines are fully isolated from the COMMON variables for stress, energy, time, etc. Thus these subroutines can be used to provide partial information about stresses (as they might for the components of a composite), or auxiliary information (for porous and fracturing material), or they may be called within an iteration loop for repetitive stress calculations at a single time.

Within PEST there are CALL's to three solid equations of state: EQST, ESA, and EQSTPF. The subroutines ESA and EQSTPF are described and listed in Appendices D and C of this report. EQST, containing the standard Mie-Grüneisen and PUFF expansion equations of state, is in Reference 31 and is similar to that in Reference 9.



GA-8678-181

FIGURE A-1 FLOW CHART OF HSTRESS, STRESS-SWITCHING ROUTINE



GA-8678-181

FIGURE A-1 FLOW CHART OF HSTRESS, STRESS-SWITCHING ROUTINE (Concluded)

### Deviator Stress Models

The special deviator stress models are described in Reference 32 (models 1, 2, 3, and 4), Reference 12 (model 5), and References 11 and 33 (model 6). The standard deviator stress option in SRI PUFF includes elastic-plastic behavior with work hardening and Coulomb friction. Except for the Coulomb friction, this model is like that given in the PUFF 66 manual.<sup>9</sup> In the standard model the yield strength at the end of a time step is given by

$$\begin{aligned} Y_c &= Y - Y_{ADD} \Delta\epsilon + \beta P && \text{(plastic)} \\ &= Y + \beta P && \text{(elastic)} \end{aligned} \tag{A-1}$$

where

- $Y$  is the yield strength at the beginning of the time step
- $Y_{ADD}$  is the work-hardening modulus in the computationally convenient form of  $\partial Y / \partial \epsilon$
- $P$  pressure
- $\beta$  Coulomb friction factor.

The value of  $\beta$  is derived by examining the usual forms of the Coulomb law:

$$\tau_Y = c + \sigma_N \tan \varphi \tag{A-2}$$

$$\sqrt{J_2} = k + 3 \alpha_c P \tag{A-3}$$

where

- $\tau_Y$  is the shear stress at yield
- $c$  is the cohesion
- $\sigma_N$  is the normal stress on the yielding surface
- $\varphi$  is the angle of internal friction
- $J_2$  is the second invariant of the deviator stress tensor
- $k, \alpha_c$  are constants.



Equation (A-2) is the usual form employed in soil mechanics, while Eq. (A-3) is that proposed by Drucker and Prager<sup>34</sup> as a three-dimensional form of (A-2).

In our calculations we took the three-dimensional form of Drucker and Prager and related the standard material constants  $c$  and  $\varphi$  to  $k$  and  $\alpha_c$

$$k = \frac{\sqrt{3} c \sqrt{N_\varphi}}{1 + N_\varphi/2} \quad (A-4)$$

$$3 \alpha_c = \frac{\sqrt{3}}{2} \frac{N_\varphi - 1}{1 + N_\varphi/2} \quad (A-5)$$

where  $N_\varphi = \tan^2(\pi/4 + \varphi/2)$ . From these relations the corresponding values of  $Y_o$  (initial yield) and  $\beta$  can be found

$$Y_o = \frac{3c\sqrt{N_\varphi}}{1 + N_\varphi/2} \quad (A-6)$$

$$\beta = \frac{3}{2} \frac{N_\varphi - 1}{1 + N_\varphi/2} \quad (A-7)$$

At the end of a time step during PUFF calculations the yield value  $Y$  is increased by  $Y_{ADD} \Delta p$  if yielding occurred but the pressure factor in Eq. (A-1) is not added on. As in other yielding models, the deviator stress is limited to  $2Y_c/3$  at each time.

Any of the above deviator models (except 6) can now be used in conjunction with PEST. An appropriate means for varying the elastic moduli and relating the one-dimensional strain to the plastic-strain in the solid for model 6 have not been found. Thus model 6 should not be used with PEST.

### Calling Procedure

PEST is called at two points in a wave propagation code. The first CALL occurs in the initializing subroutine (GENRAT in PUFF) at the place where material properties are inserted. At this CALL, the original solid density ( $\rho_{os}$ ) and the Hugoniot parameters (C, D, S,  $\Gamma = G$ ) must be available in COMMON). Also the initial porous density ( $\rho_o = \text{RHO}(M)$ ) must be available and is read in before the CALL statement. Additional material data for each model used are read in directly by PEST during the initializing CALL: they are not available to the rest of the program. All other input and output variables are inserted through the CALL statement. The CALL statement used in GENRAT is

```
CALL PEST(LS,IN,A1,A2,A3,A4,A5,M, EXMAT(M),RHO(M),A6, RHOS(M),A7,A8,A9,
```

```
A10, A11,A12,A13,C(M),D(M),S(M),G(M),A14,YO(M),A15,A16,CZQ(M),CWQ(M),
```

where the first parameter (LS) indicates initialization when set equal to zero. After initialization for the first porous material, LS is set to 1 in PEST. The second parameter (IN) is the file containing the input data. The A's represent variables that are not used during this CALL. The parameter M is the material number. EXMAT(M) is sound speed, and CZQ(M) and CWQ(M) are quadratic and linear viscosity coefficients. These three quantities (viscosity coefficients for POREQST model only) are determined during initialization in PEST and returned to GENRAT. During this CALL, the subroutine reads cards required for each of the equation-of-state models employed and initializes its internal array variables. The input information is described in the following section.

The second and all subsequent CALLs to PEST are made to obtain the pressure in a wave propagation calculation. In SRI PUFF the following CALL statement is in the subroutine HSTRESS:

```
CALL PEST(2,5,NPR(M),H(J,1),J,T(J),DT,M,CS(J),DH,DOLD,RHOS(M),RHOI(J), P(J),
PST1(J),AST1(J),EH, EOLD,F,C(M),D(M),S(M),G(M),MUM,YADDM,RVV(J),
ENV(J),CZJ,CWJ)
```

The value of the first parameter given (LS = 2) signifies that pressure is to be computed. The indicators NPR(M) and H(J,1) specify which solid equation-of-state subroutine is to be used and the state of stress in the material (compression, tension, or recompression). The J,DT,CS(J), DH, and DOLD,P(J),EH and EOLD,F,MUM,RVV(J), and ENV(J) are the cell number, time step, cell sound speed, present and previous densities, cell pressure, present and previous energies, thermal strength reduction factor, shear modulus, relative void volume, and void density, respectively. The RHOI(J), PST1(J), and AST1(J) are the previous time intermediate surface density, rate-independent pressure and rate-independent distension ratio.

#### Input Information for All Models

The subroutine PEST is in two parts: the first handles reading and initializing, and the second (beginning at location 1000) handles pressure computations. During the initializing portion, a set of six indicators is first read in to indicate which porous equation of state models are to be used under the three conditions considered: compression, tension, and recompression. Recompression is assumed to apply after fragmentation occurs. Next, one line of data that is common to all models is read in. Then data are read in for rate-independent models for each of the three conditions, and subsequently for the rate-dependent models for each of the three conditions. Arrays are repeated wherever possible.

Table A-1 gives values for each of the six model indicators: KCS, KTS, KRS, KCD, KTD, AND KRD. Non-zero values of the indicators refer to the models as shown in Table A-1. Tension and recompression model indicators are set to zero when it is desired to utilize the compression model data again. The arrays are then repeated and reinitialized with

TABLE A-1 DEFINITION OF INDICATORS FOR PEST MODEL OPTIONS

Indicator	Value	Model
Rate-independent compression	1	POREQST
KCS	2	Holt
or	3	Carroll-Holt
KRS	4	Herrmann P-alpha
	5	Hendron*
Rate-independent tension	1	Constant strength
	2	Fracture mechanics*
KTS	3	Carroll-Holt
Compression with rate effects	1	No rate dependence
	2	Linear viscous void
	3	Holt
KCD or KRD	4	Butcher P-alpha-tau
Tension with rate effects	1	No rate dependence
	2	NAG ductile fracture
KTD	3	NAG brittle fracture*

\* Not yet implemented.

appropriate changes in sign. When no rate dependence is desired, it is permissible to specify all zeros for the dynamic indicators. A sample of these indicators is shown in Figure A-1. The format used is A10,I6,I2,I2. The data for each model are provided in the order of the indicators. These data used the formats (A10,I10),4(A10,E10.3), or (A10,7E10.3). The sample data are appropriate for porous tungsten. The meaning of each parameter in the data can be found in the nomenclature list below.

In many cases, there are optional ways to insert the data. For the data common to all models, AK, the initial modulus, may be inserted as  $-G_s$ , the shear modulus of the solid. In this case PEST computes AK from Eq. (11). If the AK value provided is larger than  $K_s \rho / \rho_{so}$ , AK is reset to  $K_s \rho / \rho_{so}$ .

In the POREQST model the fifth density in the RHOP array is the consolidation density. If this value is omitted, PEST computes it by finding the density appropriate to the P2 value in the last density region. If desired, an array of quadratic and linear artificial viscosity coefficients can be inserted following the RHOP array. If these arrays are omitted, COSQ is set to 4, and C1 is 0.15. The fifth members of each of these arrays are returned to GENRAT and are used as the viscosity coefficients for the solid.

In PORHOLT the consolidation density, RHOP5, may be inserted as the consolidation pressure. Then PEST computes the appropriate consolidation density from this pressure.

Input for the Carroll-Holt model may take several forms. If  $Y_{CH}$  and  $\epsilon$  are used and YCH is named as shown in Figure A-2, these values are used directly. This value of YCH is not a pressure on the compaction curve but a solid yield strength, which governs compaction. Instead of  $Y_{CH}$ , the pressure on the compaction curve at the initial density, PY, can

SAMPLE MODEL INDICATOR DATA FOR POREQST(C) AND CARROLL-HOLT(T AND R) RATE-INDEPENDENT MODELS AND LINEAR VISCOUS VOID AND DUCTILE FRACTURE RATE-DEPENDENT MODELS:

```

KCS,TS,RS      010303 KCD,TD,KD      020000

POROUS DATA USED FOR ALL MODELS:
AK=      2.100E+12 MUP=      1.050E+12 YZERO=      6.000E+09 RHOP1=      1.456E+01
POREQST DATA:
NREG=      3
RHOP=      1.456E+01 1.845E+01 1.890E+01
CNSQ=      3.0 3.4 3.8 4.2 4.6
0 P2=      1.000E+10
1 P2=      6.500E+10 DELP=      -8.000E+09 YADDP=      2.000E+09
2 P2=      8.200E+10 DELP=      -2.000E+09 YADDP=      4.000E+09
3 P2=      2.000E+11 DELP=      0. YADDP=      6.000E+09

PORHOLT DATA:
RHOP5 =      2.083E+01 UPDRHO =      6.000E+09 PY =      1.000E+10 YADDP =      1.200E+10
CARROLL-HOLT DATA:
YCH =      9.300E+09 EPS =      1.000E-14 TER7 =      0.6
OR
PY =      1.000E+10 PC =      2.000E+11 TER7 =      0.6
OR
PY =      1.000E+10 EPS =      1.000E-14
HERRMANN P-ALPHA DATA:
PC =      2.000E+11 PY =      1.000E+10
CONSTANT STRENGTH DATA:
TER5 =      -1.000E+10 TER7 =      0.6
LINEAR VISCOUS VOID OR DUCTILE FRACTURE DATA:
TER =      -5.000E-04
OR
TER =      -5.000E-04 1.000E+10 1.000E-04 1.000E+10 1.000E+10 1.000E+10 1.000E+09 0.6
DYNAMIC PORHOLT OR BUTCHER P-ALPHA-TAU DATA:
TPM=      5.000E-08

```

FIGURE A-2 SAMPLE INPUT FOR PEST SUBROUTINE

be inserted. Also the consolidation pressure, PC, may be provided instead of  $\epsilon$ . The subroutine then computes the appropriate value of  $\epsilon$ . However, the functional form of Eq. (53) does not permit a value of  $\epsilon$  that is appropriate for all values of PC/PY. If the requested value of PC is too small, it will be adjusted upward in the program to the minimum permitted. The three possible forms of the data are shown in Figure A-1. This data card also contains TER7, the value of void volume at which separation occurs in tension. If TER7 is read in for the compression model, it is available if the tension model is a repetition of the compression model. TER7 has no meaning in compression.

Only one parameter, TER1, is used for the linear viscous void model. However all seven parameters for NAG ductile fracture can be inserted for the linear viscous model; they are then repeated, with no sign changes, for the NAG model.

The nomenclature list is followed by a flow chart for PEST in Figure A-2. A sample impact calculation is exhibited in some detail in Figures A-3 through A-7. The stress histories in Figure A-7 indicate the character of the waves produced by the impact. The subroutine listing follows the results of the sample calculation.

# NOMENCLATURE OF PEST

<u>Formal and External Parameters</u>	<u>Definition/Units</u>
LS	Initializing indicator: 0 Initialize for first porous material (Reset to 1 in PEST) 1 Initialize for other materials 2 Compute pressure for each porous material
NPRM	Indicator designating which solid equation of state pressure model to be used
H(and IH)	Indicator telling state of material: S Solid P Porous compression T Porous tension Q Porous recompression R Recompression after fragmentation Z Fragmented
J	Coordinate cell number
TJ	Spall parameter; equals zero when spallation occurs.
DT	Time increment, sec
M	Material number
C	Sound speed, cm/sec
D	Current cell density, g/cm <sup>3</sup>
DOLD	Previous cell density, g/cm <sup>3</sup>
RHOS	Solid material density, g/cm <sup>3</sup>
RHOI	Previous value of density at zero pressure and energy on the intermediate surface, g/cm <sup>3</sup>
P	Pressure at a cell, dynes/cm <sup>2</sup>
PST1	Previous value of <sup>2</sup> rate-dependent pressure, dynes/cm



ASTI	Previous distension ratio for a point on the rate-independent pressure curve
E	Current internal energy estimate for a cell, ergs/g
EOLD	Previous value of E, ergs/g
F	Thermal strength reduction factor
EQSTCM	Solid bulk modulus and first coefficient in Hugoniot relation, dynes/cm <sup>2</sup>
EQSTDM	Quadratic coefficient in Hugoniot relation, dynes/cm <sup>2</sup>
EQSTSM	Cubic coefficient in Hugoniot relation, dynes/cm <sup>2</sup>
EQSTGM	Grüneisen ratio
MUM	Current shear modulus, dynes/cm <sup>2</sup>
YADDM	Work-hardening modulus, dynes/cm <sup>2</sup>
RVV	Relative void volume
ENT	Void density, number/cm <sup>3</sup>
CZJ	Coefficient of quadratic artificial viscosity
CWJ	Coefficient of linear artificial viscosity

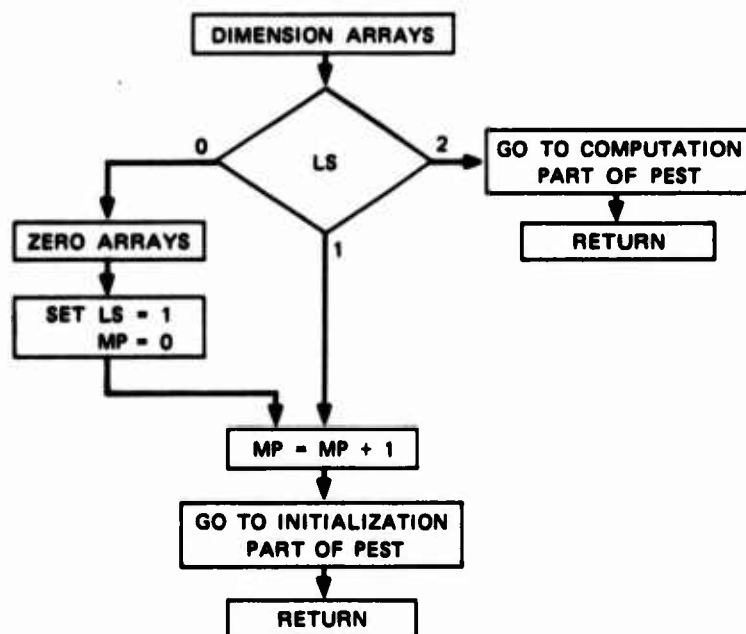
#### Input-Related Variables

AK	Porous Bulk modulus defined at density RHOP(MP,1,1), dynes/cm <sup>2</sup>
COSQ(MP, I, N)	Coefficient of quadratic artificial viscosity, with I=region number for POREQST model
Cl(MP, I, N)	Coefficient of linear artificial viscosity, with I=region number for POREQST model

DELP	Maximum deviation from linear pressure curve for given POREQST region, dynes/cm <sup>2</sup>
DPDRHO	Slope of rate-independent porous pressure equation just beyond elastic limit, dyne-cm/g
EPS	Parameter introduced to give finite consolidation pressure for Carroll-Holt model
KCD, KRD, KTD	Rate-dependent compression, recompression and tension model indicators
KCS, KRS, KTS	Rate-independent compression, recompression and tension model indicators
MP	Porous material number
N	Array subscript variable = 1,2,3 corresponding to compression, tension, and recompression
NPM	Porous material number corresponding to material number M
NREG	Number of porous regions in POREQST model
PC	Consolidation pressure for Herrmann P-alpha model
PORA, PORB, PORC(MP, I, N)	Calculated coefficients of porous rate-independent pressure or density relation
PY	Pressure corresponding to initial yield point on compaction curve
P1	Pressure on compaction curve of POREQST model at RHOP(MP,1,1)
P2	Pressure on left-hand side of each region for POREQST model, dynes/cm <sup>2</sup>
RHOP(MP,1,1)	Density used for initial porous data, g/cm <sup>3</sup>
RHOP(MP, I, N)	Porous densities for I=region number used by POREQST model, g/cm <sup>3</sup>
RHOP(MP, 5, N)	Density at consolidation, g/cm <sup>3</sup>

TER(MP,1,N)	Growth constant = $3/(4), \text{ cm}^2/\text{dyne}/\text{sec}$
TER(MP,2,N)	Growth threshold, $\text{dynes}/\text{cm}^2$
TER(MP,3,N)	Nucleation radius parameter, cm
TER(MP,4,N) and TSR(MP,6,N)	Parameters in nucleation function, no./ $\text{cm}^3/\text{sec}$ and $\text{dynes}/\text{cm}^2$ : $N = \text{TSR}(\text{MP},4,\text{N}) * \exp((P - \text{TSR}(\text{MP},5,\text{N})) / \text{TSR}(\text{MP},6,\text{N}))$
TER(MP,5,N)	Nucleation threshold for Ductile Fracture and static pressure for Constant Strength model, $\text{dynes}/\text{cm}^2$
TER(MP,7,N)	Relative void volume at which fragmentation occurs
TPH	Time constant (sec) associated with Dynamic Porholt and Butcher P-alpha- tau models
YADDP(MP,I,N)	Increment of yield strength, for I=region number in POREQST model
YCH	Pressure on compaction curve at $\text{RHOP}(\text{MP},1,1)$ in Carroll-Holt model, $\text{dynes}/\text{cm}^2$
YZERO	Initial yield strength, $\text{dynes}/\text{cm}^2$
<u>Other Internal Variables</u>	
ALFD	Dynamic distension ratio for current pressure, between elastic and rate- independent values
ALFD1	Previous value of dynamic distension ratio
ALFL	Distension ratio corresponding to current elastic pressure and density
ALFS	Current distension ratio for a point on the rate-independent pressure curve

BULK	Current value of bulk modulus, dynes/cm <sup>2</sup>
CJ	Current sound speed calculated in solid equation of state subroutines except when CJ = 1.
DREF	Density at P-V plane, computed by removing effect of thermal expansion, at constant pressure, DREF=TF*D,g/cm <sup>3</sup>
DS	Solid material density, g/cm <sup>3</sup>
P	Previous value of pressure, dynes/cm <sup>2</sup>
PEL	Pressure <sub>2</sub> based on elastic relations, dynes/cm <sup>2</sup>
PJ	Current pressure, dynes/cm <sup>2</sup>
PS	Solid pressure, dynes/cm <sup>2</sup>
PST	Pressure based on rate-independent pressure model
PTH	Threshold pressure for solid, dynes/cm <sup>2</sup>
RVV	Current relative void volume; takes on negative value to indicate fragmentation
RVV1	Previous value of relative void volume
TF	Thermal expansion factor used to relate current density on intermediate surface to reference density at zero energy and constant pressure



PEST INITIALIZES AND COMPUTES  
EQUATION-OF-STATE VARIABLES  
UNDER COMPRESSION, TENSION,  
AND RECOMPRESSION

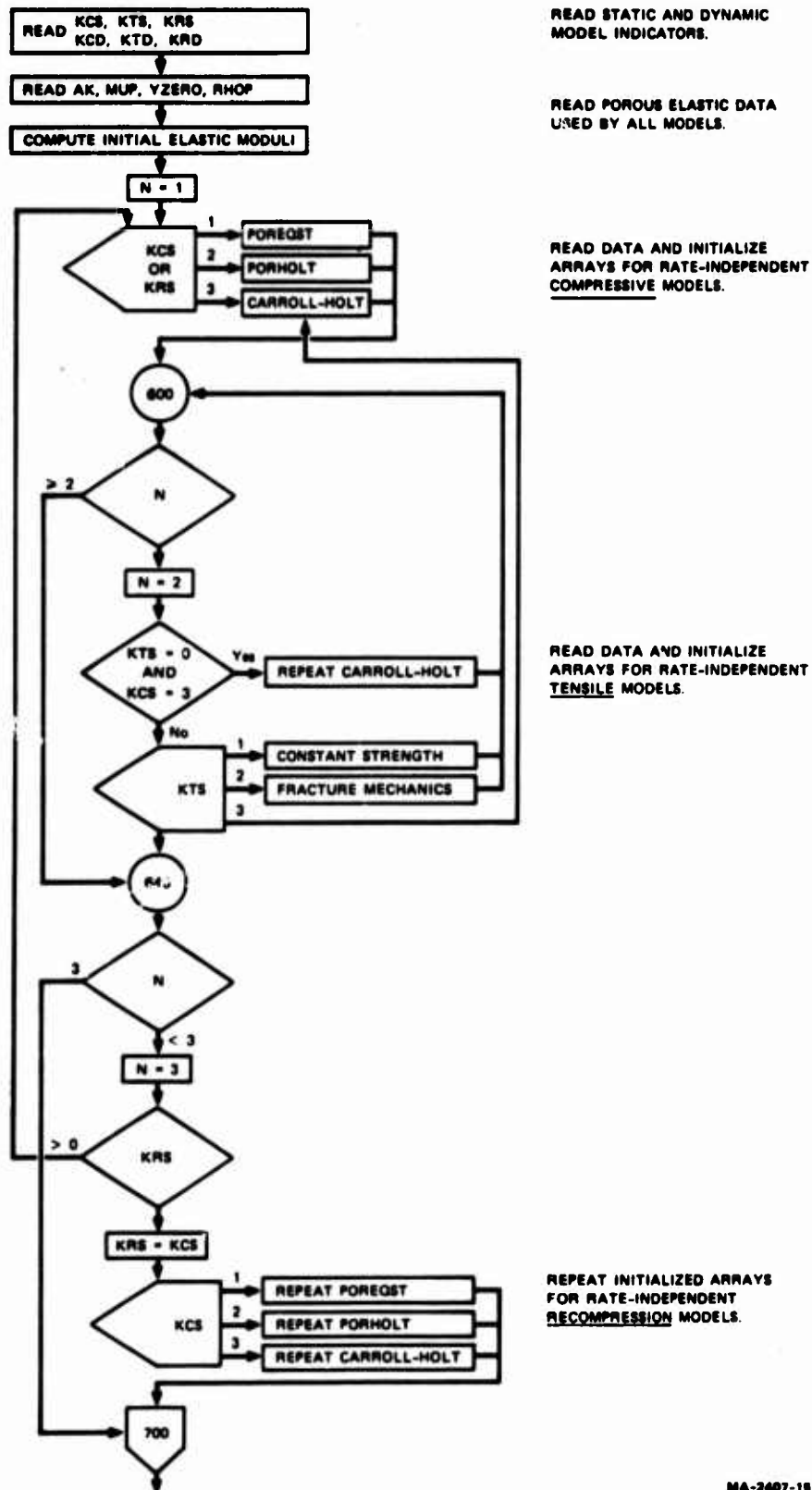
THE INDICATOR LS SETS PATH  
FOR INITIALIZATION OR  
COMPUTATION

INITIALIZE FOR EACH POROUS  
MATERIAL MP NUMBER.

MA-2407-14

FIGURE A-3 FLOW CHART FOR PEST SUBROUTINE

# PEST INITIALIZATION — RATE-INDEPENDENT MODELS



MA-2407-18

FIGURE A-3 FLOW CHART FOR PEST SUBROUTINE (Continued)

# PEST INITIALIZATION — RATE-DEPENDENT MODELS

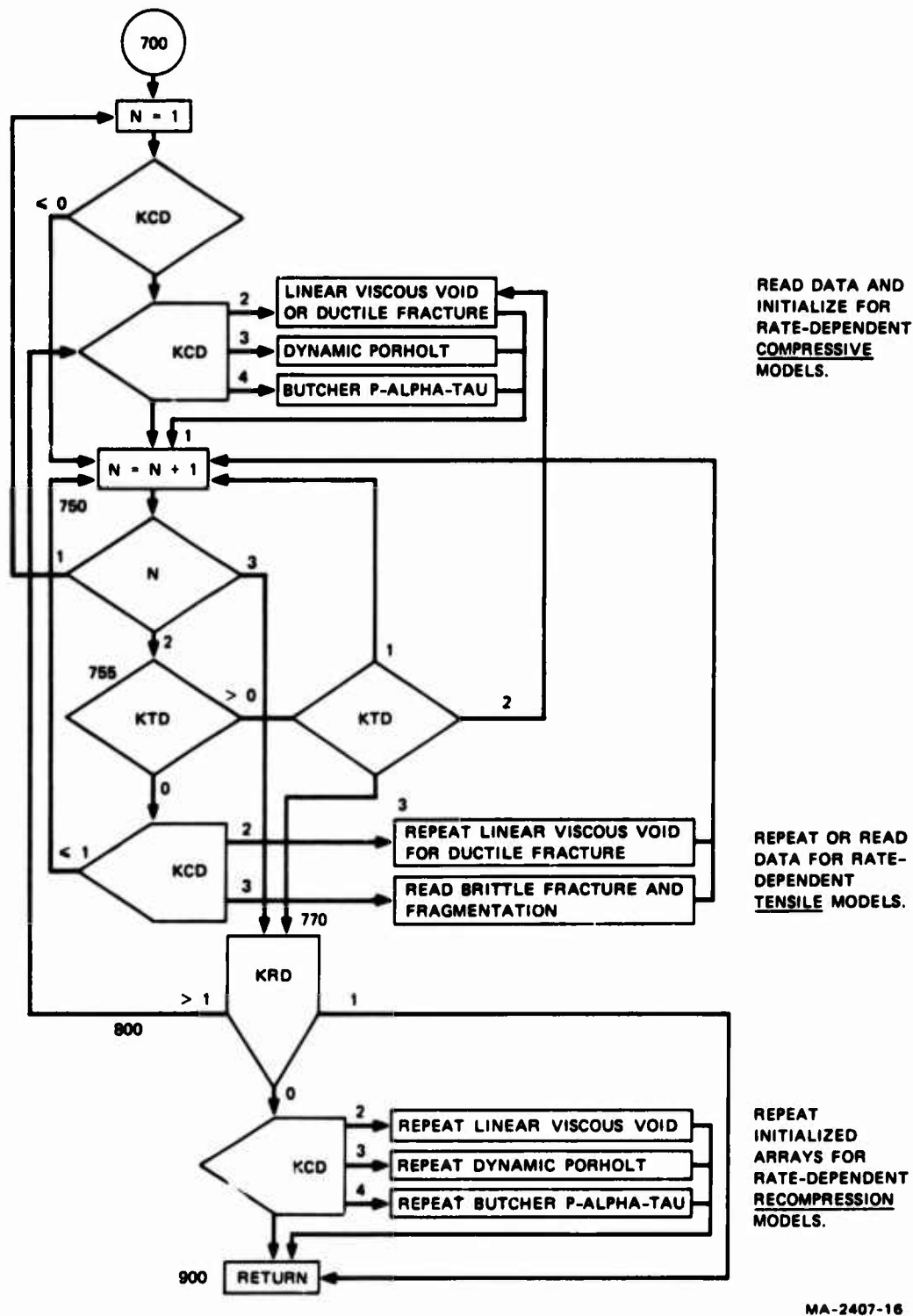
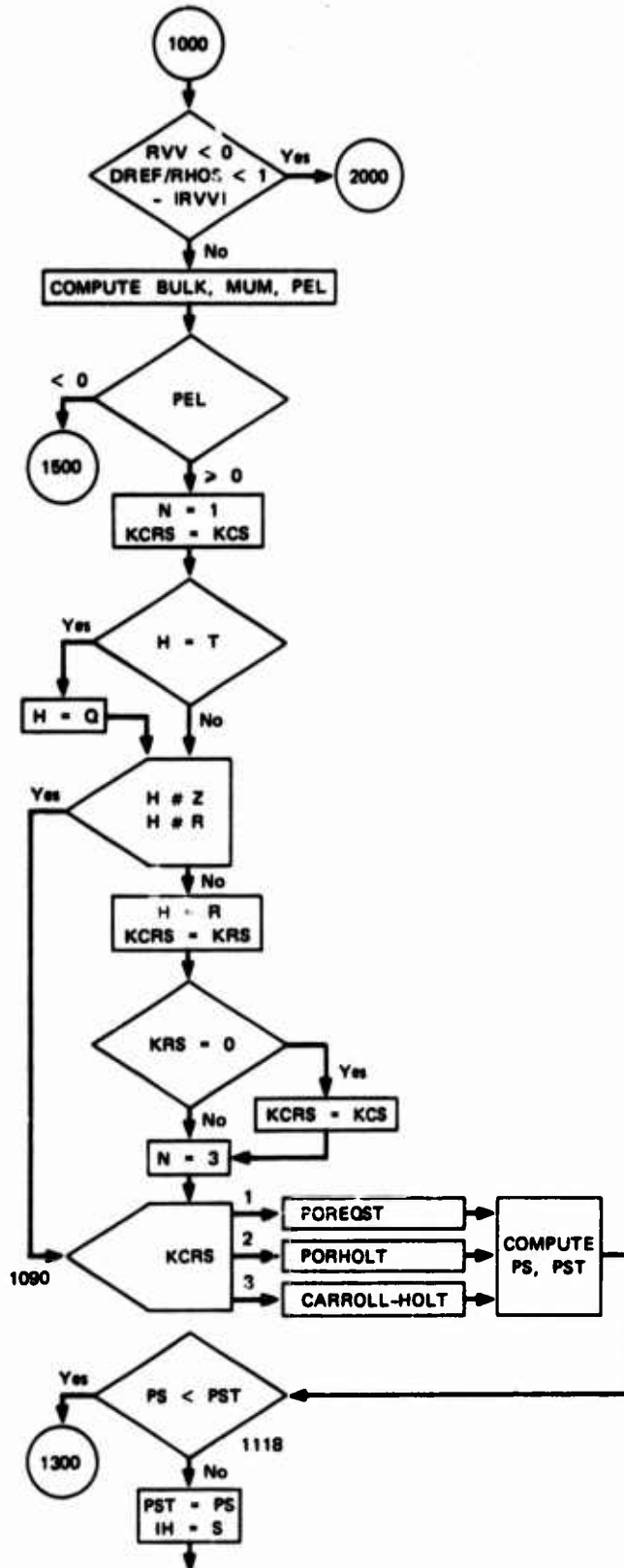


FIGURE A-3 FLOW CHART FOR PEST SUBROUTINE (Continued)

# PEST COMPUTATION OF PRESSURE — COMPRESSION PATH



TEST FOR FRAGMENTATION

COMPUTE CURRENT ELASTIC MODULI  
AND ELASTIC PRESSURE PEL

PEL > 0 IS COMPRESSION PATH;  
PEL < 0 IS TENSILE PATH.

CHOOSE BETWEEN COMPRESSION (P)  
AND RECOMPRESSION (R) ROUTES.

CALCULATE COMPACTION  
CURVE PRESSURE AND CHECK  
FOR CONSOLIDATION.  
COMPUTE SOLID AND STATIC  
PRESSURES (PS AND PST).

MA-2407-17

FIGURE A-3 FLOW CHART FOR PEST SUBROUTINE (Continued)



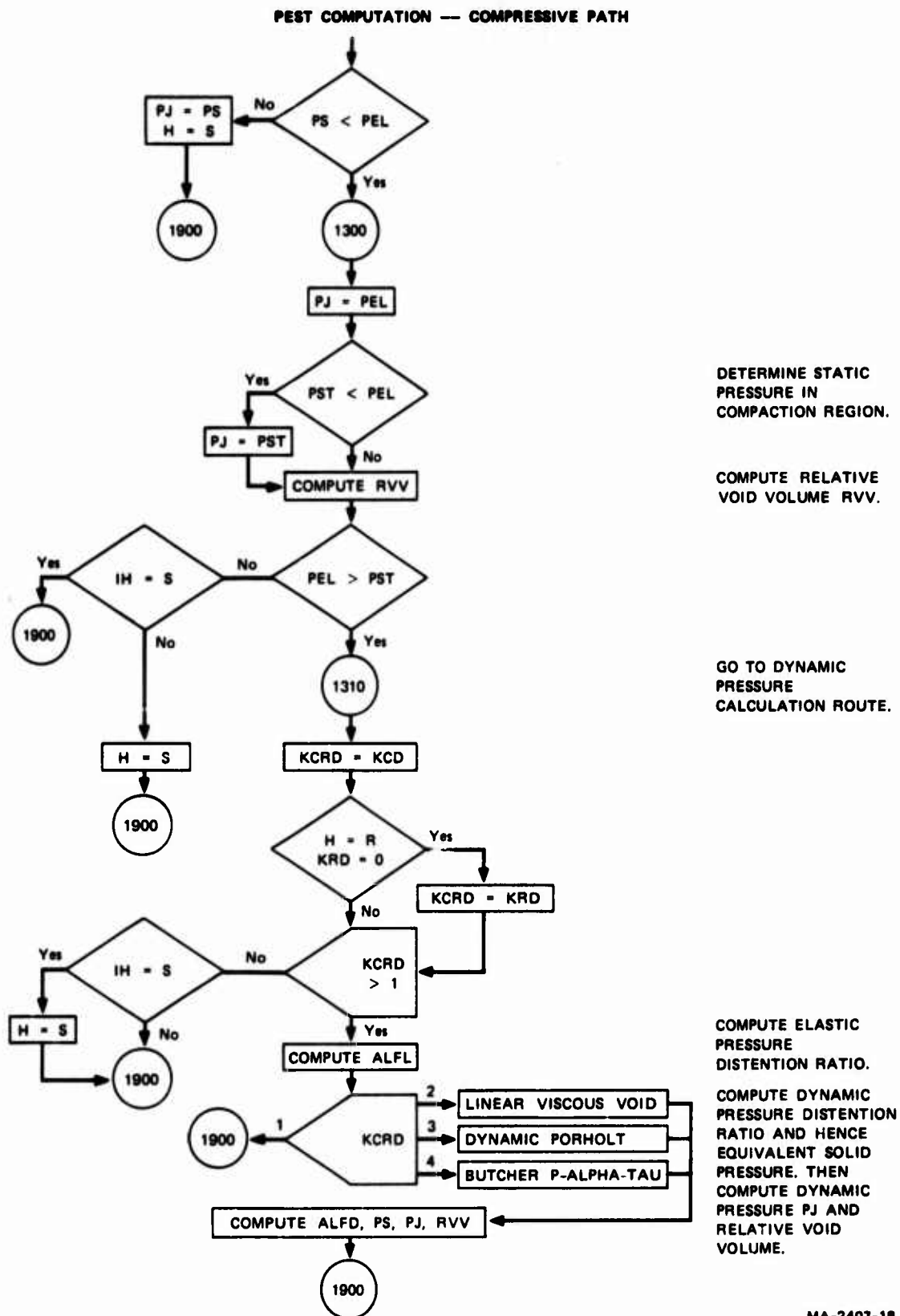


FIGURE A-3 FLOW CHART FOR PEST SUBROUTINE (Continued)

# PEST COMPUTATION — TENSILE PATH

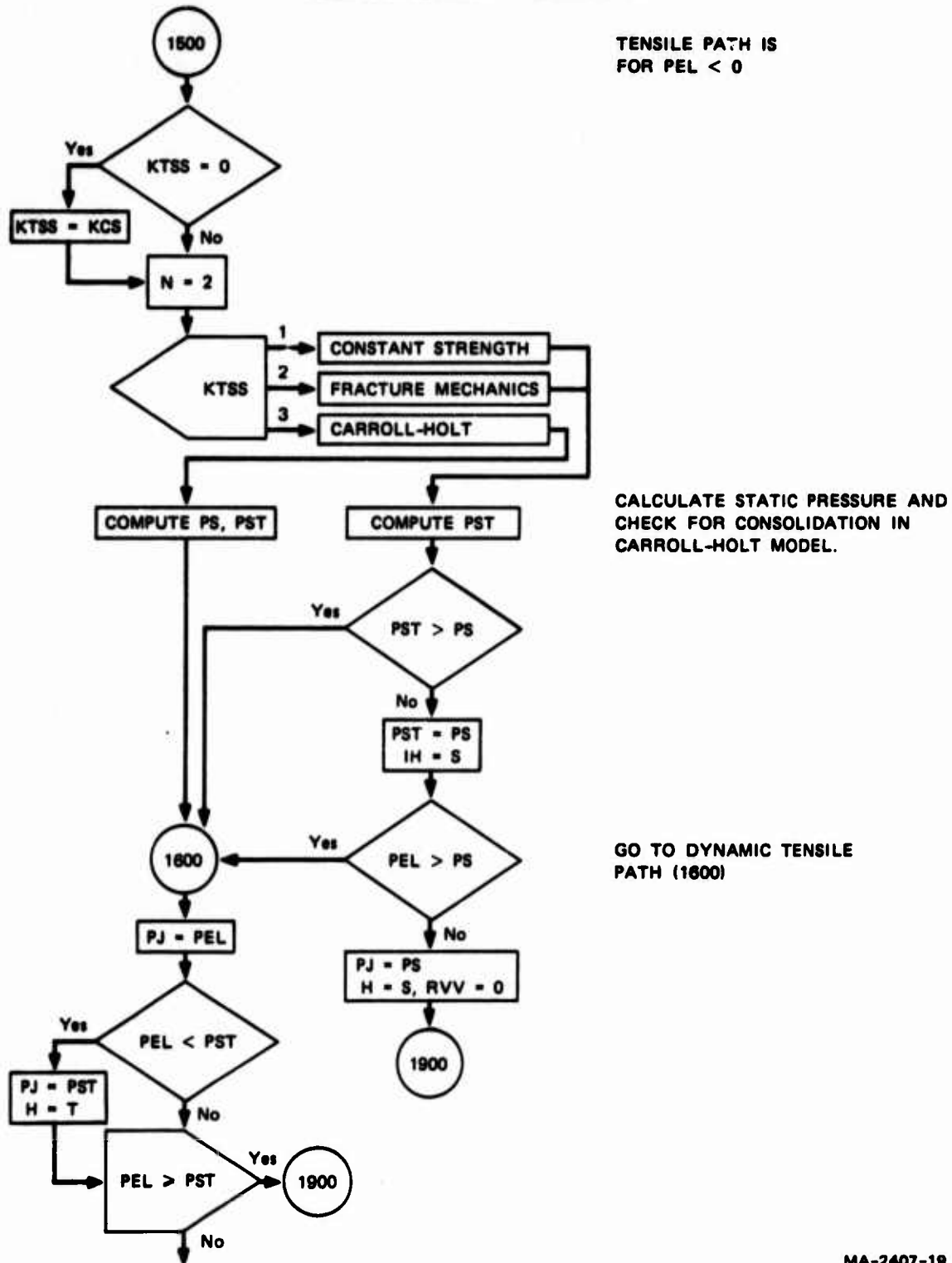
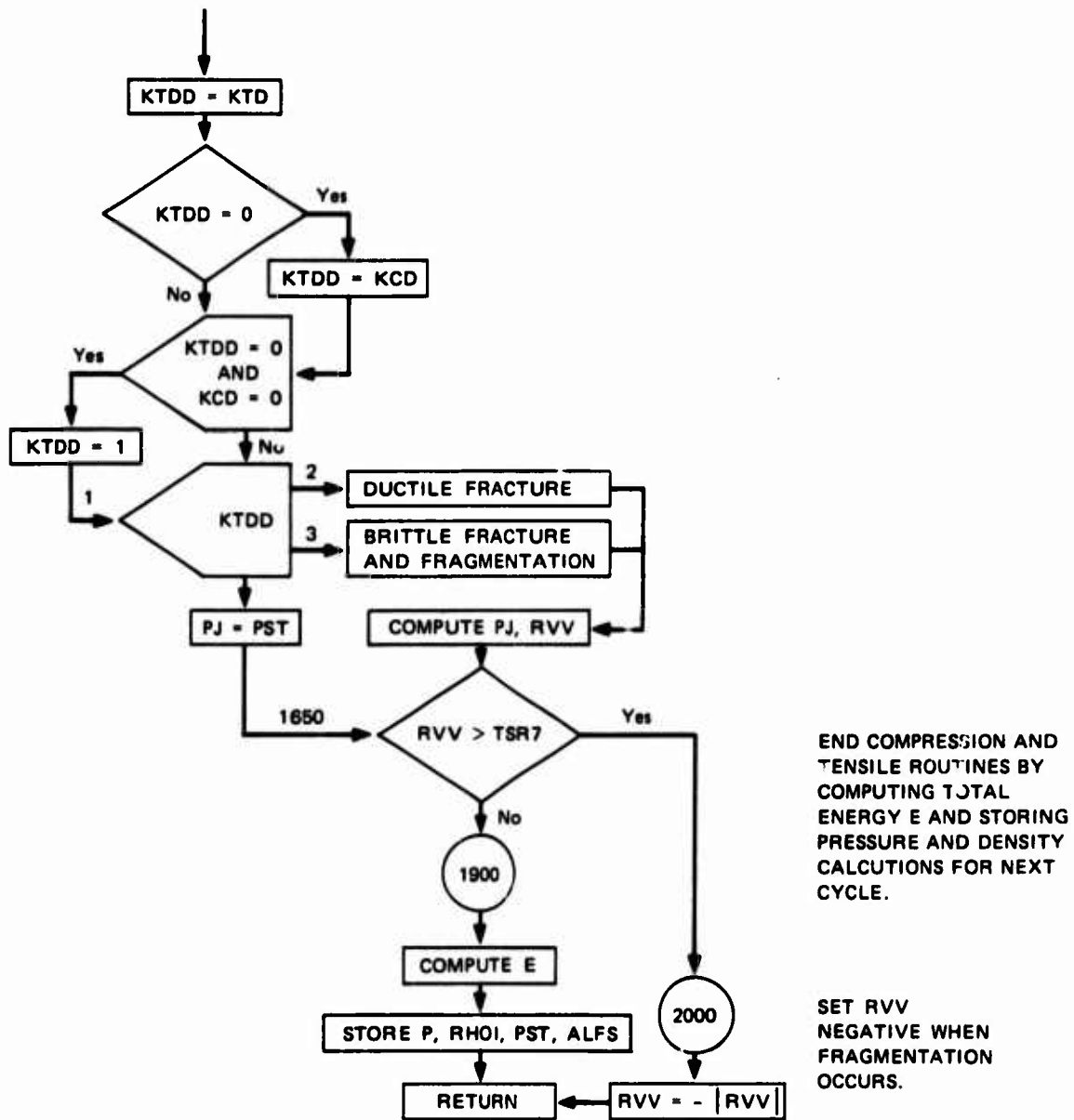


FIGURE A-3 FLOW CHART FOR PEST SUBROUTINE (Continued)

PEST COMPUTATION — TENSILE PATH (Continued)



MA-2407-20

FIGURE A-3 FLOW CHART FOR PEST SUBROUTINE (Concluded)



DATE = 06/14/74 ICDIT IMPACT TUNGSTEN-TUNGSTEN FOM IMPACT FOM CHECKOUT JK BEST COPY

J	DX	A(J)	U(J)	YAL(J)	CHL(J)	RM(J)	Y(J)	Z(J)	PHI(J)	MATERIAL	COD
1	9.000F+02	0	7.34E+04	6.667E-01	1.14E+05	1.84E+01	1.00E+01	1.34E+02	0	POLYURETH	5
2	7.556F+02	0	7.34E+04	6.667E-01	1.14E+05	1.84E+01	1.00E+01	1.34E+02	0	POLYURETH	5
3	7.111F+02	1.556E-01	7.34E+04	6.667E-01	1.14E+05	1.84E+01	1.00E+01	1.34E+02	0	POLYURETH	5
4	6.667F+02	2.267E-01	7.34E+04	6.667E-01	1.14E+05	1.84E+01	1.00E+01	1.34E+02	0	POLYURETH	5
5	6.222E+02	2.933E-01	7.34E+04	6.667E-01	1.14E+05	1.84E+01	1.00E+01	1.34E+02	0	POLYURETH	5
6	5.778F+02	3.556E-01	7.34E+04	6.667E-01	1.14E+05	1.84E+01	1.00E+01	1.34E+02	0	POLYURETH	5
7	5.333F+02	4.133E-01	7.34E+04	6.667E-01	1.14E+05	1.84E+01	1.00E+01	1.34E+02	0	POLYURETH	5
8	4.889F+02	4.667E-01	7.34E+04	6.667E-01	1.14E+05	1.84E+01	1.00E+01	1.34E+02	0	POLYURETH	5
9	4.444F+02	5.154E-01	7.34E+04	6.667E-01	1.14E+05	1.84E+01	1.00E+01	1.34E+02	0	POLYURETH	5
10	4.000F+02	5.644E-01	7.34E+04	6.667E-01	1.14E+05	1.84E+01	1.00E+01	1.34E+02	0	POLYURETH	5
11	0	6.000E-01	7.34E+04	6.667E-01	1.14E+05	1.84E+01	1.00E+01	1.34E+02	0	POLYURETH	5
12	5.150F+03	6.667E-01	7.34E+04	1.20E+01	5.135E+05	1.94E+01	1.2.00E+01	9.14E+02	0	TUNGSTEN	5
13	5.650F+03	6.750E-01	7.34E+04	1.20E+01	5.135E+05	1.94E+01	1.2.00E+01	9.14E+02	0	TUNGSTEN	5
14	5.150F+03	6.151E-01	7.34E+04	1.20E+01	5.135E+05	1.94E+01	1.2.00E+01	9.14E+02	0	TUNGSTEN	5
15	5.650F+03	6.151E-01	7.34E+04	1.20E+01	5.135E+05	1.94E+01	1.2.00E+01	9.14E+02	0	TUNGSTEN	5
16	5.150F+03	6.202E-01	7.34E+04	1.20E+01	5.135E+05	1.94E+01	1.2.00E+01	9.14E+02	0	TUNGSTEN	5
17	5.650F+03	6.252E-01	7.34E+04	1.20E+01	5.135E+05	1.94E+01	1.2.00E+01	9.14E+02	0	TUNGSTEN	5
18	5.150F+03	6.303E-01	7.34E+04	1.20E+01	5.135E+05	1.94E+01	1.2.00E+01	9.14E+02	0	TUNGSTEN	5
19	5.650F+03	6.353E-01	7.34E+04	1.20E+01	5.135E+05	1.94E+01	1.2.00E+01	9.14E+02	0	TUNGSTEN	5
20	5.150F+03	6.404E-01	7.34E+04	1.20E+01	5.135E+05	1.94E+01	1.2.00E+01	9.14E+02	0	TUNGSTEN	5
21	5.650F+03	6.454E-01	7.34E+04	1.20E+01	5.135E+05	1.94E+01	1.2.00E+01	9.14E+02	0	TUNGSTEN	5
22	0	6.505E-01	7.34E+04	1.20E+01	5.135E+05	1.94E+01	1.2.00E+01	9.14E+02	0	TUNGSTEN	5
23	3.000F+03	6.505E-01	7.34E+04	1.20E+01	5.135E+05	1.94E+01	1.2.00E+01	9.14E+02	0	TUNGSTEN	5
24	3.166E+03	6.535E-01	7.34E+04	1.20E+01	5.135E+05	1.94E+01	1.2.00E+01	9.14E+02	0	TUNGSTEN	5
25	3.331E+03	6.567E-01	7.34E+04	1.20E+01	5.135E+05	1.94E+01	1.2.00E+01	9.14E+02	0	TUNGSTEN	5
26	3.497E+03	6.600E-01	7.34E+04	1.20E+01	5.135E+05	1.94E+01	1.2.00E+01	9.14E+02	0	TUNGSTEN	5
27	3.662E+03	6.635E-01	7.34E+04	1.20E+01	5.135E+05	1.94E+01	1.2.00E+01	9.14E+02	0	TUNGSTEN	5
28	3.828E+03	6.672E-01	7.34E+04	1.20E+01	5.135E+05	1.94E+01	1.2.00E+01	9.14E+02	0	TUNGSTEN	5
29	3.993E+03	6.712E-01	7.34E+04	1.20E+01	5.135E+05	1.94E+01	1.2.00E+01	9.14E+02	0	TUNGSTEN	5
30	4.159F+03	6.750E-01	7.34E+04	1.20E+01	5.135E+05	1.94E+01	1.2.00E+01	9.14E+02	0	TUNGSTEN	5
31	4.324E+03	6.791E-01	7.34E+04	1.20E+01	5.135E+05	1.94E+01	1.2.00E+01	9.14E+02	0	TUNGSTEN	5
32	4.490E+03	6.835E-01	7.34E+04	1.20E+01	5.135E+05	1.94E+01	1.2.00E+01	9.14E+02	0	TUNGSTEN	5
33	4.655E+03	6.879E-01	7.34E+04	1.20E+01	5.135E+05	1.94E+01	1.2.00E+01	9.14E+02	0	TUNGSTEN	5
34	4.821E+03	6.926E-01	7.34E+04	1.20E+01	5.135E+05	1.94E+01	1.2.00E+01	9.14E+02	0	TUNGSTEN	5
35	4.986F+03	6.974E-01	7.34E+04	1.20E+01	5.135E+05	1.94E+01	1.2.00E+01	9.14E+02	0	TUNGSTEN	5
36	5.152E+03	7.024E-01	7.34E+04	1.20E+01	5.135E+05	1.94E+01	1.2.00E+01	9.14E+02	0	TUNGSTEN	5
37	5.317E+03	7.076E-01	7.34E+04	1.20E+01	5.135E+05	1.94E+01	1.2.00E+01	9.14E+02	0	TUNGSTEN	5
38	5.483E+03	7.124E-01	7.34E+04	1.20E+01	5.135E+05	1.94E+01	1.2.00E+01	9.14E+02	0	TUNGSTEN	5
39	5.648E+03	7.184E-01	7.34E+04	1.20E+01	5.135E+05	1.94E+01	1.2.00E+01	9.14E+02	0	TUNGSTEN	5
40	5.814E+03	7.244E-01	7.34E+04	1.20E+01	5.135E+05	1.94E+01	1.2.00E+01	9.14E+02	0	TUNGSTEN	5
41	5.979E+03	7.294E-01	7.34E+04	1.20E+01	5.135E+05	1.94E+01	1.2.00E+01	9.14E+02	0	TUNGSTEN	5
42	6.145E+03	7.358E-01	7.34E+04	1.20E+01	5.135E+05	1.94E+01	1.2.00E+01	9.14E+02	0	TUNGSTEN	5
43	6.310E+03	7.414E-01	7.34E+04	1.20E+01	5.135E+05	1.94E+01	1.2.00E+01	9.14E+02	0	TUNGSTEN	5
44	6.476E+03	7.483E-01	7.34E+04	1.20E+01	5.135E+05	1.94E+01	1.2.00E+01	9.14E+02	0	TUNGSTEN	5
45	6.641E+03	7.547E-01	7.34E+04	1.20E+01	5.135E+05	1.94E+01	1.2.00E+01	9.14E+02	0	TUNGSTEN	5
46	6.807E+03	7.614E-01	7.34E+04	1.20E+01	5.135E+05	1.94E+01	1.2.00E+01	9.14E+02	0	TUNGSTEN	5
47	6.972E+03	7.682E-01	7.34E+04	1.20E+01	5.135E+05	1.94E+01	1.2.00E+01	9.14E+02	0	TUNGSTEN	5
48	7.138E+03	7.752E-01	7.34E+04	1.20E+01	5.135E+05	1.94E+01	1.2.00E+01	9.14E+02	0	TUNGSTEN	5
49	7.303E+03	7.823E-01	7.34E+04	1.20E+01	5.135E+05	1.94E+01	1.2.00E+01	9.14E+02	0	TUNGSTEN	5
50	7.469F+03	7.896E-01	7.34E+04	1.20E+01	5.135E+05	1.94E+01	1.2.00E+01	9.14E+02	0	TUNGSTEN	5

FIGURE A-5 INITIAL LAYOUT OF FINITE DIFFERENCE GRID FOR DISTENDED TUNGSTEN IMPACT CALCULATION

Reproduced from  
best available copy.

DATE = 06/06/74 IDENT IMPTEST TUNGSTEN-TUNGSTEN FOAM IMPACT FOR CHECKOUT OF BEST CONF

J	OR	CH	X(J)	U(J)	YML(J)	CHL(J)	DHL(J)	T(J)	7M(J)	FML(J)	MATERIAL	COND
				CM/SEC	DYN/CM2	CM/SEC	GM/CM3	NYN/CM2	GM/CM2	ERG/34		
51	7.634E-03	7.971E-01	0.	0.	4.000E+09	4.933E+05	1.454E+11	1.000E+11	1.112E-01	0.	TUNG FOAM P N A	51
52	7.800E-03	8.047E-01	0.	0.	4.000E+09	4.933E+05	1.454E+11	1.000E+11	1.136E-01	0.	TUNG FOAM P N A	52
53	0.	0.125E-01	0.	0.	0.	0.	0.	0.	0.	0.	TUNG FOAM P N A	53
54	1.200E-02	6.125E-01	0.	0.	0.	2.563E+05	1.190E+00	1.000E+11	1.424E-02	0.	C7 (M) GA S N A	54
55	1.290E-02	6.245E-01	0.	0.	0.	2.563E+05	1.190E+00	1.000E+11	1.535E-02	0.	C7 (M) GA S N A	55
56	1.379E-02	6.374E-01	0.	0.	0.	2.563E+05	1.190E+00	1.000E+11	1.641E-02	0.	C7 (M) GA S N A	56
57	1.469E-02	6.512E-01	0.	0.	0.	2.563E+05	1.190E+00	1.000E+11	1.748E-02	0.	C7 (M) GA S N A	57
58	1.559E-02	6.659E-01	0.	0.	0.	2.563E+05	1.190E+00	1.000E+11	1.855E-02	0.	C7 (M) GA S N A	58
59	1.648E-02	6.815E-01	0.	0.	0.	2.563E+05	1.190E+00	1.000E+11	1.961E-02	0.	C7 (M) GA S N A	59
60	1.738E-02	6.972E-01	0.	0.	0.	2.563E+05	1.190E+00	1.000E+11	2.068E-02	0.	C7 (M) GA S N A	60
61	1.828E-02	7.130E-01	0.	0.	0.	2.563E+05	1.190E+00	1.000E+11	2.175E-02	0.	C7 (M) GA S N A	61
62	1.917E-02	7.288E-01	0.	0.	0.	2.563E+05	1.190E+00	1.000E+11	2.282E-02	0.	C7 (M) GA S N A	62
63	2.007E-02	7.446E-01	0.	0.	0.	2.563E+05	1.190E+00	1.000E+11	2.389E-02	0.	C7 (M) GA S N A	63
64	2.097E-02	7.604E-01	0.	0.	0.	2.563E+05	1.190E+00	1.000E+11	2.496E-02	0.	C7 (M) GA S N A	64
65	2.186E-02	7.762E-01	0.	0.	0.	2.563E+05	1.190E+00	1.000E+11	2.603E-02	0.	C7 (M) GA S N A	65
66	2.276E-02	7.920E-01	0.	0.	0.	2.563E+05	1.190E+00	1.000E+11	2.710E-02	0.	C7 (M) GA S N A	66
67	2.366E-02	8.078E-01	0.	0.	0.	2.563E+05	1.190E+00	1.000E+11	2.817E-02	0.	C7 (M) GA S N A	67
68	2.455E-02	8.236E-01	0.	0.	0.	2.563E+05	1.190E+00	1.000E+11	2.924E-02	0.	C7 (M) GA S N A	68
69	2.545E-02	8.394E-01	0.	0.	0.	2.563E+05	1.190E+00	1.000E+11	3.031E-02	0.	C7 (M) GA S N A	69
70	2.634E-02	8.552E-01	0.	0.	0.	2.563E+05	1.190E+00	1.000E+11	3.138E-02	0.	C7 (M) GA S N A	70
71	2.724E-02	8.710E-01	0.	0.	0.	2.563E+05	1.190E+00	1.000E+11	3.245E-02	0.	C7 (M) GA S N A	71
72	2.814E-02	8.868E-01	0.	0.	0.	2.563E+05	1.190E+00	1.000E+11	3.352E-02	0.	C7 (M) GA S N A	72
73	2.903E-02	9.026E-01	0.	0.	0.	2.563E+05	1.190E+00	1.000E+11	3.459E-02	0.	C7 (M) GA S N A	73
74	2.993E-02	9.184E-01	0.	0.	0.	2.563E+05	1.190E+00	1.000E+11	3.566E-02	0.	C7 (M) GA S N A	74
75	3.083E-02	9.342E-01	0.	0.	0.	2.563E+05	1.190E+00	1.000E+11	3.673E-02	0.	C7 (M) GA S N A	75
76	3.172E-02	9.500E-01	0.	0.	0.	2.563E+05	1.190E+00	1.000E+11	3.780E-02	0.	C7 (M) GA S N A	76
77	3.262E-02	9.658E-01	0.	0.	0.	2.563E+05	1.190E+00	1.000E+11	3.887E-02	0.	C7 (M) GA S N A	77
78	3.352E-02	9.816E-01	0.	0.	0.	2.563E+05	1.190E+00	1.000E+11	3.994E-02	0.	C7 (M) GA S N A	78
79	3.441E-02	9.974E-01	0.	0.	0.	2.563E+05	1.190E+00	1.000E+11	4.101E-02	0.	C7 (M) GA S N A	79
80	3.531E-02	1.013E-01	0.	0.	0.	2.563E+05	1.190E+00	1.000E+11	4.208E-02	0.	C7 (M) GA S N A	80
81	3.621E-02	1.031E-01	0.	0.	0.	2.563E+05	1.190E+00	1.000E+11	4.315E-02	0.	C7 (M) GA S N A	81
82	3.710E-02	1.049E-01	0.	0.	0.	2.563E+05	1.190E+00	1.000E+11	4.422E-02	0.	C7 (M) GA S N A	82
83	3.800E-02	1.067E-01	0.	0.	0.	2.563E+05	1.190E+00	1.000E+11	4.529E-02	0.	C7 (M) GA S N A	83
84	0.	1.562E-01	0.	0.	0.	2.563E+05	1.190E+00	1.000E+11	4.636E-02	0.	C7 (M) GA S N A	84

TIME TO COMPLETE 66.441 IS 1.31 SECONDS.

FIGURE A-5 INITIAL LAYOUT OF FINITE DIFFERENCE GRID FOR DISTENDED TUNGSTEN IMPACT CALCULATION (Concluded)

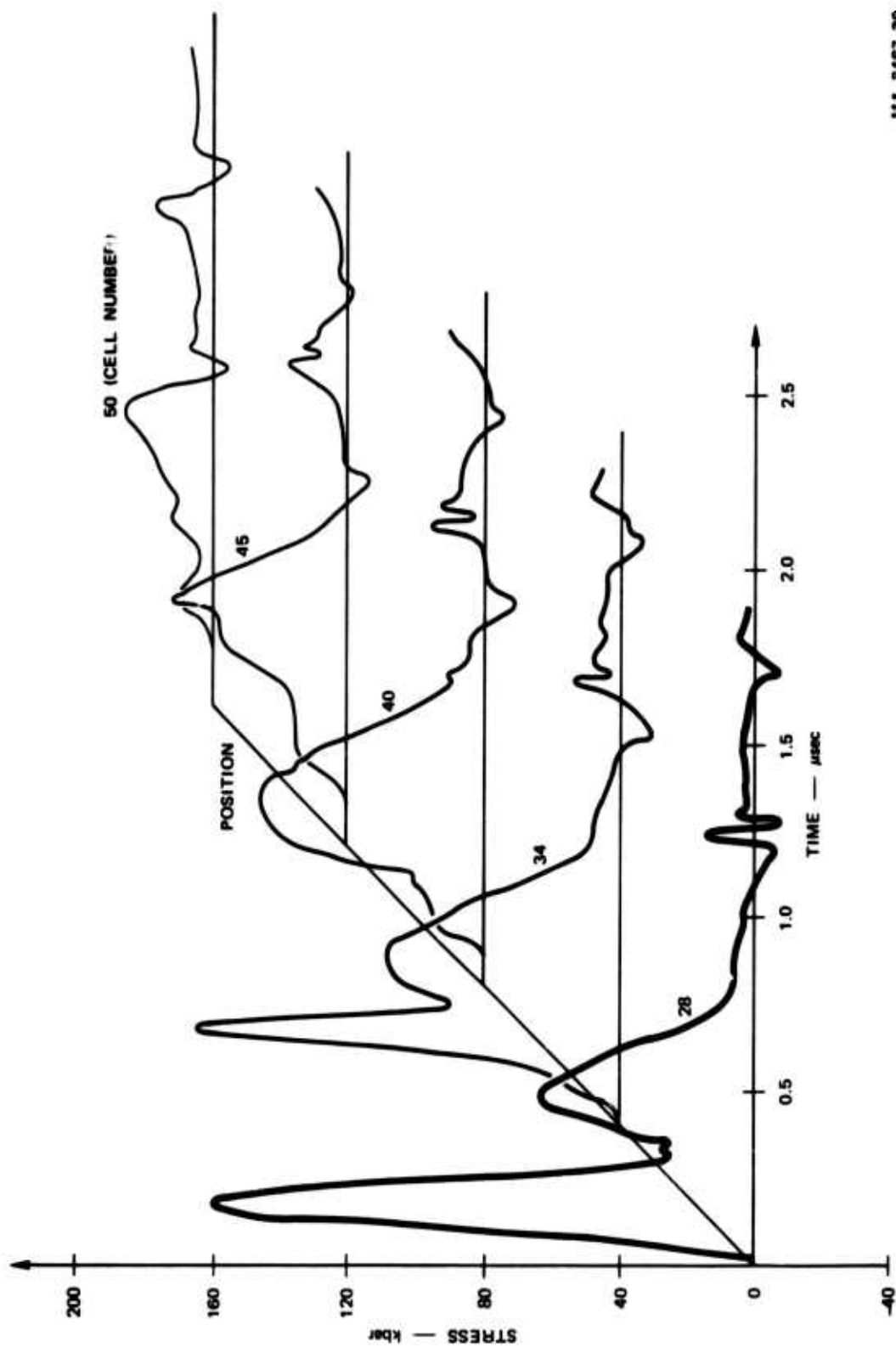


DATE = 06/06/76 IDENT IMPDET TUNGSTEN-TUNGSTEN FROM IMPACT FOR CHECKOUT OF WEST COPY  
FIRST SCRIPT INTERFACE AND JENIT STRESS HISTORIES

N	TIME MUSEC	S12 KHAM	S23 KHAM	S34 KHAM	S1 37 KHAM	S1 41 KHAM	S1 45 KHAM	S1 51 KHAM	S1 54 KHAM	JTC	NTMAM NANSEC	DELTIM SEC
1	.000	-0.00	.000	.0000	.0000	.0000	.0000	.0000	.0000	23	.122	1.145
2	.000	-0.00	7.412	.0000	.0000	.0000	.0000	.0000	.0000	23	.147	.047
3	.000	-0.00	13.138	.0000	.0000	.0000	.0000	.0000	.0000	23	.177	.024
4	.001	-0.00	19.889	.0000	.0000	.0000	.0000	.0000	.0000	23	.212	.024
5	.001	-0.00	25.594	.0000	.0000	.0000	.0000	.0000	.0000	23	.255	.024
6	.001	-0.00	33.377	.0000	.0000	.0000	.0000	.0000	.0000	23	.316	.031
7	.002	-0.00	40.917	.0000	.0000	.0000	.0000	.0000	.0000	23	.367	.032
8	.002	-0.00	49.163	.0000	.0000	.0000	.0000	.0000	.0000	23	.440	.033
9	.003	-0.00	57.886	.0000	.0000	.0000	.0000	.0000	.0000	23	.524	.031
10	.003	-0.00	67.932	.0000	.0000	.0000	.0000	.0000	.0000	23	.634	.037
11	.004	-0.00	74.506	.0000	.0000	.0000	.0000	.0000	.0000	23	.760	.038
12	.005	-0.00	84.690	.0000	.0000	.0000	.0000	.0000	.0000	23	.913	.038
13	.006	-0.00	101.372	.0000	.0000	.0000	.0000	.0000	.0000	23	1.095	.040
14	.007	-0.00	113.484	.0000	.0000	.0000	.0000	.0000	.0000	23	1.314	.042
15	.009	-0.00	126.763	.0000	.0000	.0000	.0000	.0000	.0000	23	1.577	.044
16	.011	-0.00	138.437	.0000	.0000	.0000	.0000	.0000	.0000	23	1.892	.046
17	.013	-0.00	151.454	.0000	.0000	.0000	.0000	.0000	.0000	23	2.271	.049
18	.016	-0.00	162.335	.0000	.0000	.0000	.0000	.0000	.0000	23	2.725	.050
19	.019	-0.00	168.497	.0000	.0000	.0000	.0000	.0000	.0000	23	3.200	.055
20	.022	-0.00	164.311	.0000	.0000	.0000	.0000	.0000	.0000	23	3.144	.056
21	.025	-0.00	151.646	.0000	.0000	.0000	.0000	.0000	.0000	23	3.114	.040
22	.028	-0.00	137.272	.0000	.0000	.0000	.0000	.0000	.0000	23	3.127	.043
23	.031	-0.00	124.241	.0000	.0000	.0000	.0000	.0000	.0000	23	3.141	.043
24	.035	-0.00	125.740	.0000	.0000	.0000	.0000	.0000	.0000	23	3.247	.047
25	.038	-0.00	126.808	.0000	.0000	.0000	.0000	.0000	.0000	23	3.253	.072
26	.041	-0.00	132.254	.0000	.0000	.0000	.0000	.0000	.0000	24	3.314	.042
27	.045	-0.01	134.644	.0000	.0000	.0000	.0000	.0000	.0000	24	3.341	.076
28	.049	-0.04	145.714	.0000	.0000	.0000	.0000	.0000	.0000	24	3.349	.079
29	.051	-0.11	144.495	.0000	.0000	.0000	.0000	.0000	.0000	24	3.337	.040
30	.055	-0.32	144.681	.0000	.0000	.0000	.0000	.0000	.0000	24	3.326	.041
31	.058	-0.80	152.181	.0000	.0000	.0000	.0000	.0000	.0000	24	3.322	.430
32	.061	-1.03	156.531	.0000	.0000	.0000	.0000	.0000	.0000	23	3.333	.044
33	.064	-0.374	150.722	.0000	.0000	.0000	.0000	.0000	.0000	23	3.310	.045
34	.067	-0.696	155.191	.0000	.0000	.0000	.0000	.0000	.0000	23	3.346	.044
35	.071	-1.213	155.334	.0000	.0000	.0000	.0000	.0000	.0000	23	3.349	.049
36	.074	-1.943	156.479	.0000	.0000	.0000	.0000	.0000	.0000	23	3.349	.049
37	.077	-3.037	162.577	.0000	.0000	.0000	.0000	.0000	.0000	23	3.343	.092
38	.080	-4.344	163.434	.0000	.0000	.0000	.0000	.0000	.0000	23	3.346	.093
39	.083	-5.843	161.695	.0000	.0000	.0000	.0000	.0000	.0000	23	3.343	.100
40	.086	-7.335	157.627	.0000	.0000	.0000	.0000	.0000	.0000	23	3.340	.099
41	.089	-9.631	154.127	.0000	.0000	.0000	.0000	.0000	.0000	23	3.344	.099
42	.092	-9.655	152.752	.0000	.0000	.0000	.0000	.0000	.0000	23	3.344	.102
43	.095	-10.500	154.567	.0000	.0000	.0000	.0000	.0000	.0000	23	3.343	.103
44	.098	-11.413	154.313	.0000	.0000	.0000	.0000	.0000	.0000	23	3.344	.104
45	.101	-12.657	161.465	.0000	.0000	.0000	.0000	.0000	.0000	23	3.344	.103
46	.104	-14.514	162.575	.0000	.0000	.0000	.0000	.0000	.0000	23	3.344	.103
47	.107	-16.323	162.299	.0000	.0000	.0000	.0000	.0000	.0000	23	3.344	.105
48	.111	-18.311	161.439	.0000	.0000	.0000	.0000	.0000	.0000	23	3.346	.107
49	.114	-20.678	161.437	.0000	.0000	.0000	.0000	.0000	.0000	23	3.345	.106
50	.117	-24.174	161.448	.0000	.0000	.0000	.0000	.0000	.0000	23	3.377	.104

FIGURE A-7 PORTION OF THE HISTORICAL LISTING OF STRESS AT THE IMPACT INTERFACE (S12)  
AND AT CELLS 34, 37, 41, 45, 50, AND 56 AFTER REZONING





MA-2467-30

FIGURE A-8 COMPUTED STRESS HISTORIES AT SEVERAL LOCATIONS IN THE DISTENDED TUNGSTEN OF THE TEST CASE

# SUBROUTINE PEST

```

SUBROUTINE PFST( LS, IN, NPRM, H, J, TJ, DT, M, C, D, DOLD, RHOS, RHUI, P, PST1, PEST 2
1  AST1, E, EOLD, F, FOSTCH, EOSTOM, EOSTSM, EUSTOM, MUM, YADDM, RVV, ENT, CZJ, PEST 3
2  CWJ, EOSTHM, FOSTEM, EOSTNM, NCYC) PEST 4
C PEST 5
C PEST 1: VERSION OF APRIL 1974 PEST 6
C WRITTEN AT STANFORD RESEARCH INSTITUTE BY L. SEAMAN AND R.E. TOKHEIM PEST 7
C CODE PROVIDES EQUATIONS OF STATE FOR POROUS AND SOLID MATERIALS PEST 8
C UNDER COMPRESSION(C), TENSION(T) AND RECOMPRESSION(R) BY STATIC AND PEST 9
C RATE-DEPENDENT MODELS. INITIALIZATION FOR ALL MODELS IS INCLUDED. PEST 10
C PEST 11
C INDICATORS OF MODELS TO BE CHOSEN FOR STATIC(S) AND DYNAMIC(D) PEST 12
C CONDITIONS FOLLOW: PEST 13
C KCS OR KRS: RATE-INDEPENDENT COMPRESSION PEST 14
C 1 PORQUEST PEST 15
C 2 PORHOLT PEST 16
C 3 CARROLL-HOLT PEST 17
C 4 HERRMANN P-ALPHA PEST 18
C 5 HENDON PEST 19
C KTS: RATE-INDEPENDENT TENSION PEST 20
C 1 CONSTANT STRENGTH PEST 21
C 2 FRACTURE MECHANICS PEST 22
C 3 CARROLL-HOLT PEST 23
C PEST 24
C KCD OR KRD: COMPRESSION WITH RATE EFFECTS PEST 25
C 1 NO RATE DEPENDENCE PEST 26
C 2 LINEAR VISCOUS VOID COMPRESSION PEST 27
C 3 PORHOLT PEST 28
C 4 BUTCHER P-ALPHA-TAU PEST 29
C PEST 30
C KTD: TENSION WITH RATE EFFECTS PEST 31
C 1 NO RATE DEPENDENCE PEST 32
C 2 N.A.G. DUCTILE FRACTURE PEST 33
C 3 BRITTLE FRACTURE AND FRAGMENTATION PEST 34
C PEST 35
C INDICATORS(X) ARE READ IN THREE-DIGIT PAIRS FOR S AND D CONDITIONS: PEST 36
C KCS,KTS,KRS= 0X1X0X KCD,KTD,KRD= 0A0X0X PEST 37
C PEST 38
C INDICATORS M AND IM PEST 39
C S SOLID PEST 40
C P POROUS-PRESSURE PEST 41
C T POROUS-TENSION PEST 42
C R POROUS-RECOMPRESSION PEST 43
C Z FRAGMENTATION PEST 44
C R RECOMPRESSION AFTER FRAGMENTATION PEST 45
C PEST 46
C INTERM H,OUT PEST 47
C REAL MUM,MUP,KIC PEST 48
C DIMENSION KCS(4),KCD(4),KTS(4),KTD(4),KRS(4),KRD(4) PEST 49
C DIMENSION NPRM(4),NREG(4) PEST 50
C DIMENSION TPH(4,3),DADP(4,3),KIC(4) PEST 51
C DIMENSION AK(4),MUP(4),YADDP(4,5,3),ELK(4),ELG(4),TER(4,8,3) PEST 52
C DIMENSION RHOP(4,5,3),COSQ(4,5,3),C1(4,5,3) PEST 53
C DIMENSION PORH(4,5,3),PORH(4,5,3),PORC(4,5,3) PEST 54
C DIMENSION EPS(4,3),DEL(4,3),ALE(4,3),APC(4,3) PEST 55
C DATA SHF/1.8R/EP/1.E-6/IDN/1M /,OUT/6/,JQ1/7H -PEST-/,JQ2/ PEST 56
1 10M -PORQUEST-/,JQ3/10M -CARROLL-/,JQ4/5HHOLT-/,JQ5/10M -HERRMANN PEST 57
2 /,JQ6/9M P-ALPHA-/,JQ7/10M -CONST ST/,JQ8/7HRENGTH-/ PEST 58
3 /,JQ9/10M -FRACTURE/,JQ10/6M MECH-/,JQ11/10M -LINEAR V/,JQ12/ PEST 59
4 9MISC VOID-/,JQ13/10M -DYNAMIC /,JQ14/RHPORHOLT-/,JQ15/ PEST 60
5 10M -PORHOLT-/,JQ16/RHUTCHER-/,JQ5/5HSTAT:/,JQ8/5HSTATE:/ PEST 61
6 /,JQ17/10M -DUCTILE /,JQ18/9MFRACTURE-/ PEST 62
C PEST 63
C *** 7FHUING OF ARPAYS *** CPEST 64

```

# SUBROUTINE PEST (Continued)

C	IF (IS-1) 1, A, 1000	CPEST	65
1	DO 5 I = 1, 6	PEST	66
5	NPM(I) = 0	PEST	67
	DO 40 I = 1, 4	PEST	68
	AK(I) = MUP(I) = KIC(I) = ELK(I) = ELG(I) = 0.	PEST	69
50	NRER(I) = 0	PEST	70
	DO 41 I = 1, 12	PEST	71
51	TPM(I) = UADP(I) = EPS(I) = DEL(I) = ALE(I) = APC(I) = 0.	PEST	72
	DO 42 I = 1, 40	PEST	73
52	YADNP(I) = RHOP(I) = CISO(I) = CI(I) = PORA(I) = PORB(I) = PORC(I) = 0.	PEST	74
	DO 43 I = 1, 96	PEST	75
53	TER(I) = 0.	PEST	76
	MP = 0 \$ DPDNJ = DPDEJ = 0. \$ LS = 1 \$ CJ = 1.	PEST	77
8	MP = MP + 1	PEST	78
	NPM(M) = MP	PEST	79
C		CPEST	80
C	*****	CPEST	81
C	*****	CPEST	82
C	*****	CPEST	83
C	*****	CPEST	84
C	*****	CPEST	85
C	*** READ DATA USED BY ALL MODELS. ***	CPEST	86
	READ(IN, 935) A1, KCS(MP), KTS(MP), KRS(MP), A2, KCD(MP), KTD(MP)	PEST	87
1	KNP(MP)	PEST	88
	WRITE(6, 935) A1, KCS(MP), KTS(MP), KRS(MP), A2, KCD(MP), KTD(MP)	PEST	89
1	KNP(MP)	PEST	90
	WRITE(6, 960) IDN, IN, JO1	PEST	91
C		CPEST	92
	READ(IN, 920) A1, AK(MP), A2, MUP(MP), A3, YZERO, A4, RHOP(MP, 1, 1)	PEST	93
	WRITE(6, 920) A1, AK(MP), A2, MUP(MP), A3, YZERO, A4, RHOP(MP, 1, 1)	PEST	94
	WRITE(6, 940) IDN, IN, JO1	PEST	95
	ALFO = RHOS/RHOP(MP, 1, 1)	PEST	96
	IF (AK(MP) .GT. 0. .AND. AK(MP) .LE. FUSTCM * RHOP(MP, 1, 1)	PEST	97
1	/RHOS) GO TO 20	PEST	98
	IF (AK(MP) .GT. 0.) GO TO 10	PEST	99
C	* IF AK IS NEGATIVE, IT IS INTERPRETED AS THE SHEAR MODULUS *	CPEST	100
C	* OF THE SOLID. *	CPEST	101
	GS = -AK(MP)	PEST	102
	AK(MP) = EUSTCM / (ALFO + 0.75 * FUSTCM / GS * (ALFO - 1.))	PEST	103
	MUP(MP) = GS * (1. - 5. * (1. - 1. / ALFO) * (3. * EUSTCM + 4. * GS) / (9. * EUSTCM	PEST	104
1	+ 0. * GS))	PEST	105
	GO TO 15	PEST	106
C	* IF AK IS TOO LARGE, IT IS REDUCED TO THE MAXIMUM PERMITTED. *	CPEST	107
10	AK(MP) = EUSTCM * RHOP(MP, 1, 1) / RHOS	PEST	108
15	WRITE(6, 950) AK(MP), MUP(MP)	PEST	109
	WRITE(6, 960) IDN, OUT, JO1	PEST	110
20	ELK(MP) = (FUSTCM / AK(MP) - ALFO) / (ALFO - 1.)	PEST	111
	YADNP = 0.666667 * YZERO \$ MUP(MP) = 1.333333 * MUP(MP)	PEST	112
	C = SORT((AK(MP) * AMAX1(0., MUP(MP))) / AMIN1(0., RHOP(MP, 1, 1)))	PEST	113
	J2 = 5HCUMP. \$ J3 = J4 = 14	PEST	114
	N = 1	PEST	115
	KCSM = KCS(MP) \$ KCDM = KCD(MP) \$ KISM = KIS(MP) \$ KIDM = KID(MP)	PEST	116
	KRSM = KRS(MP) \$ KNDM = KND(MP)	PEST	117
	IF (KISM .EQ. 0) J3 = 5HTENS. \$ IF (KRSM .EQ. 0) J4 = 5HRECOM	PEST	118
C		CPEST	119
C	*** READ FOR RATE-INDEPENDENT COMPRESSIVE MODEL. ***	CPEST	120
C		CPEST	121
	GO TO (490, 510, 520, 530, 540, 550) KCSM	PEST	122
490	CONTINUE	PEST	123
C		CPEST	124
C	** READ AND INITIALIZE FOR POREGIST. **	CPEST	125
	READ(IN, 940) A1, NREG(MP)	PEST	126
	WRITE(6, 940) A1, NREG(MP)	PEST	127
	WRITE(6, 960) IDN, IN, JO2, IDN, JO5, J2, J3, J4	PEST	128
	READ(IN, 910) A1, (RHOP(MP, I, N), I = 1, 5)	PEST	129
	WRITE(6, 910) A1, (RHOP(MP, I, N), I = 1, 5)	PEST	130

# SUBROUTINE PEST (Continued)

	WRITE(6,960)IND,IN,J02	PEST 131
	DO 498 I=1,5	PEST 132
	C050(MP,I,N) = 4.0	PEST 133
498	C1(MP,I,N) = 0.15	PEST 134
501	READ(IN,915)A1,A2	PEST 135
	BACKSPACE IN	PEST 136
	IF (A1.EQ.1MC.AND.(A2.EQ.1HO.OH.A2.EQ.1HO)) GO TO 502	PEST 137
	IF (A1.EQ.1MC.AND.A2.EQ.1H1) GO TO 503	PEST 138
	GO TO 504	PEST 139
502	READ(IN,910)A1.(C050(MP,I,N),I=1,5)	PEST 140
	WRITE(6,910)A1.(C050(MP,I,N),I=1,5)	PEST 141
	WRITE(6,960)IND,IN,J02	PEST 142
	GO TO 501	PEST 143
503	READ(IN,910)A1.(C1(MP,I,N),I=1,5)	PEST 144
	WRITE(6,910)A1.(C1(MP,I,N),I=1,5)	PEST 145
	WRITE(6,960)IND,IN,J02	PEST 146
504	CZJ = C050(MP,5,1)	PEST 147
	CWJ = C1(MP,5,1)	PEST 148
	NP=NRPG(MP)	PEST 149
	READ(IN,920)A1,P1	PEST 150
	WRITE(6,920)A1,P1	PEST 151
	WRITE(6,960)IND,IN,J02	PEST 152
	POH(MP,I,N) = P1 \$ PORH(MP,I,N) = PORC(MP,I,N) = 0.	PEST 153
	DO 505 N0=1,NP	PEST 154
	READ(IN,920)A1,P2,A2,DELPA3,YADDP(MP,N0,N)	PEST 155
	WRITE(6,920)A1,P2,A2,DELPA3,YADDP(MP,N0,N)	PEST 156
	WRITE(6,960)IND,IN,J02	PEST 157
	IF (N0.NE.1P) GO TO 5045	PEST 158
	IF (RHOP(MP,NP+1,N).GT.RHOS) GO TO 5045	PEST 159
	RHOP(MP,NP+1,N) = RHOS*(1.+TSQF(0,P2,0.,EQSTCM,EGSTDM,EGSTSM,	PEST 160
	1 EQSTGM,F0STHM,F0STEM,RHOS,F0STNM,0.))	PEST 161
	WRITE(6,932)RHOP(MP,NP+1,N)	PEST 162
	WRITE(6,960)IND,OUT,J02	PEST 163
5045	DRHO=RHOP(MP,N0+1,N)-RHOP(MP,N0,N)	PEST 164
	AA=P2-P1=4.*DELPA/RHOP(MP,N0,N)/DRHO	PEST 165
	POHA(MP,N0+1,N)=P1+RHOP(MP,N0+1,N)/DRHO*AA	PEST 166
	RR=P2-P1=4.*DELPA*(RHOP(MP,N0+1,N)+RHOP(MP,N0,N))/DRHO	PEST 167
	PORA(MP,N0+1,N)=RHOP(MP,N0+1,N)+RHOP(MP,N0,N)/DRHO*RR	PEST 168
	PORC(MP,N0+1,N)=4.*DELPA*(RHOP(MP,N0+1,N)+RHOP(MP,N0,N)/DRHO)**2	PEST 169
	YADDP(MP,N0,N) = YADDP(MP,N0,N)/DRHO	PEST 170
505	P1=P2	PEST 171
	YADDP(MP,NP+1,N) = 0.	PEST 172
	RHOP(MP,5,N) = RHOP(MP,NP+1,N)	PEST 173
	GO TO 600	PEST 174
510	CONTINUE	PEST 175
C		CPEST 176
C **	READ AND INITIALIZE FOR POWHOLT.	** CPEST 177
	READ(IN,920)A1,RHOP(MP,5,N),A2,DPDRHO,A3,PY,A4,YADDP(MP,1,N)	PEST 178
	WRITE(6,920)A1,RHOP(MP,5,N),A2,DPDRHO,A3,PY,A4,YADDP(MP,1,N)	PEST 179
	WRITE(6,960)IND,IN,J015,IND,IO5,J2,J3,J4	PEST 180
	IF (RHOP(MP,5,N).LT.100.) GO TO 512	PEST 181
	P2 = RHOP(MP,5,N)	PEST 182
	RHOP(MP,5,N)=RHOS*(1.+TSQF(0,P2,0.,EQSTCM,EGSTDM,F0STSM,EGSTGM,	PEST 183
	1 EQSTHM,F0STEM,RHOS,F0STNM,0.))	PEST 184
	WRITE(6,932)RHOP(MP,5,N)	PEST 185
	WRITE(6,960)IND,OUT,J015	PEST 186
512	RHOP(MP,2,N)=RHOP(MP,1,1)*(PY/AK(MP)+1.)	PEST 187
	RHOP(MP,3,N)=RHOS/(1.-RHOS*PY/RHOP(MP,2,N)/EQSTCM)	PEST 188
	ALFF=RHOP(MP,3,N)/RHOP(MP,2,N)	PEST 189
	R=RHOP(MP,3,N)-RHOS	PEST 190
	PORA(MP,1,N)=ALFF*(ALFF+RHOP(MP,2,N)/EQSTCM*(DPDRHO-R/RHOS)	PEST 191
	R1=POHA(MP,1,N)/(RHOP(MP,5,N)-RHOP(MP,2,N))	PEST 192
	POHA(MP,1,N)=(RHOP(MP,5,N)-RHOP(MP,3,N))/	PEST 193
	1 (RHOP(MP,5,N)-RHOP(MP,2,N))**2-R1	PEST 194
	YADDP(MP,1,N) = YADDP(MP,1,N)/(RHOP(MP,5,N)-RHOP(MP,2,N))	PEST 195
	WRITE(6,930)	PEST 196

# SUBROUTINE PEST (Continued)

	IF (N .GE. 2) GO TO 640	PEST 197
	GO TO 600	PEST 198
520	CONTINUE	PEST 199
C		CPEST 200
C **	READ AND INITIALIZE FOR CARROLL-MOLT.	** CPEST 201
	HEAD(IN,920)A1,YCH,A2,FPS(MP,N),A3,TER(MP,7,N)	PEST 202
	WRITE(6,920)A1,YCH,A2,FPS(MP,N),A3,TER(MP,7,N)	PEST 203
	WRITE(6,960)J00,IN,J03,J04,J05,J2,J3,J4	PEST 204
	IF (A1 .EQ. 10) YCH = 1 GO TO 525	PEST 205
	PY = YCH	PEST 206
	IF (ABS(FPS(MP,N)) .LT. 1.) GO TO 526	PEST 207
	P2 = FPS(MP,N)	PEST 208
	RV = 1.-RHOP(MP,1,1)/RHOS	PEST 209
C *	PY AND PC KNOWN	* CPEST 210
	RHOP(MP,5,N)=RHOS*(1.+TSQF(0,P2,0.,EUSTCM,EUSTDM,EQSTSM,EQSTGM,	PEST 211
	1 EOSTNM,EUSTFM,RHOS,EOSTNM,1.))	PEST 212
	BB = HHMTN = (RHOP(MP,5,N)/RHOS-1.)*EQSTCM/PY	PEST 213
	ALFA = 1./((1.-V)	PEST 214
	DEL(MP,N) = PY/(EQSTCM*ALOG(1.-RHOP(MP,1,1)/RHOS))	PEST 215
	IF (YCH .LT. 0.) HHMTN = AMIN1(BB,1./DEL(MP,N))	PEST 216
	HHMTN = AMAX1(HHMTN,0.24627*ALFA**2+.8512*ALFA-1.9633)	PEST 217
	IF (RH .GT. HHMTN) GO TO 521	PEST 218
	HB = HHMTN	PEST 219
	RHOP(MP,5,N) = RHOS*(1.+RH*PY/EQSTCM)	PEST 220
	F0 = 1./RH	PEST 221
	WRITE(6,927)	PEST 222
	GO TO 5215	PEST 223
521	E0 = PY**HH	PEST 224
5215	R0 = ALOG(E0)/ALOG(RV+E0)	PEST 225
	F2 = F1 = (RV+E0)**RH	PEST 226
	IF (ABS(F2-F1) .LT. 1.E-05*E1) GO TO 524	PEST 227
	R1 = ALOG(E1)/ALOG(RV+E1)	PEST 228
	NW = 0	PEST 229
522	NW = NW+1	PEST 230
	E2 = E1*EXP((RH-R1)*(ALOG(RV+E1)/(1.-RH*E1/(RV+E1))))	PEST 231
	H2 = ALOG(F2)/ALOG(RV+E2)	PEST 232
	AW = NW	PEST 233
	IF (ABS(R2-H1) .LT. 1.E-5 .OR. AW .GE. 10.) GO TO 524	PEST 234
	E0 = F1 * RC = R1 * E1 = E2 & H1 = H2	PEST 235
	GO TO 522	PEST 236
524	FPS(MP,N) = F2	PEST 237
	DEL(MP,N) = (1.-RHOP(MP,5,N)/RHOS)/ALOG(FPS(MP,N))	PEST 238
	IF (RH .LE. HHMTN) GO TO 5275	PEST 239
	GO TO 528	PEST 240
C *	YCH AND FPS KNOWN	* CPEST 241
525	DEL(MP,N) = 0.66667*YCH/EQSTCM	PEST 242
	IF (YCH .LT. 0.) FPS(MP,N) = AMAX1(FPS(MP,N),ABS(DEL(MP,N)))	PEST 243
	PY = -0.666667*YCH*ALOG(1.-RHOP(MP,1,1)/RHOS*FPS(MP,N))	PEST 244
	GO TO 527	PEST 245
C *	PY AND FPS KNOWN	* CPEST 246
526	DEL(MP,N) = -PY/EQSTCM/ALOG(1.-RHOP(MP,1,1)/RHOS*FPS(MP,N))	PEST 247
	IF (YCH .LT. 0.) FPS(MP,N) = AMAX1(FPS(MP,N),ABS(DEL(MP,N)))	PEST 248
527	RHOP(MP,5,N) = RHOS*(1.-DEL(MP,N)*ALOG(FPS(MP,N)))	PEST 249
5275	CALC EUST(0.,RHOP(MP,5,N),P2,M,1.)	PEST 250
C *	ALL C-H	* CPEST 251
528	ALE(MP,N) = DEL(MP,N)*ALOG(FPS(MP,N))	PEST 252
	APC(MP,N) = RHOS/RHOP(MP,5,N)	PEST 253
	WRITE(6,925)PY,P2,FPS(MP,N)	PEST 254
	WRITE(6,960)J00,OUT,J03,J04	PEST 255
	WRITE(6,932)RHOP(MP,5,N)	PEST 256
	WRITE(6,960)J00,OUT,J03,J04	PEST 257
	FPS(MP,N) = 1.+FPS(MP,N)	PEST 258
	GO TO 600	PEST 259
530	CONTINUE	PEST 260
C		CPEST 261
C **	READ INPUT AND INIT FOR MEHRMANN P-ALPHA.	** CPEST 262

# SUBROUTINE PEST (Continued)

READ(IN,920)A1,PC,A2,PY	PEST 263
WRITE(6,920)A1,PC,A2,PY	PEST 264
WRITE(6,960)TDD,IN,J05,J06,J05,J2,J3,J4	PEST 265
PORA(MP,1,N) = PY \$ PORC(MP,1,N) = PC	PEST 266
GO TO 600	PEST 267
CONTINUE	PEST 268
C	CPEST 269
C ** READ AND INIT FOR WENDRON.	** CPEST 270
GO TO 600	PEST 271
550 CONTINUE	PEST 272
C	CPEST 273
C ** READ AND INIT FOR THS.	** CPEST 274
GO TO 600	PEST 275
600 IF (N,RF, 2) GO TO 640	PEST 276
N = 2	PEST 277
J2=KHTENS * J3=J4=1H	PEST 278
C	CPEST 279
C *** READ FOR RATE-INDEPENDENT TENSION MODEL.	*** CPEST 280
C	CPEST 281
IF (KTSM.EQ. 1.AND. KCSM.EQ. 3) GO TO 610	PEST 282
GO TO (615,620,570) KTSM	PEST 283
C	CPEST 284
C ** REPEAT CARROLL-MOLT ARRAY FOR N=2.	** CPEST 285
610 ALE(MP,2)=ALE(MP,1) \$ EPS(MP,2)=EPS(MP,1)	PEST 286
DEL(MP,2)=DEL(MP,1) \$ TER(MP,7,2) = TER(MP,7,1)	PEST 287
APC(MP,2)=1./(1.-ALE(MP,N))	PEST 288
KHOP(MP,5,N)=RHOS/APC(MP,2)	PEST 289
WRITE(6,932)KHOP(MP,5,N)	PEST 290
WRITE(6,960)TDD,OUT,J03,J04,J05,J2	PEST 291
GO TO 600	PEST 292
615 CONTINUE	PEST 293
C	CPEST 294
C ** READ AND INIT FOR CONSTANT STRENGTH.	** CPEST 295
READ(IN,920)A1,TER(MP,5,N),A2,TER(MP,7,N)	PEST 296
WRITE(6,920)A1,TER(MP,5,N),A2,TER(MP,7,N)	PEST 297
WRITE(6,960)TDD,IN,J07,J08,J05,J2	PEST 298
GO TO 600	PEST 299
620 CONTINUE	PEST 300
C	CPEST 301
C ** READ AND INIT FOR KIC.	** CPEST 302
READ(IN,945)A1,KIC(MP),A2,TER(MP,7,N)	PEST 303
WRITE(6,945)A1,KIC(MP),A2,TER(MP,7,N)	PEST 304
WRITE(6,960)TDD,IN,J09,J010,J05,J2	PEST 305
GO TO 600	PEST 306
630 CONTINUE	PEST 307
IF (N,FO, 3) GO TO 700	PEST 308
N = 2	PEST 309
J2=KHECOM	PEST 310
C	CPEST 311
C *** READ FOR RATE-INDEPENDENT RECOMPRESSION MODEL.	*** CPEST 312
C	CPEST 313
IF (KHSM.GT. 0) GO TO 640	PEST 314
C	CPEST 315
C ** REPEAT ARRAYS KHS=KCS.	** CPEST 316
GO TO (641,645,647,648) KCSM	PEST 317
C	CPEST 318
C ** POWEQST.	** CPEST 319
641 MPP = MP	PEST 320
DO 642 NO = 1,MPP	PEST 321
PORA(MP,NO,3)=PORA(MP,NO,1) \$ YADDP(MP,NO,3)=YADDP(MP,NO,1)	PEST 322
PORC(MP,NO,3)=PORC(MP,NO,1) \$ PORC(MP,NO,3)=PORC(MP,NO,1)	PEST 323
642 CONTINUE	PEST 324
DO 644 N=1,5	PEST 325
KHOP(MP,NO,3)=KHOP(MP,NO,1) \$ COSQ(MP,NO,3)=COSQ(MP,NO,1)	PEST 326
C1(MP,NO,3)=C1(MP,NO,1)	PEST 327
IF (NO.EQ. 5) GO TO 644	PEST 328

# SUBROUTINE PEST (Continued)

```

644 CONTINUE                                PEST 329
      GO TO 700                                PEST 330
C                                          CPEST 331
C **      PORHOLT.                                ** CPEST 332
645 PORH(MP,1,3)=PORH(MP,1,1) $ PORH(MP,1,3)=PORH(MP,1,1) PEST 333
      RHOP(MP,5,3) = RHOP(MP,5,1) $ RHOP(MP,2,3) = RHOP(MP,2,1) PEST 334
      RHOP(MP,3,3) = RHOP(MP,3,1) $ YADP(MP,1,3) = YADP(MP,1,1) PEST 335
      GO TO 700                                PEST 336
C                                          CPEST 337
C **      CARROLL-HOLT MODEL.                                ** CPEST 338
647 APC(MP,3)=APC(MP,1) $ EPS(MP,3)=EPS(MP,1) PEST 339
      DEL(MP,3)=DEL(MP,1) $ RHOP(MP,5,3)=RHOP(MP,5,1) PEST 340
      GO TO 700                                PEST 341
C                                          CPEST 342
C **      WERHMANN P-ALPHA MODEL.                                ** CPEST 343
648 PORH(MP,1,3) = PORH(MP,1,1) $ PORC(MP,1,3) = PORC(MP,1,1) PEST 344
      RHOP(MP,1,3) = RHOP(MP,1,1) PEST 345
      GO TO 700                                PEST 346
660 GO TO (400,510,520,530,540,550) KRSM PEST 347
C                                          CPEST 348
C ***      READ FOR RATE EFFECTS IN COMPRESSION.                                *** CPEST 349
C                                          CPEST 350
700 N = 1 PEST 351
      J2=KCOMP, $ J3=J4=1H PEST 352
      IF (KTUM.EQ. 0) J3=5HTENS, $ IF (KHUM.EQ. 0) J4=5HRECOM PEST 353
      IF (KCUH.EQ. 1) GO TO 740 PEST 354
      GO TO (750,720,730,740) KCUH PEST 355
720 CONTINUE                                CPEST 356
C                                          CPEST 357
C **      READ AND INIT FOR LINEAR VISCOUS VOID (C) OR DUCTILE FRACTURE (T) PEST 358
      HEAD(IN,010)A1,(TFH(MP,I,N),I=1,7) PEST 359
      WRITE(6,010)A1,(TFH(MP,I,N),I=1,7) PEST 360
      IF (N.EQ. 1 .OR. N.EQ. 3) WRITE(6,060)IDD,IN,JQ11,JQ12,JUR, PEST 361
      J2,J3,J4 PEST 362
      IF (N.EQ. 2) WRITE(6,060)IDD,IN,JQ17,JQ18,JQ19,J2 PEST 363
      IF (TFH(MP,N,N).EQ. 0.)TFH(MP,N,N)=0.3,14159*TFR PEST 364
      (MP,3,N)**3*TFH(MP,4,N) PEST 365
      GO TO 750 PEST 366
730 CONTINUE                                CPEST 367
C                                          CPEST 368
C **      READ AND INIT DYNAMIC PORHOLT.                                ** CPEST 369
      READ(IN,020)A1,TPH(MP,N) PEST 370
      WRITE(6,020)A1,TPH(MP,N) PEST 371
      WRITE(6,060)IDD,IN,JQ13,JQ14,JUR,J2,J3,J4 PEST 372
      GO TO 750 PEST 373
740 CONTINUE                                CPEST 374
C                                          CPEST 375
C *      READ AND INIT DYNAMIC BUTCHER P-ALPHA-TAU.                                ** CPEST 376
      HEAD(IN,020)A1,TFH(MP,N) PEST 377
      WRITE(6,020)A1,TFH(MP,N) PEST 378
      DADP(MP,N)=-ALFO/AK(MP)*(1.-AK(MP)*ALFO/ECST(M) PEST 379
      WRITE(6,060)IDD,IN,JQ13,JQ14,JUR,J2,J3,J4 PEST 380
750 N = N+1 PEST 381
C                                          CPEST 382
C ***      READ FOR RATE EFFECTS IN TENSION.                                *** CPEST 383
C                                          CPEST 384
      GO TO (700,755,770,900) A PEST 385
755 J2=HTENS PEST 386
      IF (KTUM.GT. 0) GO TO (750,720,760) KTUM PEST 387
      IF (KCUH.EQ. 0) GO TO 750 PEST 388
C                                          CPEST 389
C **      REPEAT ARRAYS KTD=KCD.                                ** CPEST 390
      IF (KCUH.EQ. 1) GO TO 750 PEST 391
      IF (KCUH.GT. 2) GO TO 756 PEST 392
C                                          CPEST 393
C **      REPEAT LINEAR VISCOUS VOID FOR DUCTILE FRACTURE.                                ** CPEST 394
      TFR(MP,1,2)=TFR(MP,1,1) $ TFR(MP,2,2)=-TFR(MP,2,1)

```

# SUBROUTINE PEST (Continued)

```

TER(MP,3,2)=TFW(MP,3,1) $ TER(MP,4,2)=TER(MP,4,1)          PEST 395
TER(MP,5,2)=TER(MP,5,1) $ TER(MP,6,2)=TER(MP,6,1)          PEST 396
TER(MP,7,2) = TER(MP,7,1) $ TER(MP,8,2) = TER(MP,8,1)      PEST 397
GO TO 750                                                    PEST 398
750 IF (KCDM .GT. 3) GO TO 750                                PEST 399
C                                                            CPEST 400
C ** READ WRITTLE FRACTURE AND FRAGMENTATION.              ** C PEST 401
750 CONTINUE                                                  PEST 402
760 CONTINUE                                                  PEST 403
GO TO 750                                                    PEST 404
C                                                            CPEST 405
C ** READ FOR RATE EFFECTS IN RECOMPRESSION.                *** CPEST 406
770 J2=5HRECOM                                                PEST 407
IF (KNDM .GT. 0) GO TO 800                                    PEST 408
C                                                            CPEST 409
C ** REPEAT ARRAYS KND=KCD AS FOLLOWS.                      ** CPEST 410
IF (KCDM .EQ. 0) GO TO 400                                    PEST 411
GO TO (900,700,705,790) KCDM                                PEST 412
C                                                            CPEST 413
C ** REPEAT FOR LINEAR VISCOUS VOID COMPRESSION MODEL.      ** CPEST 414
780 TER(MP,1,3)=TER(MP,1,1) $ TER(MP,2,3)=TER(MP,2,1)      PEST 415
TER(MP,3,3) = TER(MP,3,1) $ TER(MP,4,3) = TER(MP,4,1)      PEST 416
TER(MP,5,3) = TER(MP,5,1) $ TER(MP,6,3) = TER(MP,6,1)      PEST 417
TER(MP,7,3) = TER(MP,7,1) $ TER(MP,8,3) = TER(MP,8,1)      PEST 418
GO TO 400                                                    PEST 419
C                                                            CPEST 420
C ** REPEAT FOR DYNAMIC PORHOLT MODEL.                      ** CPEST 421
785 TPH(MP,3)=TPH(MP,1)                                       PEST 422
GO TO 400                                                    PEST 423
C                                                            CPEST 424
C ** REPEAT FOR BUTCHER P-ALPHA-TAU MODEL.                  ** CPEST 425
790 TPH(MP,3)=TPH(MP,1) $ DAUP(MP,3)=DANP(MP,1)            PEST 426
GO TO 400                                                    PEST 427
800 GO TO (900,720,730,740) KNDM                             PEST 428
900 NETIWN                                                    PEST 429
910 FORMAT(A10,7F10,3)                                       PEST 430
915 FORMAT(1X,2A1)                                           PEST 431
920 FORMAT(4(A10,E10,3))                                     PEST 432
925 FORMAT(* PY=E10,3,* PC=E10,3,* EPS=E10,3)               PEST 433
927 FORMAT(* ABSOLUTE VALUE OF CONSOLIDATION PRESSURE WAS CHANGED TO
1 BE WITHIN ALLOWABLE RANGE*)                               PEST 435
930 FORMAT(/)                                                 PEST 436
932 FORMAT(* CONSOLIDATION DENSITY=E10,3)                    PEST 437
935 FORMAT(2(A10,16,12,12))                                  PEST 438
940 FORMAT(A10,I10,A10,E10,3)                                PEST 439
945 FORMAT(A1,E10,3)                                          PEST 440
950 FORMAT(* BULK AND SHEAR MODULI ARE CHANGED TO *2E12,3,* DYN/CM2*) PEST 441
960 FORMAT(1H*,7QX,5H IND=A2,5H, IN=I2,A10,A9,4A5)          PEST 442
C                                                            CPEST 443
C *****                                                    CPEST 444
C COMPUTATION OF PRESSURE DURING WAVE PROPAGATION.          CPEST 445
C *****                                                    CPEST 446
C                                                            CPEST 447
1000 MP = NPM(N)                                             PEST 448
IMH=                                                         PEST 449
C                                                            CPEST 450
C ** COMPUTE BULK AND SHEAR MODULI APPROPRIATE TO CURRENT E AND O. CPEST 451
C                                                            CPEST 452
TF = 1.+F*EOSTGM*HMOS/EOSTCM                                PEST 453
DREF = D*TF                                                  PEST 454
HVV1 = ARS(RVV) $ ALFD1 = 1./(1.-RVV1) $ PHO1 = RHO1        PEST 455
IF (RVV .LT. 0. .AND. DREF/HMOS .LT. 1.-ARS(HVV1)) GO TO 2000 PEST 456
IF (RHO1 .EQ. 0.) RHO1=DOLD                                  PEST 457
IF (FLG(MP).EQ.0. .AND. MUM .NE. 0.) ELG(MP)=(1.-MUP(MP)*F/MUM) PEST 458
1 / (1.-PHOP(MP,1,1)/HMOS) _ PEST 459
IF (F .EQ. 0.) GO TO 1000 PEST 460

```



# SUBROUTINE PEST (Continued)

IF (M.EQ. 5R S.OR. M.EQ. 5R M) GO TO 1800	PEST 461
ALF=RHO5/RHO1	PEST 462
RULK=ELSTCM*F/(ALF*ELK(MP)*(ALF-1))	PEST 463
MUM=AMAX1(0.,MUM*(1.-ELG(MP)*ELG(MP)/ALF))	PEST 464
C=SORT((RULK*MUM)/D)	PEST 465
C	CPEST 466
C *** COMPUTE PRESSURE FROM ELASTIC RELATIONS.	*** CPEST 467
PEL=RULK*(D/RHO1*TF-1.)	PEST 468
C	CPEST 469
C ** BRANCH TO TENSILE OR COMPRESSIVE ROUTES.	** CPEST 470
C	CPEST 471
IF (PEL.LT. 0.) GO TO 1500	PEST 472
C	CPEST 473
C *** COMPRESSION PATH.	*** CPEST 474
C	CPEST 475
KCHS=KCS(MP) S N=1	PEST 476
IF (M.EQ. 5R T) M = 5R Q	PEST 477
IF (M.NE. 5R Z.AND. M.NE. 5R M) GO TO 1090	PEST 478
M = 5R M	PEST 479
KCRS = KRS(MP)	PEST 480
IF (KRS(MP).EQ. 0) KCHS = KCS(MP)	PEST 481
N = 1	PEST 482
1090 GO TO (1100,1120,1140,1160,1180) KCRS	PEST 483
C	CPEST 484
C *** CALCULATION OF COMPACTION CURVE.	*** CPEST 485
C	CPEST 486
C ** POROSITY MODEL.	** CPEST 487
1100 NC = 0	PEST 488
PST = 0.	PEST 489
IF (DREF.GT. RHOP(MP,5,N)) GO TO 1109	PEST 490
1105 NC = NC+1	PEST 491
IF (DREF.GT. RHOP(MP,NC,N)) GO TO 1105	PEST 492
PST = 1*(POHA(MP,NC,N)+POHB(MP,NC,N)/DREF+PORC(MP,NC,N)/DREF**2)	PEST 493
NQ = MAX0(1,NC-1)	PEST 494
CZJ = CPCS(MP,NQ,N) S CWJ = C1(MP,NQ,N)	PEST 495
YADDN = YADDP(MP,NQ,N)	PEST 496
C	CPEST 497
C * CHECK FOR CONSOLIDATION IN LAST POROUS REGION.	* CPEST 498
1108 IF (DREF.LT. RHOS) GO TO 1300	PEST 499
1109 GO TO (1110,1112,1114) NPRM	PEST 500
1110 CALL FUST(E,D,PS,M,CJ,DPDDJ,DPDEJ)	PEST 501
GO TO 1114	PEST 502
1112 CALL FSA(1,5,M,CJ,D,E,PS,DPDDJ,DPDEJ)	PEST 503
GO TO 1114	PEST 504
1114 CALL EUSTPF(1,5,M,CJ,D,E,PS)	PEST 505
1116 IF (PS.LT. PST) GO TO 1300	PEST 506
PST = PS	PEST 507
JH = 5R S	PEST 508
IF (PS.LT. PFL) GO TO 1300	PEST 509
PJ = PS S M = 5R S S PVV = 0.	PEST 510
GO TO 1900	PEST 511
C	CPEST 512
C ** BOWHOLT MODEL.	** CPEST 513
1120 DREF=AMAX1(DREF,RHOP(MP,1,N))	PEST 514
ALFS = (RHOP(MP,2,N)*(POHA(MP,1,N)+POHB(MP,1,N)*(DREF-RHOP(MP,2,N)	PEST 515
1))*(DREF-RHOP(MP,2,N)))/DREF	PEST 516
ALFS=AMAX1(ALFS,1.)	PEST 517
DS = ALFS*DREF	PEST 518
GO TO (1126,1128,1130) NPRM	PEST 519
1126 CALL FUST(0.,DS,PS,M,CJ,DPDDJ,DPDEJ)	PEST 520
GO TO 1134	PEST 521
1128 CALL FSA(1,5,M,CJ,DS,D.,PS,DPDDJ,DPDEJ)	PEST 522
GO TO 1134	PEST 523
1130 CALL EUSTPF(1,5,M,CJ,DS,D.,PS)	PEST 524
1134 PST = PS/ALFS*F	PEST 525
YADDN = YADDP(MP,1,N)	PEST 526

# SUBROUTINE PEST (Continued)

GO TO 1104	PEST 527
C	CPEST 528
C ** CARROLL-MOLT MODEL.	** CPEST 529
1140 RNEW = 1.0	PEST 530
IF (ORLF .GT. RHOP(MP,5,N)) GO TO 1143	PEST 531
RNEW = RD = DREF/PHOS	PEST 532
IF (RNEW .GT. 2.-1./APC(MP,N)) RNEW = 1.+0.5*(HP-1./APC(MP,N))	PEST 533
NW = N	PEST 534
1141 H1 = H*DEL(MP,N)*ALOG(EPS(MP,N)-RNEW)	PEST 535
RNEW = A*IN1(RNEW*(H)-RNEW)/(1.+DEL(MP,N)/(EPS(MP,N)-RNEW))*0.9999	PEST 536
19999)	PEST 537
NW = NW+1	PEST 538
AW = NW	PEST 539
IF (ABS(RNEW-R1) .GT. 1.E-6 .AND. AW .LT. 10.) GO TO 1141	PEST 540
1143 US = DREF/RNEW	PEST 541
GO TO (1145,1147,1149) NPHM	PEST 542
1145 CALL EUST(0.,05,PS,N,CJ,DPDDJ,DPDEJ)	PEST 543
GO TO 1155	PEST 544
1147 CALL FSA(1.5,M,CJ,DS,N.,PS,DPDDJ,DPDEJ)	PEST 545
GO TO 1155	PEST 546
1149 CALL EUSTPF(1.5,M,CJ,DS,N.,PS)	PEST 547
1155 PST = PS*RNEW*F	PEST 548
GO TO 1104	PEST 549
1160 CONTINUE	PEST 550
C	CPEST 551
C ** HERRMANN P-ALPHA.	** CPEST 552
PST = 0.	PEST 553
UC = RHOS*(PORC(MP,1,N)*F/EQSTCM+1.)/TF	PEST 554
UC = RHOS*(1.+TSOE(N,PORC(MP,1,N)*F,EQSTGM*UC*F,EQSTCM,	PEST 555
1 EQSTLM,EUSTGM,EUSTHM,EUSTHM,EQSTFM,RHOS,EQSTNM,F))	PEST 556
IF (DC .LT. 0) GO TO 1104	PEST 557
DY = RHOP(MP,1,N)/TF*(1.+POWA(MP,1,N)/AK(MP))	PEST 558
ALFY = 1./(DY*TF/RHOS-PORA(MP,1,N)*F/EQSTCM)	PEST 559
UD = AMAX1(0,DY)	PEST 560
UYU = UY*ALFY/UD	PEST 561
DCU = UC/UD	PEST 562
H1 = (UCD-UYU)**2/(ALFY - 1.)	PEST 563
H2 = DCD*H1/2.	PEST 564
ALFC = H2-SQRT(H2*H2-DCD*UCD-H1)	PEST 565
DS = ALFC*UD	PEST 566
GO TO (1170,1172,1174) NPHM	PEST 567
1170 CALL EUST(E,DS,PS,N,CJ,DPDDJ,DPDEJ)	PEST 568
GO TO 1174	PEST 569
1172 CALL FSA(1.5,M,CJ,DS,F,PS,DPDDJ,DPDEJ)	PEST 570
GO TO 1174	PEST 571
1174 CALL EUSTPF(1.5,M,CJ,DS,E,PS)	PEST 572
1174 IF (D .GE. DY) GO TO 1179	PEST 573
UYU = UY*ALFY/D	PEST 574
UCU = UC/D	PEST 575
H1 = (UCD-UYU)**2/(ALFY - 1.)	PEST 576
H2 = DCD*H1/2.	PEST 577
ALFC = H2-SQRT(H2*H2-DCD*UCD-H1)	PEST 578
1179 PST = PS/ALFC	PEST 579
IF (PEL .LT. PST) GO TO 1300	PEST 580
PJ = PST	PEST 581
1180 CONTINUE	PEST 582
1300 PJ = PEL	PEST 583
IF (PST .LT. PEL) PJ = PST	PEST 584
C	CPEST 585
C * COMPUTE RELATIVE VOID VOLUME (RVV)	* CPEST 586
C	CPEST 587
PTH=TSOF(1,F,RHOS/D,EQSTGM*RHOS*E,EUSTGM,EUSTDM,EUSTSM,EQSTGM,	PEST 588
1 EUSTHM,EUSTEM,PHOS,EQSTNM,F)	PEST 589
IF (PJ .NE. 0.) RVV=AMAX1(1.-PJ/PTH,0.)	PEST 590
IF (PJ .EQ. 0.) RVV=AMAX1(0.,1.-D/PTH)	PEST 591
ALFC=1./(1.-RVV)	PEST 592

# SUBROUTINE PEST (Continued)

```

IF (AST1 .EQ. 0.) AST1 = ALFS                                PEST 593
IF (PEL .GT. PST) GO TO 1310                                  PEST 594
IF (IM .NE. SR S) GO TO 1900                                  PEST 595
RVV = 0. S H = SR S S GO TO 1900                             PEST 596
C                                                                CPEST 597
C *** DYNAMIC PRESSURE. *** CPEST 598
C                                                                CPEST 599
1310 KCRD=KLD(MP)                                              PEST 600
IF (H .EQ. 5R R .AND. KRD(MP) .NE. 0) KCRD = KRD(MP)        PEST 601
IF (KCRD .GT. 1) GO TO 1320                                   PEST 602
C                                                                CPEST 603
C ** NO RATE-DEPENDENCE. ** CPEST 604
IF (IM .EQ. SR S) H = 5R S                                     PEST 605
GO TO 1900                                                     PEST 606
1320 PEL=TSOF(1,PEL*RHUS/D,EQSTGM*RHUS*E,EQSTCM,FQSTDM,EQSTSM,EQSTGM, PEST 607
1 EQSTHM,FQSTFM,RHUS,FQSTNM,E)                                PEST 608
IF (PEL .NE. 0.) ALFL=PELS/PEL                                PEST 609
IF (PEL .EQ. 0.) ALFL=PELS/D                                  PEST 610
ALFD = (ALFS-AST1)/DT                                          PEST 611
ALFLD = (ALFL - ALFD)/DT                                       PEST 612
GO TO (1900,1340,1380,1440) KCRD                               PEST 613
C                                                                CPEST 614
C ** LINEAR VISCOUS VOID COMPACTION. ** CPEST 615
1340 VVE = 1.-1./ALFL                                          PEST 616
DV = DVO = 1./D-1./DOLD                                       PEST 617
NLOOP=MAX(1,1.-DV*EQSTCM/D/AMAX1(PST,P)/ALF*0.0,-4.*TER(MP,1,N)*DT) PEST 618
1 *(P-PST1))                                                    PEST 619
VOLN = 1./DOLD * VSO = (1.-RVV1)/DOLD                         PEST 620
NTRY = 0                                                        PEST 621
RVV1 = RVV1                                                    PEST 622
PTH1 = PTH0 = PST1*AST1                                         PEST 623
PSO = AMAX1(P,PST1)/(1.-RVV1)                                   PEST 624
IF (PST1 .LT. 0.) PSO=PTH1=PTH0=0.                               PEST 625
IF (1.-RVV1 = 1./AST1 .LT. 0. .AND. PSO .GT. PTH0) GO TO 13401 PEST 626
RVPO = -1./((DOLD*EQSTCM)                                       PEST 627
DRVP = 0.                                                       PEST 628
GO TO 13403                                                     PEST 629
13401 RVPO = (1.-RVV1-1./AST1)/DOLD/(PSO-PTH0)                 PEST 630
DRVP = (RVV-VVE)/D/(PELS-PTH)-RVPO                             PEST 631
13403 VSTH = 1./((DOLD*AST1)                                     PEST 632
IF (PST1 .LE. 0. .OR. PST1 .GT. P) PTH1=PTH0=PTH              PEST 633
DVSTH = (1.-RVV1)/D-VSTH                                        PEST 634
DVDP = (VVE/D-RVV1/DOLD)/(PELS-PSO)                             PEST 635
DPH = PTH-PTH0                                                  PEST 636
1341 DELV = DV/NLOOP S VH = VOLN S DTN = DELV/DVO*DT          PEST 637
A1 = TER(MP,1,N)*DTN                                            PEST 638
C BEGIN DO LOOP FOR SUBCYCLING                                  PEST 639
DO 1347 NL = 1,NLOOP                                           PEST 640
VH = VH+DELV S RATIO = (VH-1./DOLD)/DVO                       PEST 641
RVP = RVPO+DRVP*RATIO                                           PEST 642
VSTH = VSTH+DVSTH*RATIO                                         PEST 643
PTHH = PTH0+DPH*RATIO                                           PEST 644
C FIRST ESTIMATE OF PRESSURE IN SOLID                          PEST 645
DP = AMAX1(0.,PSO-PTHH)                                         PEST 646
XG = 1. S IF (DP .GE. 0.) XG = EXP(A1*DP)                       PEST 647
PLO = PTHH * PHP = PELH = AMAX1(P,PST1)/(1.-RVV1)+(PELS-AMAX1(P, PEST 648
1 PST1)/(1.-RVV1))*RATIO                                         PEST 649
PSA = PELH * ZR = RVVL*VH                                        PEST 650
IF (PTHH .GT. PELH) GO TO 1345                                   PEST 651
PSJ = (DELV+VSO-VSTH+PTHH+RVP+PSO+DVDP+RVVL*VH*(XG*(1.+A1/2.* PEST 652
1 (-PTHH-PSO+PTH1))-1.))/(RVP+DVDP+RVVL*VH*XG*A1/2.)          PEST 653
NC = 0                                                         PEST 654
1342 NC = NC+1                                                  PEST 655
DP = (AMAX1(0.,PSJ-PTHH)*AMAX1(0.,PSO-PTH1))/2.               PEST 656
ZG = RVVL*VH S IF (DP .GE. 0.) ZG = ZG*EXP(A1*DP)             PEST 657
DELVA = VSTH-VSO+RVP*(PSJ-PTHH)+DVDP*(PSJ-PSO)+ZG-RVVL*VH    PEST 658

```

# SUBROUTINE PEST (Continued)

PSA = PSJ	PEST 659
AC = NC	PEST 660
IF (ABS(DELVA-DELV) .LT. 1.E-5*VH .OR. (PSJ .LE. PTHH .AND. AC	PEST 661
1 .GT. 1.)) GO TO 1346	PEST 662
IF (AC .GE. 1) GO TO 1344	PEST 663
IF (DELVA .GT. DELV) PLO = AMAX1(PSA,PLO)	PEST 664
IF (DELVA .LT. DELV) PUP = AMIN1(PSA,PUP)	PEST 665
C MAKE 2ND ESTIMATE OF PRESSURE IN THE SOLID	PEST 666
IF (MOD(AC,2) .EQ. 0) GO TO 1343	PEST 667
PSJ = PSJ + (DELV-DELVA)/(RVP+DVDP+ZG*41/2.)	PEST 668
GO TO 1344	PEST 669
C INTERPOLATION ESTIMATE OF PRESSURE IN SOLID	PEST 670
1343 PSJ = PSA + (DELV-DELVA)/(DELVB-DELVA)*(PSH-PSA)	PEST 671
1344 CONTINUE	PEST 672
IF (PSJ .GT. PUP) PSJ = PUP+.E7	PEST 673
IF (PSJ .LT. PLO) PSJ = PLO+.E7	PEST 674
IF (AC .EQ. 1) GO TO 1345	PEST 675
IF (ABS(DELVA-DELV) .GT. ABS(DELVB-DELV)) GO TO 1342	PEST 676
1345 PSB = PSA + DELVB - DELVA \$ GO TO 1342	PEST 677
C CONCLUSION OF LOOP	PEST 678
1346 RVVL = ZG/VH \$ PTHL = PTHH \$ PSA = PSB = AMAX1(PTHH,AMIN1	PEST 679
1 (PELH,PSA))	PEST 680
VSO = VH-ZG \$ ENT = ENT*VH/D/VH	PEST 681
1347 CONTINUE	PEST 682
PJ = (1.-RVVL)*PSA \$ RVV = RVVL \$ GO TO 1900	PEST 683
C PROVISION FOR ABORT FOR ITERATION FAILURE	PEST 684
1348 NTRY = NTRY+1 \$ IF (NTRY .GE. 5) GO TO 1349	PEST 685
VOLD = VH-DELV \$ DV = 1./D-VOLD	PEST 686
ALUP = MAX1(3.,-2.*NTRY*DV*EUSTCM/D/AMAX1(PST,P)/ALF+0.8)	PEST 687
GO TO 1341	PEST 688
1349 WRITE(6,2349)M,P,DV,DELVA,DELVB	PEST 689
GO TO 1346	PEST 690
C	CPEST 691
C ** PORHOUT MODEL = DYNAMIC.	** CPEST 692
1380 ALFD = TPH(MP,N)*ALFLD +AST1 +ALFSD*(DT-TPH(MP,N))*(ALFD1-TPH(	PEST 693
1 MP,N)*ALFLD-AST1+TPH(MP,N)*ALFSD)*EXP(-DT/TPH(MP,N))	PEST 694
1382 DS = ALFD/D	PEST 695
GO TO (1385,1390,1395) NPRM	PEST 696
1385 CALL FUST(E,DS,PS,M,CJ,DPDDJ,DPDEJ)	PEST 697
GO TO 1400	PEST 698
1390 CALL ESA(1.5,M,CJ,DS,E,PS,UPDDJ,UPDEJ)	PEST 699
GO TO 1400	PEST 700
1395 CALL EUSTPH(1.5,M,CJ,DS,E,PS)	PEST 701
1400 PJ=AMIN1(PEL,AMAX1(PST,PS/ALFD))	PEST 702
PS1=TSUE(1,PJ,RHOS/D,FUSTGM*RHOS+E,FUSTCM,EUSTDM,FOSTSM,EUSTGM,	PEST 703
1 EOSTHM,FUSTFM,RHOS,FOSTNM,F)	PEST 704
IF (PJ .NE. 0.) RVV=AMAX1(0.,1.-PJ/PS)	PEST 705
IF (PJ .EQ. 0.) RVV=AMAX1(0.,1.-D/PS)	PEST 706
1420 CONTINUE	PEST 707
GO TO 1900	PEST 708
C ** BUTCHER P=ALPHA-TAU	** CPEST 709
1440 CONTINUE	PEST 710
HT=TPH(MP,N)*(ALFL-ALFS)/DADP(MP,N)/(PEL-PST)	PEST 711
ALFD=((ALFL-ALFD1)*RT/(DT-ALFS+ALFD1)*EXP(DT/HT)+ALFS-(ALFL-ALFD1)*	PEST 712
1 HT/D)	PEST 713
IF (ALFD .LT. ALFS) ALFD = ALFS	PEST 714
IF (ALFD .GT. ALFL) ALFD = ALFL	PEST 715
GO TO 1342	PEST 716
C	CPEST 717
C *** TENSILE PATH.	*** CPEST 718
C ** STATIC FRACTURE THRESHOLD CURVE.	** CPEST 719
C	CPEST 720
1500 KTSS = KTS(MP)	PEST 721
IF(KTSS .EQ. 0) KTSS = KCS(MP)	PEST 722
N = 2	PEST 723
GO TO (1520,1540,1560) KTSS	PEST 724

# SUBROUTINE PEST (Continued)

C		CPEST 725
C **	CONSTANT STRENGTH.	** CPEST 726
1520	PTH = 1FR(MP,5,N)*F	PEST 727
	PST = UPTH*(1./RHOS*EOSTGM*F/EOSTCM)/(1.+PTH/EOSTCM)	PEST 728
	GO TO 1600	PEST 729
C		CPEST 730
C **	FRACTURE MECHANICS.	** CPEST 731
1540	GO TO 1520	PEST 732
C		CPEST 733
C **	CARROLL-HOLT THRESHOLD STRESS.	** CPEST 734
1560	PST = PFI	PEST 735
	IF (DREF .GT. WHOP(MP,5,N)) GO TO 1600	PEST 736
	RNEW = R0 = DREF/RHOS	PEST 737
	NW = 1	PEST 738
1565	H1 = R0*DEL(MP,N)*ALOG(FPS(MP,N)-BNEW)	PEST 739
	BNEW = AMIN(RNEW*(H1-RNEW)/(1.+DEL(MP,N)/(EPS(MP,N)-RNEW)),0.9999)	PEST 740
19990		PEST 741
	NW = NW+1	PEST 742
	AW = NW	PEST 743
	IF (ARS(RNEW-R1) .GT. 1.E-6 .AND. AW .LT. 10.) GO TO 1565	PEST 744
	US = DREF/RNEW	PEST 745
	GO TO (1570,1572,1574) NPHM	PEST 746
1570	CALL EUST(0.,05,PS,M,CJ,DPDQJ,DPDEJ)	PEST 747
	GO TO 1580	PEST 748
1572	CALL ESA(1.5,M,CJ,US,0.,PS,DPDQJ,DPDEJ)	PEST 749
	GO TO 1580	PEST 750
1574	CALL EUSTPF(1.5,M,CJ,US,0.,PS)	PEST 751
1580	PST = P0HNEW*F	PEST 752
	IF (PST .GT. PS) GO TO 1600	PEST 753
	PST = PS	PEST 754
	IM = SM S	PEST 755
	IF (PEL .GT. PS) GO TO 1600	PEST 756
	KJ = PS	PEST 757
	M = SM S C RVV = 1.	PEST 758
	GO TO 1600	PEST 759
1600	PJ = PEL	PEST 760
	IF (M .NE. 50 S) M = 50 T	PEST 761
	IF (PEL .LT. PST) M = 50 T	PEST 762
	IF (PEL .LT. PST) KJ = PST	PEST 763
C		CPEST 764
C **	COMPUTE RELATIVE VOID VOLUME (RVV)	** CPEST 765
C		CPEST 766
	PTH=TSUF(1,PJ,RHOS/D,EOSTGM*RHOS*E,EOSTCM,EUSTDM,F0STSM,EOSTGM,	PEST 767
1	EOSTHM,F0STFM,RHOS,F0STNM,F)	PEST 768
	IF (PJ .NE. 1.) RVV = AMAX1(0.,1.-PJ/PTH)	PEST 769
	IF (PJ .EQ. 1.) RVV=AMAX1(0.,1.-D/PTH)	PEST 770
	ALFS = 1./(1.-RVV)	PEST 771
	IF (RVV .GT. TER(MP,7,N)) GO TO 2000	PEST 772
	IF (PEL .GE. PST) GO TO 1600	PEST 773
C		CPEST 774
C **	DYNAMIC TENSILE PRESSURE.	** CPEST 775
C		CPEST 776
	KTD0 = KTD(MP)	PEST 777
	IF (KTD0 .EQ. 0.) KTD0 = KCD(MP)	PEST 778
	IF (KTD0 .EQ. 0 .AND. KCDM .EQ. 0) KTD0 = 1	PEST 779
	GO TO (1615,1620,1640) KTD0	PEST 780
C		CPEST 781
C **	NO RATE DEPENDENCE.	** CPEST 782
1615	PJ = PST	PEST 783
	GO TO 1625	PEST 784
C		CPEST 785
C **	N. A. G. DUCTILE FRACTURE MODEL.	** CPEST 786
1620	DV = DVO = 1./D-1./DOLD	PEST 787
	VVE = 1.-PEL/TSUF(1,PEL*RHOS/D,EOSTGM*RHOS*E,F0STCM,E0STDM,E0STSM,	PEST 788
1	E0STGM,F0STHM,F0STFM,RHOS,E0STNM,E)	PEST 789
	IF (AST1 .EQ. 0.) AST1 = ALFS	PEST 790

# SUBROUTINE PEST (Continued)

```

PELS = PFL/(1.-VVV)
NLOOP=MAX(1.,-DV*EQSTCM)/AMIN1(PST,P)/ALF*0.8,4.*TER(MP,1,N)*DT
1 * (P-PST))
VOLN = 1./DOLD * VSO = (1.-RVV1)/DOLD
NTRY = 0
RVV1 = RVV1
PTH1 = PTH0 = PST1*AST1
PSO = AMIN1(P,PST1)/(1.-RVV1)
IF (PST1 .GT. 0.) PSO=PTH1=PTH0=0.
IF (1.-RVV1) = 1./AST1 .GT. 0. .AND. PSO .LT. PTH0) GO TO 16201
DRVP = 0.
RVPO = -1./ (DOLD*EQSTCM)
GO TO 16203
16201 RVPO = (1.-RVV1-1./AST1)/DOLD/(PSO-PTH0)
DRVP = (RVV-VVE)/D/(PFLS-PTH)-RVPO
16203 VSTH0 = 1./ (DOLD*AST1)
NVSTH = (1.-RVV1)/D-VSTH0
DVDP = (VVE/D-RVV1)/DOLD/(PELS-PSO)
IF (PS1) .EQ. 0. .OR. PST1 .LT. P) PTH1 = PTH0 = PTH
PTH1 = PTH-PTH0
1621 DELV = DV/NLOOP * VM = VOLN * DTN = DELV/DV*DT
A1 = TER(MP,1,N)*DTN
C
  AFGJA DO LOOP FOR SUNCYCLING
  NO 1632 NL = 1,NLOOP
  VM = VM*DELV * RATIO = (VM-1./DOLD)/DVO
  RVP = RVPO+DRVP*RATIO
  VSTH = VSTH0+NVSTH*RATIO
  PTH1 = PTH0+PTH*RATIO
C
  FIRST ESTIMATE OF PRESSURE IN SOLID
  DP = AMIN1(0.,PSO-PTH1)
  XG = 1. * YN = 0.
  IF (DP .GE. 0.) GO TO 1622
  XG = EXP(A1*DP)
  XN = EXP(DP/TER(MP,6,N))
1622 PLU = PTH1 * PUP = PFLH = AMIN1(P,PST1)/(1.-RVV1)*(PELS-AMIN1(P,
1 PST1)/(1.-RVV1))*RATIO
ZG = RVV1*VM * ZN = 0. * PSA = PELH
IF (PTH1 .LT. PELH) GO TO 1630
PSJ = (DFLV-VSO-VSTH*PTH1+RVP*PSO+DVDP-RVV1*VM*(XG*(1.+A1/2.*
1 (-PTH1+PSO*PTH1))-1.)-TER(MP,8,N)*VM*DTN*XN*(1.- (PTH1+PSO-PTH1)/PEST 830
2 2./TER(MP,6,N)))/(RVP+DVDP+RVV1*VM*XG*A1/2.+TER(MP,8,N)*VM*DTN* PEST 831
3 XN/2./TER(MP,6,N)) PEST 832
NC = 0 PEST 833
1623 NC = NC+1 PEST 834
DP = (AMIN1(0.,PSJ-PTH1)+AMIN1(0.,PSO-PTH1))/2. PEST 835
ZG = RVV1*VM * ZN = 0. PEST 836
IF (DP .GE. 0.) GO TO 1624 PEST 837
ZG = ZG*EXP(A1*DP) PEST 838
ZN = TER(MP,8,N)*VM*DTN*EXP(DP/2./TER(MP,6,N)) PEST 839
1624 DELVA = VSTH-VSO+RVP*(PSJ-PTH1)+DVDP*(PSJ-PSO)+ZG-RVV1*VM*ZN PEST 840
PSA = PSJ PEST 841
AC = NC PEST 842
IF (ABS(DELVA-DELV) .LT. 1.E-5*VM .OR. (PSJ .GE. PTH1 .AND. AC PEST 843
1 .GT. 1.)) GO TO 1630 PEST 844
IF (NC .GE. 10) GO TO 1640 PEST 845
IF (DELVA .LT. DELV) PLO = AMIN1(PLO,PSA) PEST 846
IF (DELVA .GT. DELV) PUP = AMAX1(PSA,PUP) PEST 847
C
  MAKE 2ND ESTIMATE OF PRESSURE IN THE SOLID PEST 848
IF (MOD(NC,2) .EQ. 0) GO TO 1625 PEST 849
PSJ = PSJ+(DELV-DELVA)/(RVP+DVDP+ZG*A1/2.+ZN/2./TER(MP,6,N)) PEST 850
GO TO 1626 PEST 851
C
  INTERPOLATION ESTIMATE OF PRESSURE IN SOLID PEST 852
1625 PSJ = PSA+(DELV-DELVA)/(DELVA-DELVA)*(PSB-PSA) PEST 853
1626 IF (PSJ .LT. PUP) PSJ = PUP+.1.E7 PEST 854
IF (PSJ .GT. PLO) PSJ = PLO-1.E7 PEST 855
IF (NC .EQ. 1) GO TO 1627 PEST 856

```

# SUBROUTINE PEST (Concluded)

IF (ABS(DELVA-DELV) .GT. ABS(DELVB-DELV)) GO TO 1623	PEST 857
1627 PSH = PSA * DELVM = DELVA	PEST 858
GO TO 1623	PEST 859
C CONCLUSION OF LOOP	PEST 860
1630 RVVL = (7G+ZN)/VM * PTHL = PTHM * PSA=PSO=AMIN1(PTHM,AMAX1	PEST 861
1 (PFLM,PSA))	PEST 862
VSO = VM-2G-7N	PEST 863
FNT = ENT0VOLD/VM+TFH(MP,4,N)*EXP((DP/2./TFH(MP,4,N))*DTN	PEST 864
1632 CONTINUE	PEST 865
PJ = (1.-RVVL)*PSA	PEST 866
RVV = RVVL	PEST 867
1635 IF (RVV .GT. TFH(MP,7,N)) GO TO 2000	PEST 868
GO TO 1900	PEST 869
C PROVISION FOR SHORT FOR ITERATION FAILURE	PEST 870
1640 NTRY = NTRY+1	PEST 871
IF (NTRY .GE. 5) GO TO 1643	PEST 872
VOLD = VM-DELV * DV = 1./D-VOLD	PEST 873
NLOOP = MAX1(3.,-2.*NTRY*(DV+EUSTCM0)/AMIN1(PST,P)/AIF+G,N)	PEST 874
GO TO 1621	PEST 875
1643 WRITE(6,2749)M,P,DV,DELVA,DELVB	PEST 876
GO TO 1630	PEST 877
C WRITE FRACTURE AND FRAGMENTATION.	PEST 878
1660 GO TO 1901	PEST 879
C	PEST 880
C ** SOLID AND POROUS MELT AND SOLID BEHAVIOR	** CPEST 881
C	CPEST 882
1800 GO TO (1805,1810,1815) NPM	PEST 883
1805 CALL FUST(E,D,PS,M,C,DPMUJ,DPDEJ)	PEST 884
GO TO 1840	PEST 885
1810 CALL FSA(1,5,M,C,D,E,PS,DPMUJ,DPDEJ)	PEST 886
GO TO 1840	PEST 887
1815 CALL FUSTMF(1,5,M,C,D,E,PS)	PEST 888
1840 IF (M .GE. 5E -5) GO TO 1850	PEST 889
IF (E .EQ. 0.) GO TO 1850	PEST 890
PJ=PST=PFL=PS	PEST 891
GO TO 1840	PEST 892
1850 PJ = PST = PFL = AMAX1(0.,PS)	PEST 893
IF (PJ .GT. 0.) GO TO 1855	PEST 894
PTH = 1G0F(1, PJ*RHOS/10, FUSTGM*RHOS*E, FOSTCM, FOSTNM, EQSTSM,	PEST 895
1 EUSTGM, FUSTNM, FUSTFM, RHOS, EQSTNM, E)	PEST 896
RVV = AMAX1(0., 1. - D/PTH)	PEST 897
M = 5E -5	PEST 898
GO TO 1840	PEST 899
1855 M=5E -5 * RVV	PEST 900
1860 IF (PFL .LT. 1.) GO TO 1900	PEST 901
C	CPEST 902
C ** FINDING ROUTINE.	** CPEST 903
C	CPEST 904
1900 E = F+G.*P-PJ*(1./D-1./DOL1)	PEST 905
P = P.J	PEST 906
IF (F .NE. 0.) RHOI=(FOSTCM*F)*TF-P*RHOS*(1.+FLK(MP))/(EQSTCM*F-	PEST 907
1 P*FLK(MP))	PEST 908
IF (F .EQ. 0.) RHOI=D*TF	PEST 909
RHOI=AMIN1(RHOI,RHOS)	PEST 910
1910 PST=PST * AST=ALFS	PEST 911
RETURN	PEST 912
C FRAGMENTATION.	PEST 913
2000 M=PST*STJN0. * RHOI=D*TF	PEST 914
RVV = -ABS(RVV)	PEST 915
AST = 1./(1.+RVV)	PEST 916
M = 5E -2	PEST 917
RETURN	PEST 918
2349 FORMAT(* ITERATION FAILURE,M=12,* P=10.3,* DV=E10.3,* DFLVA	PEST 919
1 =F10.3,* DFLVB=F10.3)	PEST 920
END PEST	PEST 921

## APPENDIX B

### INVERSE SOLUTION OF THE MIE-GRÜNEISEN EQUATION OF STATE

At several points in the PEST subroutine it is necessary to find solid densities, given the pressure and internal energy. The subroutine described here for determining these densities is called TSQE. The pressure used may be either the pressure in the solid or the pressure in the porous material. In either case a direct solution for pressure is unobtainable so iterations are required. The following form of the Mie-Gruneisen equation is used

$$P_s = (C\mu + D\mu^2 + S\mu^3) \left(1 - \frac{\Gamma\mu}{2}\right) + \Gamma\rho_s E \quad (B-1)$$

where  $\mu = \rho_s / \rho_{so} - 1$ . For compression ( $\rho_s > \rho_{so}$ ), the product  $\Gamma\rho_s$  is treated as a constant  $\Gamma_o\rho_{so}$  and  $\Gamma\mu/(1 + \mu)$ . For extension,  $\Gamma$  is treated as constant, and  $D = S = 0$ . If the pressure  $P$  in the porous material is known instead of  $P_s$ , the following relation holds:

$$\frac{P\rho_{so}}{\rho} = \frac{P_s(\mu, E)}{1 + \mu} = P'_s(\mu, E) \quad (B-2)$$

Since variables on the left are all known, the same kind of iteration procedure is used to obtain  $\mu$  here as for Eq. (B-1).

The iteration scheme used is a combination of regula falsi and Newton-Raphson. A first estimate of  $\mu$  is made from a linearization of  $P_s(\mu, E)$  or  $P'_s(\mu, E)$ .

$$\mu_1 = \frac{P_s - \Gamma_o\rho_{so} E}{K_s} \quad (B-3)$$



or

$$\mu_1 = \frac{P\rho_{so}/\rho - \Gamma_o \rho_{so} E}{K_S} \quad (B-4)$$

Then the right-hand side of Eq. (B-1) or (B-2) is evaluated with  $\mu = \mu_1$  to obtain  $P_{s1}$  or  $P'_{s1}$ . The next computed value of  $\mu$  in the solution of Eq. (B-1) is

$$\mu_{i+1} = \mu_i + \frac{P_s - P_{s1}}{2 \left( \frac{\partial P_s}{\partial \mu} \right)_{\mu=\mu_i}} + \frac{P_s - P_{s1}}{2 \left( \frac{P_{s1} - P_{s1-1}}{\mu_i - \mu_{i-1}} \right)} \quad (B-5)$$

where the second term on the right is the Newton-Raphson part and the third is the regula falsi term. Equation (B-5) is used to compute successive iterations of  $\mu$  until the difference between  $\mu_{i+1}$  and  $\mu_i$  is sufficiently small.

Four paths are shown in the listing of TSQE, corresponding to whether solid or porous pressure is known and whether density is greater or less than  $\rho_{so}$ . The nomenclature is given below, followed by the listing of the subroutine.

#### Nomenclature

IP            Indicator

0    Solution for  $\mu$  with the solid pressure known

1    Solution with the porous pressure known

PP            Input pressure,  $P_s$  or  $P\rho_{so}/\rho$ , dyne/cm<sup>2</sup>

GRE            $\Gamma\rho_{so}E$ , an input quantity, dyne/cm<sup>2</sup>

C,D,S        Coefficients of the Hugoniot expansion, dyne/cm<sup>2</sup>

G            Grüneisen ratio

EMU            $\mu = \rho_s/\rho_{so} - 1$

# FUNCTION TSQE

```

FUNCTION TSQF(IP,PP,GHE,C,D,S,G,H,F5,RUS,EN,F)
C
C**      CALCULATES MU ON PTH FROM KNOWN PRESSURE AND EOS RELATION. **C
C      TP = 0. INVERSE EOS. IP = 1. INVERSE EOS FOR PTH = ALFA*PST.
C
NC = 0 * PA = FMU0 = 0. * G2 = G/2.
AMIXY
IF (LEGVAR(A) .NE. 0) IX = 0
IND = 1
IF (PP .LE. RPE) IND = IND+2
FMU1 = (PP-GPE)/C
8 NC = NC+1
GO TO (10,15,20,25) IND
C      PATH FOR COMPRESSION = SOLID PRESSURE KNOWN. ** CTSQE
10 WMU = 1.+FMU1
PH = FMU1*(C+FMU1*(D+FMU1*S))
P1 = GHE+PH*(1.-C)*FMU1/WMU
FMU2 = TSQE = FMU1*(PP-P1)*(0.5/(PH*G2/WMU**2)+(C+FMU1)*(2.*D+FMU1)*3)
1. *C)*(1.-G*FMU1/WMU)+0.5*(FMU1-FMU2)/(P1-P0))
GO TO 30
C      PATH FOR EXPANSION = SOLID PRESSURE KNOWN. ** CTSQE
20 WMU1 = FMU1
S1 = GHE+WMU1
S2 = H*(G-H)*S0
S4 = EXP((H+FMU1)/WMU**2)
S3 = F5*(1.-S4)
P1 = C1+S2+S3
(DP)H1 = H*(S2+S3+C)/2.*(G-H)/S1+S3+C)*S2+F5*S4/WMU**3*(1.-FMU1)
FMU2 = FMU1*(PP-P1)/(DP)H1
FMU2 = AMAX1(-1.,+1.,F-R*NC,AMIN1(FMU2,+,E-R*NC))
GO TO 30
C      PATH FOR COMPRESSION = POROUS PRESSURE KNOWN. ** CTSQE
15 WMU = 1.+FMU1
ETA = 1.-G2*FMU1/WMU
PH = FMU1*(C+FMU1*(D+FMU1*S))
P1 = (PH*ETA+GHE)/WMU
FMU2 = FMU1*(PP-P1)*(C.5/(ETA*(C+FMU1)*(2.*D+FMU1)*3*S))-(P1-PH*G2/
1 WMU**2)/WMU)+0.5*(FMU1-FMU2)/(P1-P0))
GO TO 30
C      PATH FOR EXPANSION = POROUS PRESSURE KNOWN. ** CTSQE
25 WMU = 1.+FMU1
S0 = GHE+WMU1
S2 = H*(G-H)*S0
S4 = EXP((H+FMU1)/WMU**2)
S3 = F5*(1.-S4)
P1 = R*NC+S2+S3
(DP)H1 = H*(S2+S3/2.*(G-H)*S3/S0+PUS*S2+F5*S4*(1.-FMU1)/WMU**3
FMU2 = FMU1*(PP-P1)/(DP)H1
FMU2 = AMAX1(-1.,+1.,F-R*NC,AMIN1(FMU2,+,E-R*NC))
30 CONTINUE
IF (IP .GT. 1) PRINT 32,IP,PP,GHE,P1,FMU2,FMU1,FMU0,NC,IX
32 FORMAT(' IP=13. PP,GHE,P1=3E10.3. FMU2,FMU1,FMU0=3E12.5. NC,
1 IX=213)
IF (NC .EQ. 12) IX = IX+1
IF (IX .GT. 20) STOP
IF (PP .NE. C. .AND. ABS(FMU2-FMU1) .GT. 1.E-4*MAX1(ABS(FMU1),1,ETSQE
1-3)) GO TO 75
IF (PP .EQ. C. .AND. ABS(FMU2-FMU1) .GT. 1.E-3*MAX1(ABS(FMU1),1,ETSQE
1-3)) GO TO 75
TSQE = FMU2
65 IF (IP .EQ. 1) TSQE = PTH = PP*(1.+FMU2)
IF (PP .EQ. 0.) TSQE = PUS*(1.+FMU2)
70 RETURN
75 CONTINUE
IF (NC .EQ. 13) GO TO 65
IF (ABS(PP-PP) .LT. ABS(P1-PP)) GO TO 80
P0 = P1 * FMU0 = FMU1
80 IF (PP .GT. GHE) FMU1 = FMU2
IF (PP .LT. GHE) FMU1 = 0.5*(FMU1+FMU2)
GO TO 6
END

```

## APPENDIX C

### PHILCO-FORD EQUATION OF STATE

This appendix contains a listing of the subroutine incorporating the Philco-Ford<sup>10</sup> equation of state, plus instructions for using it in a wave propagation calculation.

The subroutine, termed EQSTPF, is called at two points in a wave propagation code. The first CALL is from the initializing subroutine (GENRAT in PUFF) at the point where material properties are inserted. At this CALL, the original solid density ( $\rho_{so}$ ) and the Hugoniot parameters (C, D, S,  $\Gamma$ ) must be available in COMMON. Additional material data are read in directly by EQSTPF during the initializing CALL: they are not available to the rest of the program. All other input and output variables are inserted through the CALL statement. The CALL statement used in GENRAT is simply

```
CALL EQSTPF (0,IN,M)
```

where the first parameter (NCALL) indicates initialization, the second (IN) is the file containing the input data, and the third (M) is the material number. During this CALL, the subroutine reads two cards and initializes its internal array variables. These data cards contain identifiers and 14 constants in the following form:

```
TI-PF 1  1.800E 00 3.970E 00 0.          1.750E 00 2.612E 10 1.490E 10 1.170E 10
TI-PF 2  1.159E 11 1.060E 11 3.550E 03 1.160E 04 1.950E 03 4.790E 01 5.638E 00
```

The cards contain an alphanumeric title in A10 format and 14 variables in E10.3 format. The variables are C1, DLM, DSM, D1, HLB, HLM, HSM, HVB, HVM, TBK, TCK, TMK, WT, AND ZKO. These variables are listed for aluminum, beryllium, and titanium in Table C-1 as they were taken from Goodwin et al.<sup>10</sup>

TABLE C-1 PHILCO-FORD EQUATION-OF-STATE DATA FOR ALUMINUM,  
BERYLLIUM, AND TITANIUM<sup>10</sup>

Variable	Aluminum	Beryllium	Titanium
RHOS, $\rho_{so}$ g/cm <sup>3</sup>	2.71	1.85	4.5
EQSTC, C dyn/cm <sup>2</sup>	$7.72 \times 10^{11}$	$1.203 \times 10^{12}$	$1.016 \times 10^{12}$
EQSTD, D dyn/cm <sup>2</sup>	$4.908 \times 10^{11}$	$8.212 \times 10^{11}$	$7.222 \times 10^{11}$
EQSTS, S dyn/cm <sup>2</sup>	$6.076 \times 10^{11}$	$-3.79 \times 10^{11}$	$-5.685 \times 10^{11}$
EQSTG, $\Gamma$	2.11	1.15	1.09
C1	1.80	1.80	1.80
DLM g/cm <sup>3</sup>	2.380	1.690	3.97
DSM g/cm <sup>3</sup>	2.537	1.808	(4.25)
D1	1.75	1.75	1.75
HLB erg/g	$3.020 \times 10^{10}$	$8.983 \times 10^{10}$	$2.612 \times 10^{10}$
HLM erg/g	$1.061 \times 10^{10}$	$4.976 \times 10^{10}$	$1.494 \times 10^{10}$
HSM erg/g	$6.658 \times 10^9$	$3.674 \times 10^{10}$	$1.170 \times 10^{10}$
HVB erg/g	$1.400 \times 10^{11}$	$4.202 \times 10^{11}$	$1.157 \times 10^{11}$
HVM erg/g	$1.260 \times 10^{11}$	$3.925 \times 10^{11}$	$1.060 \times 10^{11}$
TBK °K	8000	8000	11,600
TMK °K	932	1556	1950
WT g/mole	26.98	9.013	47.90
ZKO	5.626	5.626	5.638

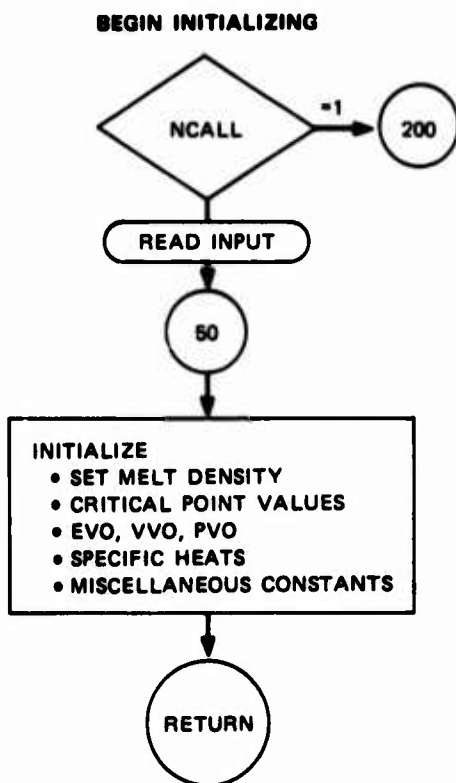
The second CALL to EQSTPF is made to obtain the pressure in a wave propagation calculation. In SRI PUFF, this CALL statement is in HSTRESS:

```
CALL EQSTPF (1, 5, M, C(J), D(J), E(J), P(J))
```

The first parameter (NCALL) signifies that pressure is to be computed. C, D, E, P are the sound speed, density, energy, and pressure. C is unused, D and E are provided to the subroutine, and P is output.

A pictorial view of the EQSTPF is given in the simplified flow chart in Figure C-1. The subroutine is actually in two parts: the first handles reading and initializing and the second (beginning at location 200) handles pressure computations. The second part contains three subsections. The first of these selects the appropriate phase for material, the second contains two functions for numerical evaluation of quantities on the phase boundaries, and the third contains five sections for computing pressures in each of the three phases and two mixed phase regions.

A nomenclature list is provided containing the input variables and other principal variables of the subroutine. This list is followed by a listing of the subroutine in FORTRAN IV.

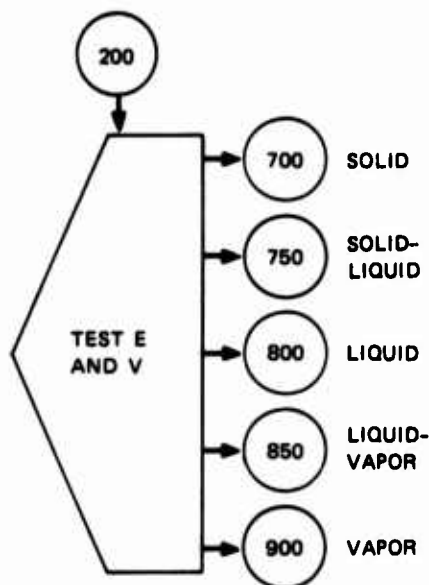


NCALL IS ZERO FOR INITIALIZING, ONE FOR COMPUTING PRESSURE.

READ 2 CARDS CONTAINING MATERIAL NAME, AND 14 VARIABLES: C1, DLM, DSM, D1, HLB, HLM, HSM, HVB, HVM, T8K, TCK, TMK, WT, ZKO.

COMPUTE THE MELT DENSITY TO BE CONSISTENT WITH ESO. COMPUTE PRESSURE, ENERGY, AND Z AT CRITICAL POINT. COMPUTE INTERNAL ENERGY, SPECIFIC VOLUME AND PRESSURE CORRECTION AT ZERO PRESSURE ON THE VAPOR TO LIQUID-VAPOR PHASE LINE. COMPUTE SPECIFIC HEATS FROM THE RATIO OF ENTHALPIES TO TEMPERATURE CHANGES.

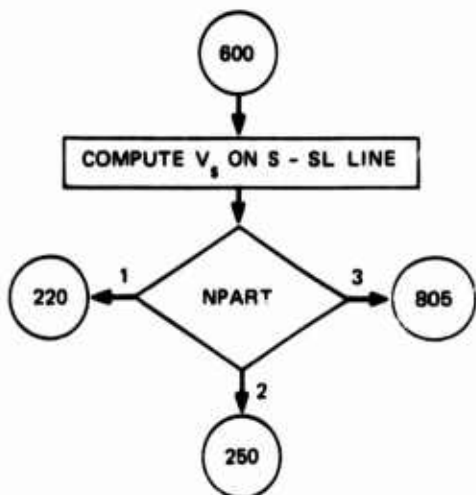
**BEGIN PRESSURE COMPUTATIONS**



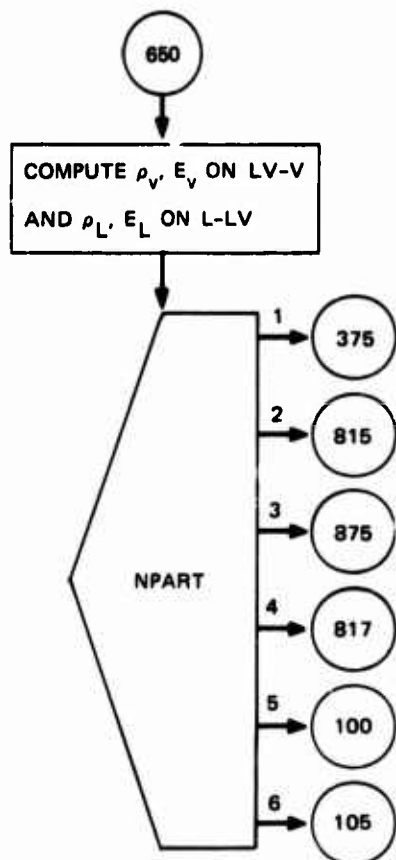
TEST INTERNAL ENERGY AND SPECIFIC VOLUME AGAINST THE ENERGIES AND VOLUMES ALONG THE PHASE LINES TO DETERMINE THE APPROPRIATE PHASE.

MA-2407-21

FIGURE C-1 SIMPLIFIED FLOW CHART FOR EQSTPF SUBROUTINE



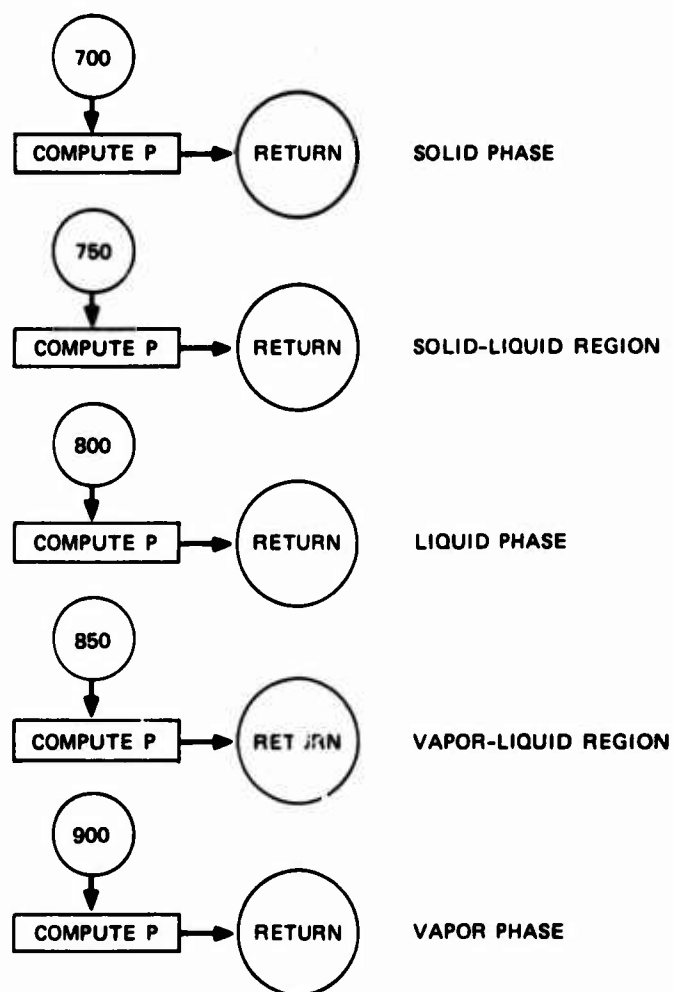
LOCATION 600 STARTS A SPECIAL FUNCTION FOR COMPUTING SPECIFIC VOLUME ON THE PHASE LINE BETWEEN SOLID AND SOLID-LIQUID REGIONS FOR GIVEN INTERNAL ENERGY. FOLLOWING COMPUTATIONS, CONTROL RETURNS TO THE POINT INDICATED BY NPART.



LOCATION 650 STARTS A SPECIAL FUNCTION FOR COMPUTING STATE POINTS ON BOTH LEFT AND RIGHT BOUNDARIES OF THE LIQUID-VAPOR REGION. CONTROL RETURNS TO THE POINT INDICATED BY NPART.

MA-2407-22

FIGURE C-1 SIMPLIFIED FLOW CHART FOR EQSTPF SUBROUTINE (Continued)



MA-2407-23

FIGURE C-1 SIMPLIFIED FLOW CHART FOR EQSTPF  
SUBROUTINE (Concluded)



# NOMENCLATURE OF INPUT AND PRINCIPAL VARIABLES

A1, A2, ( $\alpha_a, \alpha_b$ )	Constants in vapor-liquid equation of state
B, BP, (b, b')	Constants in vapor equation of state
CBT, ( $\bar{C} \cdot T_M$ )	Average of specific heats at constant pressure in solid and liquid phases, times the melting temperature, erg/g
CC	$(c_1/d_1)^3/27$
C1, ( $c_1$ ), D1, ( $d_1$ )	Coefficients in the relation for density at the phase line between the liquid and liquid-vapor regions
DEDV	$(E_{LO}-E_{SO})/(V_{LO}-V_{SO}) = \Delta E_O/\Delta V_O$ , erg/cm <sup>3</sup>
DLM	Density of liquid at melting and atmospheric pressure, g/cm <sup>3</sup>
DSM	Density of solid at melting and atmospheric pressure, g/cm <sup>3</sup>
EBL	Internal energy of liquid at boiling, erg/g
EBS	Internal energy of solid at boiling, erg/g
EC	Internal energy at critical point, erg/g
ELO, ( $E_{LO}$ )	Internal energy at atmospheric pressure on phase line between liquid and solid-liquid regions, erg/g
EO, ( $E_O$ )	Internal energy of the ideal gas at zero temperature, erg/g
EQSTC, (C)	Bulk modulus, dyne/cm <sup>2</sup>
EQSTD, (D)	Second coefficient of Hugoniot expansion, dyne/cm <sup>2</sup>
EQSTG, ( $\Gamma$ )	Grüneisen ratio
EQSTS, (S)	Third coefficient of Hugoniot expansion, dyne/cm <sup>2</sup>
ESO, ( $E_{SO}$ )	Internal energy at atmospheric pressure on phase line between solid and solid-liquid regions, erg/g
EVO	Internal energy of vapor at line between liquid-vapor and vapor at zero pressure, erg/g

HLB	Enthalpy of liquid at boiling and atmospheric pressure, erg/g
HLM	Enthalpy of liquid at melting and atmospheric pressure, erg/g
HSM	Enthalpy of solid at melting and atmospheric pressure, erg/g
HVB	Enthalpy of vapor at boiling and atmospheric pressure, erg/g
HVM	Enthalpy of vapor at melting temperature, erg/g
NCALL	Indicator in the formal parameter list  0 means reading and initializing is required  1 means pressure is to be computed
P	Pressure, dyne/cm <sup>2</sup>
PC, (P <sub>c</sub> )	Critical pressure, dyne/cm <sup>2</sup>
PVO	Correction to pressure of vapor to force a zero pressure point on the phase line <sup>2</sup> between liquid-vapor and vapor, dyne/cm <sup>2</sup>
RHOS, (ρ <sub>o</sub> )	Initial solid density, g/cm <sup>3</sup>
R1, (R)	Gas constant, 8.3144 x 10 <sup>7</sup> ergs/ <sup>o</sup> C/mole
TBK	Boiling temperature, <sup>o</sup> K
TCK, (T <sub>c</sub> )	Critical temperature, <sup>o</sup> K
TM	TMK/TCK, reduced temperature
TMK, (T <sub>M</sub> )	melting temperature, <sup>o</sup> K
V	Specific volume, cm <sup>3</sup> /g
VC, (V <sub>c</sub> )	Specific volume at the critical point, cm <sup>3</sup> /g
VLO	Specific volume of liquid at <sub>3</sub> melting and atmospheric pressure, cm <sup>3</sup> /g
VO	Initial specific volume of solid, cm <sup>3</sup> /g
VSO	Specific volume of solid <sub>3</sub> at melting and atmospheric pressure, cm <sup>3</sup> /g

VVO	Specific volume on phase line between liquid-vapor and vapor at zero pressure, cm <sup>3</sup> /g
WT	Molecular weight, g/mole
Y1	$2\bar{C} \cdot T_M$
Y3	$2\bar{C} \cdot \Delta C \cdot T_M^2$
ZC, (Z <sub>c</sub> )	$P_c V_c / RT_c$ , compressibility factor at critical point
ZKO, ZK1, ZK2, (k <sub>0</sub> , k <sub>1</sub> , k <sub>2</sub> )	Constants in the vapor equation of state
ZM, ZN	Constants in an approximate fit to the $\rho_v$ -T relation on the boundary between liquid vapor and vapor:

$$\rho_{v c} = 1 - ZM \left(1 - \frac{T}{T_c}\right)^{ZN}$$

# SUBROUTINE EQSTPF

```

C      SUBROUTINE EQSTPF (NCALL, IN, M, CJ, D, E, P)
C
C      EQSTPF COMPUTES PRESSURE FROM A THREE-PHASE EQUATION OF STATE
C      DEVELOPED BY PHILCO-FORD. ROUTINE HAS TWO PARTS, ONE FOR
C      READING AND INITIALIZING AND THE OTHER FOR COMPUTING PRESSURE.
C
C      READ INPUT (NCALL=1). CALL IS FROM GENMAT.
C      INPUT = NCALL, IN, M, AND MATERIAL PROPERTY CARDS
C      OUTPUT = PRINTS CARD IMAGES, ORGANIZES DATA INTO ARRAYS
C      COMPUTE PRESSURE (NCALL=1) CALL IS FROM HSTRESS USUALLY
C      INPUT = NCALL, M, CJ, D, E
C      OUTPUT = P (CURRENT PHASE ON STATE OF MATERIAL IS AVAILABLE)
C
C      NAMED COMMON
C      REAL MU, MUM
C      COMMON /EUS/ EQSTA(6), EUSTC(6), EUSTD(6), EUSTF(6), EUSTG(6),
1 EUSTH(6), EUSTI(6), EQSTS(6), EUSTV(6), CZU(6), CMU(6), C2(6)
C      COMMON /MFL/ EMELT(6,5), SHM(6)
C      COMMON /RHU/ RHO(6), RHOS(6)
C      COMMON /TSH/ TSH(6,30), FPMAT(6,20), TENS(6,3)
C      COMMON /Y/ Y0(6), YAUD(6), MU(6), MUM, YAUDM
C      DIMENSION A1(6), A2(6), R(6), BP(6), C1(6), CBT(6), CC(6), CV(6), D1(6),
1 DEOV(6), EBL(6), EHS(6), EC(6), EES(6), ELU(6), EU(6), EUVO(6), EPS1(6),
2 EPS2(6), ESU(6), EVU(6), MUCT(6), PC(6), PVO(6), TH(6), VC(6), VLU(6),
3 VO(6), VSO(6), VVO(6), WT(6), Y1(6), Y3(6), ZC(6), ZK0(6), ZK1(6), ZK2(6),
4 ZN(6), ZM(6)
C      DATA ACC, M1 /1.E-4, 8.3144E7/
C
C      ***** BRANCH TO INITIALIZATION OR COMPUTATION PORTIONS
C      IF (NCALL .EQ. 1) GO TO 200
C
C      ***** READ INPUT DATA AND INITIALIZE CONSTANTS *****
C
C      IND = 5M
C      READ (IN, 1101) Z1, C1(M), ULM, USM, U1(M), HLB, HLM, HSM
C      WRITE (6, 1101) Z1, C1(M), ULM, USM, U1(M), HLB, HLM, HSM
C      WRITE (6, 1102) IND, IN
C      READ (IN, 1101) Z1, HVB, HVM, THK, TCK, TMK, WT(M), ZK0(M)
C      WRITE (6, 1101) Z1, HVB, HVM, THK, TCK, TMK, WT(M), ZK0(M)
C      WRITE (6, 1102) IND, IN
C      VU(M) = 1./RHOS(M)
C      ESU(M) = HSM
C      IF (DSM .GT. 0.) GO TO 50
C
C      COMPUTE -NSM- IF UNSPECIFIED
C      ENG = EUSTG(M) * RHOS(M) * ESU(M)
C      EMU = -ERG/(EUSTC(M) * ENG)
C      EMU = -ERG/(EUSTC(M) * (EUSTD(M) * EQSTS(M) * EMU) * CMU * ERG)
C      NC2 = 0
C40 EMU0 = EMU
C      NC2 = NC2 + 1
C      IF (NC2 .GT. 20) GO TO 42
C      P = EMU * (EUSTC(M) * EMU * (EUSTD(M) * EMU * EUSTS(M)) * ENG) * ENG
C      PP = EUSTC(M) * ENG * EMU * (2. * EUSTD(M) + 3. * EMU * EUSTS(M))
C      EMU = EMU - P/PP
C      IF (ABS(EMU - EMU0) .GT. ACC) GO TO 40
C      GO TO 44
C42 PRINT 1103, EMU0, P, PP, EMU, M
C      STOP 42
C44 CONTINUE
C      VSO(M) = VO(M) / (EMU + 1.)
C      GO TO 60
C
C      ADJUST -ESO- , -VSO- TO AGREE WITH -USM-

```

# SUBROUTINE EQSTPF (Continued)

```

51  VSO(M) = 1./USM
    FNU = USM/MMOS(M)-1.
    FSO(M) = -FNU*(FUSTC(M)+FNU*(EUSTD(M)+FNU*EUSTS(M)))/(EUSTG(M)+
1  MMOS(M)*(1.+FNU))
60  FLO(M) = FSO(M)*MLM+MSM
    C      COMPUTE -OLM- IF UNSPECIFIED
    IF (OLM .LE. 0.) OLM = 0.935/VSO(M)
    VLO(M) = 1./OLM
    TLM(M) = TMR/TCK
    TM = TMR/TCK
    FLH = MVM-MLM
    C      SOLVE FOR -CL- FROM EQ. 3.21
    CL = (MLM-FLH)/(TMR-TMK)
    CV(M) = (MVM-MVM)/(TMR-TMK)
    DLTC = CV(M)-CL
    C      SOLVE FOR -A1- , -A2- AND -ALPHA- FROM EQS. 3.24
    A1(M) = (1/CL)*WT(M)
    A2(M) = (FLH-DLTC*TCK)/(M1*TCK)*WT(M)
    C      SOLVE FOR -AK- FROM EQ. 3.25
    X = 36./TM+0.*TM**6-42.
    AM = (A2(M)/TM+A1(M)*0.31425*X)/(1.+0.0838*X)
    A2(M) = A2(M)-A1(M)
    C      SOLVE FOR -ZC- FROM EQ. 3.27
    ZC(M) = 1./(3.72+0.26*(AM-7.))
    C      SOLVE FOR -VC- FROM EQ. 3.33
    VC(M) = (1.+C1(M)*(1.-TM(M))*((1./3.)*D1(M)*(1.-TM(M)))/OLM
    C      SOLVE FOR CRITICAL PRESSURE -PC- FROM EQ. 3.34
    PC(M) = ZC(M)*R1*TCK/VC(M)/WT(M)
    C      SOLVE EQ. 3.6H FOR H1 = BETA. COMPUTE B,BP
    H1 = 3.
    H2 = 1.5*(1./ZC(M)-1.)
    H3 = 2.65/ZC(M)**2-5.5/ZC(M)-0.75
70  BU = H1
    H1 = H2+SQRT(H3-1./H1)
    IF (ABS((H1-BU)/H1) .GT. ACC) GO TO 70
    B(M) = ((3.*H1-6)*H1-1.)/(H1*(3.*H1-1.))
    BP(M) = (H1-3.)/(3.*H1-1.)
    C      COMPUTE -K0- , -K1- , AND -K2- (EQS. 3.7)
    IF (ZK0(M) .EQ. 0.) ZK0(M) = B1
    ZK1(M) = H1-ZK0(M)
    ZK2(M) = (1.+7K1(M)+H1)-A1(M)-A2(M))/2.
    EPS1(M) = ZC(M)*TCK*H1/WT(M)
    EPS2(M) = TCK*(CV(M)-H1/WT(M))
    FU(M) = MVM-CV(M)*TCK
    C      SOLVE EQ. 3.2R FOR RV TO FIND EVO, PVO, DVO, VVO
    T = TM(M)
    PV = EXP(A2(M)*(1.-1./T)+A1(M)*ALOG(T))
    X1 = T/ZC(M)
    A = ZK0(M)+ZK1(M)/T
    AP = ZK2(M)*(T-1./T)
    C      SOLVE EQ. 4.5 FOR RV
    RV = PV/X1
    NC3=0
80  HV1 = RV
    NC3=NC3+1
    IF (NC3 .GT. 20) GO TO H2
    X2 = 1.-(H(M)-BP(M)*HV1)*HV1
    PO = X1*HV1/X2-(A+AP*RV1)*HV1**2
    POP = X1/X2+(X1*HV1*(B(M)-2.*BP(M)*RV1))/(X2*X2)-(2.*A+3.*AP*RV1)
1  *HV1
    HV=AMAX1(RV1+(PV-PO)/POP,1.E-12)
    IF (ABS(PV-HV1) .GT. ACC*HV .AND. ABS(RV-HV1) .GT. 1.E-12) GO TO 80
    GO TO H3
82  PRINT 1104,HV1,PO,POP,RV,M
    STOP A2

```

EQSTPF57  
EQSTPF58  
EQSTPF59  
EQSTPF60  
EQSTPF61  
EQSTPF62  
EQSTPF63  
EQSTPF64  
EQSTPF65  
EQSTPF66  
EQSTPF67  
EQSTPF68  
EQSTPF69  
EQSTPF70  
EQSTPF71  
EQSTPF72  
EQSTPF73  
EQSTPF74  
EQSTPF75  
EQSTPF76  
EQSTPF77  
EQSTPF78  
EQSTPF79  
EQSTPF80  
EQSTPF81  
EQSTPF82  
EQSTPF83  
EQSTPF84  
EQSTPF85  
EQSTPF86  
EQSTPF87  
EQSTPF88  
EQSTPF89  
EQSTPF90  
EQSTPF91  
EQSTPF92  
EQSTPF93  
EQSTPF94  
EQSTPF95  
EQSTPF96  
EQSTPF97  
EQSTPF98  
EQSTPF99  
EQSTP100  
EQSTP101  
EQSTP102  
EQSTP103  
EQSTP104  
EQSTP105  
EQSTP106  
EQSTP107  
EQSTP108  
EQSTP109  
EQSTP110  
EQSTP111  
EQSTP112  
EQSTP113  
EQSTP114  
EQSTP115  
EQSTP116  
EQSTP117  
EQSTP118  
EQSTP119  
EQSTP120  
EQSTP121

# SUBROUTINE EQSTPF (Continued)

```

N3  CONTINUE
C      SOLVE FOR S, 0.4C, 10, AND E FOR EV, HL, EL
EV = F0(M)*FMS2(M)*FMS1(M)*(1/ZK0(M)+2.*ZK1(M)/T)-ZK2(M)*RV/T)*RV
HL = 1.+C1(M)*(1.-T)**(1./3.)*D1(M)*(1.-T)
EL = EV-FMS1(M)*RV*(1./MV-1./HL)*(A2(M)/T*A1(M)-1.)
F1 = F0(M)*D1(M)-EL
EV0(M) = EV-E1-FU(M)
RV0(M) = RV
VV0(M) = VC(M)/MV
FU(M) = F1
C      SOLVE FOR 0.4C, 10, AND E WITH T = 1, MV = 1
EC(M) = F0(M)*FMS2(M)-FMS1(M)*(ZK0(M)+2.*ZK1(M)-ZK2(M))
DEIV(M) = (EL0(M)-FS0(M))/(VLU(M)-VSD(M))
FUVU(M) = DEIV(M)
FVS(M) = VU(M)*E(V(M))
C(M) = (C1(M)/D1(M))*3./27.
L(M) = FSD(M)/(TMK-29M.)
CT(M) = 0.5*(CL-CS0)*TMK
CHT(M) = 0.5*(CL+CS0)*TMK
EHL(M) = FLU(M)-CS0*TMK
EHS(M) = FSU(M)-C*TMK
Y1(M) = 2.*CHT(M)
Y3(M) = Y1(M)*(CL-CS0)*TMK
C      CONSTRUCT A FIT TO APPROXIMATE MV=1 RELATION ON LV=V BOUNDARY
T1=0.95
NPANT=5
GO TO 650
100  H1=HV
T2=0.9
NPANT=5
GO TO 650
105  H2=HV
ZA(M) = ALOG((1.-H1)/(1.-H2))/ALOG((1.-T1)/(1.-T2))
ZH(M) = (1.-H1)/(1.-T1)**ZN(M)
RETURN
C *****
C      CALCULATIONS TO FIND P(V,E)
C *****
C *****
C      SELECT REGION OF PHASE DIAGRAMS
200  CONTINUE
V = 1./U
C      SELECT S, SL, L, LH, LV, AND V REGIONS
IF (V.GF. VLN(M)) GO TO 300
C      TEST FOR COOL SOLID
IF (F.LE. ESD(M)) GO TO 700
C      SOLVE FOR VS ON S-SL BOUNDARY WITH ES=E
Y2 = F-EHS(M)
EZ = F
NPANT = 1 & GO TO 600
C      SECOND BRANCH FOR SOLID MATERIAL, CONTINUE WITH SL AND L
220  IF (V.LT. VS) GO TO 700
C      TEST FOR COOL LIQUID
IF (F.LT. EL0(M)) GO TO 750
C      SOLVE FOR TEMP OF E AS IF E IS ON SL-L LINE
Y2 = E-EL1(M)
TF = (Y2+SQRT(Y2*Y2-Y3(M)))/Y1(M)
C      COMPUTE ES FOR IF
EZ = FS = EHS(M)+CHT(M)*TF+MDCT(M)/TF
C      GO TO 600 TO GET VS ON S-SL LINE
NPANT = 2 & GO TO 602
C      COMPUTE VLM OR SL-L LINE
250  VLM = VS*(F-ES)/DEDV(M)
NL = 1
C      SEPARATE SOLID-LIQUID AND LIQUID
IF (V-VLM) 755,755,810
C
C      BEGIN SWITCHING FOR L, LV, AND V REGIONS

```

EQSTP122  
 EQSTP123  
 EQSTP124  
 EQSTP125  
 EQSTP126  
 EQSTP127  
 EQSTP128  
 EQSTP129  
 EQSTP130  
 EQSTP131  
 EQSTP132  
 EQSTP133  
 EQSTP134  
 EQSTP135  
 EQSTP136  
 EQSTP137  
 EQSTP138  
 EQSTP139  
 EQSTP140  
 EQSTP141  
 EQSTP142  
 EQSTP143  
 EQSTP144  
 EQSTP145  
 EQSTP146  
 EQSTP147  
 EQSTP148  
 EQSTP149  
 EQSTP150  
 EQSTP151  
 EQSTP152  
 EQSTP153  
 EQSTP154  
 EQSTP155  
 EQSTP156  
 EQSTP157  
 EQSTP158  
 EQSTP159  
 EQSTP160  
 EQSTP161  
 EQSTP162  
 EQSTP163  
 EQSTP164  
 EQSTP165  
 EQSTP166  
 EQSTP167  
 EQSTP168  
 EQSTP169  
 EQSTP170  
 EQSTP171  
 EQSTP172  
 EQSTP173  
 EQSTP174  
 EQSTP175  
 EQSTP176  
 EQSTP177  
 EQSTP178  
 EQSTP179  
 EQSTP180  
 EQSTP181  
 EQSTP182  
 EQSTP183  
 EQSTP184  
 EQSTP185  
 EQSTP186  
 EQSTP187  
 EQSTP188  
 EQSTP189

# SUBROUTINE EQSTPF (Continued)

```

300 IF (V .LT. VC(M)) GO TO 350
C      BRANCH FOR HIGHLY VAPORIZED MATERIAL
IF (V .GT. VVO(M)) GO TO 900
C      COMPUTE EC(V) AT CRITICAL TEMP TO COMPARE WITH F
ECV = EV(M)*EPS2(M)-EPS1(M)*(ZK0(M)+2.*ZK1(M))*RV/(K2(M)*RV*RV)
C      SECOND PARTIAL ISOLATION OF V FROM LV REGION
IF (F .GT. ECV) GO TO 900
C      COMPUTE T AND THEN EV ON LV=V LINE TO MAKE THIRD TEST FOR
C      SEPARATING LV AND V
RV = VC(M)/V
X1 = RV/(ZC(M)*(1.-(M(M)-MP(M)*RV)*RV))-ZK2(M)*RV**3
X2 = -ZK0(M)*RV*RV
X3 = (ZK2(M)*RV-ZK1(M))*RV*RV
TMIN = 0.0
IF (X1 .GT. 0.0 .AND. X3 .GT. 0.0) TMIN=SQRT(X3/X1)
FMAX = (F-ELO(M))/(EVO(M)-ELO(M))
IF (V .GT. FMAX*VVO(M)+(1.-FMAX)*VLO(M)) GO TO 900
T = 1.0
PV = EXP(AZ(M)*(1.-1./T)*A1(M)*ALOG(T))
NC4=0
310 PVT = PV
NC4=NC4+1
IF (NC4 .GT. 20) GO TO 312
TA = T
PG = X1*T+X2+X3/T
PVP = PV*(AZ(M)/T+A1(M))/T
PGP = AMAX1(0.,X1-X3/(T*T))
T = AMAX1(TA+(PG-PV)/(PVP-PGP),TMIN+ACC)
IF (PVP-PGP .LT. 0.) T=TA+0.05
T = AMIN1(1.,0.8*TA+0.199)
PV = EXP(AZ(M)*(1.-1./T)*A1(M)*ALOG(T))
IF (ABS((PV-PVT)/PV) .GT. ACC) GO TO 310
EV = FO(M)*EPS2(M)*T-EPS1(M)*(ZK0(M)+2.*ZK1(M))/T-K2(M)*RV/T)*RV
C      BRANCH TO EITHER V OR LV REGIONS
IF (T .LT. TM(M)) GO TO 905
IF (E-EV) .MOD. 900,900
312 PRINT 1105,TA,PG,PVP,PGP,T,PV,M
STOP 312
C
C ***      TEST TO SEPARATE L AND LV REGIONS
C      FIRST COMPUTE T ON L-LV LINE, THEN EL
350 NL = 2
IF (F .GT. EC(M)) GO TO 800
RL = VC(M)/V
X1 = (1.-RL)/D(M)/2.
X = SQRT(X1*X1+CC(M))
T = 1.-((X-X1)**(1./3.)-(X+X1)**(1./3.))**3
C      GO TO 650 TO OBTAIN EL
NPART = 1
GO TO 650
C      BRANCH TO EITHER L OF LV REGIONS
375 NL = 3
IF (E-EL) .MOD. 855,855,800
C      *****
C      BUILT-IN SUBROUTINES
C      *****
C      *****
C ***      SOLVE FOR VS ON S-SL LINE, GIVEN ES-EZ
600 TF = (Y2+SQRT(Y2*Y2-Y3(M)))/Y1(M)
602 RGE = WHOS(M)*EQSTG(M)*EZ
DEN = EUSTC(M)*RGE
ENUM = EVO(M)*(TF-1.)-RGE
EMUJA = 0.
EMUJA = ENUM/DEN
NC1=0

```

EUSTP191  
EUSTP192  
EUSTP193  
EUSTP194  
EUSTP195  
EUSTP196  
EUSTP197  
EUSTP198  
EUSTP199  
EUSTP200  
EUSTP201  
EUSTP202  
EUSTP203  
EUSTP204  
EUSTP205  
EUSTP206  
EUSTP207  
EUSTP208  
EUSTP209  
EUSTP210  
EUSTP211  
EUSTP212  
EUSTP213  
EUSTP214  
EUSTP215  
EUSTP216  
EUSTP217  
EUSTP218  
EUSTP219  
EUSTP220  
EUSTP221  
EUSTP222  
EUSTP223  
EUSTP224  
EUSTP225  
EUSTP226  
EUSTP227  
EUSTP228  
EUSTP229  
EUSTP230  
EUSTP231  
EUSTP232  
EUSTP233  
EUSTP234  
EUSTP235  
EUSTP236  
EUSTP237  
EUSTP238  
EUSTP239  
EUSTP240  
EUSTP241  
EUSTP242  
EUSTP243  
EUSTP244  
EUSTP245  
EUSTP246  
EUSTP247  
EUSTP248  
EUSTP249  
EUSTP250  
EUSTP251  
EUSTP252  
EUSTP253  
EUSTP254

# SUBROUTINE EQSTPF (Continued)

```

605  FMOJA = FMOJ / (FMOJ*EMUIH*(EUSTH(M)*EMUIH+EUSTS(M)))
      MCJ = MCJ / (1.0)
      IF (NCJ .GT. 20) GO TO 620
      FMOJ = (EMUIH*EMOJA - EMUIH*EMOJA) / (EMUIH*EMOJA + EMUIA*EMUIH)
      IF (FMOJ*EMOJA .LT. ACC) GO TO 610
      FMOJA = FMOJ
      FMOJA = FMOJ
      FMOIH = FMOJ
      GO TO 605
610  VS = 1. / (PMUS(M)*EMOJ)
      GO TO (200,250,405) NPART
620  PRINT 1,06,1F,2F,3F,EMOJA,EMUIH
      STOP 420

C
C ***      SOLVE FOR P,HL,EL,HV,EV, ON LV=V BOUNDARY
C
650  PV = EXP(A2(M)*(1.-1./T)*A)(M)*ALOG(T)
      X1 = T / C(M)
      A = ZK0(M) / ZK1(M) / T
      AP = ZK2(M) * (1.-1./T)
      PA = PV / X1
      MAX = M(M) - A / A
      IF (PA*MAX .LT. -1.25 .AND. NPART .LT. 5) GO TO 653
      MV = PX * (1.-MAX*MAX)
      IF (PA*MAX .LT. -0.05) MV = PV / (X1 / (1. + (-B(M)*H(M)*HV)*HV) - (A*AP*HVE
1) * HV)
      GO TO 654
653  MV = 1. - ZP(M) * (1.-T) ** ZN(M)
654  NL7 = 0
655  MV1 = MV
      NL7 = NL7 + 1
      IF (NL7 .GT. 20) GO TO 670
      X2 = 1. - (H(M) - HP(M)*HV) * HV
      PO = X1 * HV / A2 - (A*AP*HV) * HV ** 2
      POP = X1 / X2 + (X1 * HV * (M(M) - 2. * HP(M) * HV)) / A2 ** 2 - (2. * A + 3. * AP * HV) * HV
      MV = AMAX1(MV, (PV - PO) / (P - 1.0))
      IF (ABS(FV - MV)) .GT. ACC * HV .AND. ABS(RV - MV)) .GT. 1.E-12) GO TO 655
      FV = FO(M) + EPS2(M) * 1 - EPS1(M) * ((ZK0(M) + 2. * ZK1(M) / T) - ZK2(M) * HV / T) * HV
      IF (NPART .GT. 1) HL = 1. + C1(M) * (1.-T) ** (1./3.) * D1(M) * (1.-T)
      EL = FV - EPS1(M) * HV * (1./HV - 1./HL) * (A2(M) / T + A1(M) - 1.)
      GO TO (375,0) 5,075,017,100,105) NPART
670  PRINT 1,0,MV,MV1,FV,PO,POP,EV,HL,EL,T,M
      STOP 470

C
C *****
C      CALCULATIONS FOR EACH PHASE
C *****
C *****
C
C ***      SOLID PHASE
700  FMO = 1. / (PMUS(M) / V - 1.
      HGE = HICS(M) * EUSTG(M) * E
      P = FMO * (FUSTC(M) * FMO * (EUSTL(M) * EMU * EUSTS(M)) * HGE) * HGE
      GO TO 1000

C
C ***      SOLID - LIQUID MIXED PHASE
750  FMAX = (F - ESU(M)) / (ELU(M) - ESU(M))
      IF (V .GT. FMAX * V(0(M)) + (1.-FMAX) * VSO(M)) GO TO 990
      FIND T FOR V, E IN SL REGION
755  EPS = E - (F * EV(M) * V
      ES = EPS + (F * EV(M) * VS
      Y2 = ES - FMS(M)
      TF = (Y2 + SUM(T(Y2 * Y2 - Y3(M))) / Y1(M)
      NCS = 0

```



# SUBROUTINE EQSTPF (Continued)

```

760  TFO = TF
    NCS=NCS+1
    IF (NCS.GT. 20) GO TO 781
    EIA = VC(M)/VC
    EMU = EIA-1.
    ESP = (CB1(M)-HDC1(M))/TF**2
    ETAP = -ESC*ETA**2/EFS(M)
    PGE = HHOS(M)*EUSTG(M)*FS
    M = FOVO(M)*(TF-1.)-EMU*(FOSTC(M)+EMU*(EUSTL(M)+EMU*FOSTS(M))+MGE
1  )-MGE
    MP = FOVO(M)-(FOSTC(M)+EMU*(2.*EUSTL(M)+EMU*3.*FOSTS(M))+MGE)*ETAP
1  -EUSTG(M)*HHOS(M)*EIA*FSK
    TF = TF-M/MP
    ES = EHS(M)+CH1(M)*TF+HDC1(M)/TF
    VS = (FS-FMS)/DERIV(M)
    IF (ABS(TF-TFO)/TF.GT. ACC) GO TO 760
    P = FOVO(M)*(TF-1.)
    GO TO 1000
780  PRINT 11(7,TF,TFO,T,M
    STOP 780
C
C ***      I IWDU PHASE
C      SOLVE FOR PLM, VLM, ON SL-L LINE
800  Y2 = F-CHI(M)
    TF = (Y2+SQRT(Y2**2-Y3(M)))/Y1(M)
    EZ = FS = EHS(M)+CH1(M)*TF+HDC1(M)/TF
    GO TO 600 TO GET VS ON S-SL LINE
C
    NPANT = 3
    GO TO 602
805  VLM = VS*(1-ES)/DERIV(M)
810  PLM = EOVO(M)*(TF-1.)
C      SOLVE FOR PLM, VLM ON L-LV LINE
    IF (NL.FO. 3) GO TO 815
    IF (F.OF. 2C(M)) GO TO 820
    IF (NL.EO. 1) GO TO 812
    NL = VC(M)/V
    X1 = (1.-NL)/N(M)/C.
    A = SQRT(X1)*X1+CC(M)
    T = 1.-((X-A)**(1./3.)-(X+A)**(1./3.))**3
C      GO TO 650 TO OBTAIN EL
    NPANT = 2
    GO TO 650
812  T = TM(M)
    EL = ELU(M)
C
C      BEGIN ITERATION LOOP TO FIND VLM ON L-LV BOUNDARY, GIVEN F
C
C
815  TL=TL & ETI=EL & TIU=1.0 & ETU=EC(M)
    TLAST = 0.5*(TIU+TL)
C      USE PARABOLIC ESTIMATE OF SLOPES TO OBTAIN T FOR E
    S2=S23=(TIU-TL)/(ETU-ETL)
    IF (ETL.NE. ELO(M))
1  S2 = (TL-TM(M))/(FTL-ELO(M))+S23-(TIU-TM(M))/(FTU-ELO(M))
    T = TI+(S2*(S23-S2)*(E-FTL)/(ETU-ETL))*(E-FTL)
    TLAST = 0.5*(TIU+T)
    NCB=N & NPANT=N
816  NCB=NCH+1
    IF (T.GI. TU) T=0.1*TLAST+0.9*TI
    IF (T.LI. TL) T=0.1*TLAST+0.9*TL
    IF (NCH.GT. 20) GO TO 827
C
C      GO TO 650 TO COMPUTE HL,EL,RV,EV FOR GIVEN F
C
C
    GO TO 650

```

# SUBROUTINE EQSTPF (Continued)

817	IF (ABS(E-EL) .LE. ACC*AMAX(ABS(E),ELO(M))) GO TO 819	EQSTP381
	S12 = (1-TL)/(EL-ETL)	EQSTP382
	S23 = (TU-T)/(ETU-EL)	EQSTP383
	S2 = S12+S23-(TU-TL)/(ETU-ETL)	EQSTP384
	TLAST = T	EQSTP385
	IF (EL .LT. E) GO TO 818	EQSTP386
	T = T*(S2+(S12-S2)*(E-EL)/(ETL-EL))*(E-EL)	EQSTP387
	ETU=EL & TU=TLAST & GO TO 816	EQSTP388
818	T = T*(S2+(S23-S2)*(E-EL)/(ETU-EL))*(E-EL)	EQSTP389
	ETL=EL & TL=TLAST & GO TO 816	EQSTP390
819	VLB=VC(M)/RL	EQSTP391
	PLB=PC(M)*PV	EQSTP392
	GO TO 825	EQSTP393
C	SOLVE FOR PLB ABOVE CRITICAL POINT ON V = VC LINE	EQSTP394
820	VLB = VC(M)	EQSTP395
	RV = 1.	EQSTP396
	X1 = E-ELO(M)*EPS1(M)*ZK1(M)*RV	EQSTP397
	X2 = EPS1(M)*(ZK2(M)*RV-2.*ZK1(M))*RV	EQSTP398
	T = (X1+SQRT(X1*X1-4.*EPS2(M)*X2))/(2.*EPS2(M))	EQSTP399
	PG = RV*T/(ZC(M)*(1.-(B(M)-BP(M)*RV)*RV))-(ZK1(M)+ZK2(M)/T)*ZK2(M)*RV	EQSTP400
	PLB = PL(M)*PG	EQSTP401
825	RM = 1./VLM	EQSTP402
	RB = 1./VLB	EQSTP403
	Z1 = (PLM-PLB)/(RM-RB)	EQSTP404
	Z2 = (RB*PLM-PLB)/(RM-RB)	EQSTP405
	P1 = Z1/V-Z2	EQSTP406
	Z3 = ALOG(PLM/PLB)/ALOG(RM/RB)	EQSTP407
	Z4 = (ALOG(RB)*ALOG(PLM)-ALOG(RM)*ALOG(PLB))/ALOG(RM/RB)	EQSTP408
	ALP2 = Z3*ALOG(1./V)-Z4	EQSTP409
	F = (PLM/(RM-1./VLO(M))-Z3*PLM/RM)/(Z1-Z3*PLM/RM)	EQSTP410
	F = AMIN1(1.,AMAX1(0.,F))	EQSTP411
	P = EXP(F*ALOG(P1)*(1.-F)*ALP2)	EQSTP412
	GO TO 1000	EQSTP413
827	PRINT 1110,I,TMIN,TMAX,TU,TL,E,ET,ETL,ETU	EQSTP414
	STOP 827	EQSTP415
C		EQSTP416
C ***	LIQUID-VAPOR MIXED PHASE	EQSTP417
850	RL = 1.+C1(M)*(1.-T)*(1./3.)*D1(M)*(1.-T)	EQSTP418
	EL = EV-EPS1(M)*PV*(1./RV-1./RL)*(A2(M)/T+A1(M)-1.)	EQSTP419
C	CONSTRUCT UPPER AND LOWER BOUNDS ON E, T	EQSTP420
C	BEGIN ITERATION LOOP FOR E WITH T AS A PARAMETER	EQSTP421
	ETU = EV	EQSTP422
	GO TO 860	EQSTP423
C	ENTER FROM 375 FOR V LESS THAN VC	EQSTP424
855	ETU = EL	EQSTP425
860	ETL = (V-VLO(M))/(VVO(M)-VLO(M))*(EVO(M)-ELU(M))*ELO(M)	EQSTP426
	FMAX=(E-ELO(M))/(EVO(M)-ELO(M))	EQSTP427
	IF (V .GT. FMAX*VVO(M)+(1.-FMAX)*VLO(M)) GO TO 990	EQSTP428
	TU = T & TL = TM(M)	EQSTP429
	TLAST=0.5*(TU+TL)	EQSTP430
C	LINEAR INTERPOLATION TO ESTIMATE T	EQSTP431
	NC6=0	EQSTP432
	NPART=3	EQSTP433
	T = TL+(E-ETL)*(TU-TL)/(ETU-ETL)	EQSTP434
870	NC6=NC6+1	EQSTP435
	IF (NC6 .GT. 20) GO TO 892	EQSTP436
	IF (T .GT. TU) T=0.1*TLAST+0.8999*TU	EQSTP437
	IF (T .LT. TL) T=0.1*TLAST+0.8999*TL	EQSTP438
C	GO TO 650 TO COMPUTE RL, EL, RV, EV FOR GIVEN T	EQSTP439
	GO TO 650	EQSTP440
		EQSTP441

# SUBROUTINE EQSTPF (Concluded)

875	ET = (HL*V-1.)/(RL/HV-1.)*(EV-EL)*EL	EQSTP442
	IF (ABS(E-FI) .LE. ACC*AMAX1(ABS(E),ELU(M))) GO TO 890	EQSTP443
	TLAST=T	EQSTP444
	IF (ABS(ET-FIL) .GT. 1.) S12=(T-TL)/(ET-ETL)	EQSTP445
	IF (ABS(ETU-ET) .GT. 1.) S23=(TU-T)/(ETU-ET)	EQSTP446
	S2=S12*S23*(TU-TL)/(ETU-ETL)	EQSTP447
	IF (ET .LT. E) GO TO 880	EQSTP448
	T=T*(S2*(S12-S2)*(E-ET)/(ETL-ET))*(E-ET)	EQSTP449
	ETU=ET & TU=TLAST & GO TO 870	EQSTP450
880	T=T*(S2*(S23-S2)*(E-ET)/(ETU-ET))*(E-ET)	EQSTP451
	ETL=ET & TL=TLAST & GO TO 870	EQSTP452
890	P = PC(M)*(PV-PVO(M))	EQSTP453
	GO TO 1000	EQSTP454
892	PRINT 1100,T,TMIN,TMAX,TU,TL,E,ET,ETL,ETU	EQSTP455
	STOP 892	EQSTP456
C		EQSTP457
C ***	VAPOR PHASE	EQSTP458
900	HV = VC(M)/V	EQSTP459
	X1 = E-EO(M)*FPS1(M)*ZK0(M)*RV	EQSTP460
	X2 = FPS1(M)*(ZK2(M)*HV-2.*ZK1(M))*RV	EQSTP461
	T = (X1+SQRT(X1*X1-4.*EPS2(M)*X2))/(2.*EPS2(M))	EQSTP462
	P = PC(M)*(HV*V/(7C(M)*(1.-(B(M)-BP(M)*HV)*HV))-(ZK0(M)+ZK1(M)/T.	EQSTP463
	1 ZK2(M)*(T-1./T)*HV)*RV*RV-PVO(M))	EQSTP464
	GO TO 1000	EQSTP465
985	CONTINUE	EQSTP466
C		EQSTP467
C ***	CUTOFF AT ZERO PRESSURE	EQSTP468
990	P = 0.	EQSTP469
1000	RETURN	EQSTP470
1100	FORMAT(6A10)	EQSTP471
1101	FORMAT(A10,7E10,3)	EQSTP472
1102	FORMAT(1H,79X,5H IN=42,5H IN=12,* HEAD IN EQSTPF*)	EQSTP473
1103	FORMAT(1H,* LOC=42 IN EQSTPF*,5X,* EMUO,P,PP,EMU,M=*,5E10,3///)	EQSTP474
1104	FORMAT(1H,* LOC=42 IN EQSTPF*,5X,* RV1,PO,POP,RV,M=*,5E10,3///)	EQSTP475
1105	FORMAT(1H,* LOC=312 IN EQSTPF*,5X,* TA,PG,PVP,PGP,T,PV,M=*,3E10,	EQSTP476
	13/4E10,3///)	EQSTP477
1106	FORMAT(1H,* LOC=620 IN EQSTPF *,5X,* T,EZ,M,EMU1A,EMU1B=*,5E10,3/	EQSTP478
	1///)	EQSTP479
1107	FORMAT(1H,* LOC= 780 IN EQSTPF *,5X,* TF,TFU,T,M=*,4E10,3///)	EQSTP480
1108	FORMAT(1H,* LOC=892 IN EQSTPF*,5X,* T,TMIN,TMAX,TU,TL,E,ET,ETL,	EQSTP481
	1ETU *,5E10,3/4E10,3///)	EQSTP482
1109	FORMAT(1H,* LOC=670 IN EQSTPF*,5X,* HV,RV1,PV,PO,POP,EV,RL,EL,T,M	EQSTP483
	1=*,5E10,3/5E10,3///)	EQSTP484
1110	FORMAT(1H,* LOC=827 IN EQSTPF*,5X,* T,TMIN,TMAX,TU,TL,E,ET,ETL,	EQSTP485
	1ETU *,5E10,3/4E10,3///)	EQSTP486
	END	EQSTP487

## APPENDIX D

### EXTENDED TWO-PHASE EQUATION OF STATE:ESA

The subroutine incorporating the extended equation of state is listed in this appendix together with a description of the CALL statement and the nomenclature.

The subroutine, termed ESA, is called at two points in a wave propagation code. The first CALL is made from the initialization routine (GENRAT in SRI PUFF) while material properties are read in. All subsequent CALLS are made from the routine that controls stress calculations during wave propagation (HSTRESS in SRI PUFF). In preparation for the initializing CALL, the solid density ( $\rho_{so}$ ) and the Hugoniot parameters (C, D, S,  $\Gamma$ ) must be available in COMMON. Additional material data are read in directly by the subroutine ESA during the initializing CALL: they are unavailable to the rest of the program. All other input and output variables are inserted through the CALL statement. The initializing CALL is

CALL ESA (NCALL, IN, M)

where NCALL indicates the type of CALL: a zero value is for  
initializing, one is for computing pressure

IN is the file containing data

M is the material number

During this CALL the subroutine ESA reads two data cards and initializes its array variables. These cards each contain an identifier in the first 10 columns (in A10 format) and 6 constants in E10.3 format. A sample set for titanium follows:

```
ESA T1 1 -5.000E-01 0.      0.      0.      3.970E 00 1.490E 10
ESA T1 2  5.914E 09 9.560E-01 1.182E 11 0.      5.300E-10 1.026E 11
```

The first three constants are the parameters  $\Gamma_1$ ,  $F_1$ , and  $F_2$ , which appear in Eq. (93), the expression used for compressed states. The other three values are the pressures, densities, and energies associated with three points on the expansion equation-of-state surface:  $P_1, \rho_1, E_1$ ;  $P_2, \rho_2, E_2$ ;

and  $P_3$ ,  $\rho_3$ ,  $E_3$ . These nine values are used to construct the coefficients  $g_0$ ,  $g_1$ ,  $h_0$ ,  $h_1$ ,  $b_0$  ...  $b_3$ , which describe the expansion surface.

The second and all subsequent CALLs are made during the wave propagation calculations to obtain the pressure. The form of this CALL is

```
CALL ESA (NCALL, 5, M, C(J), D(J), E(J), P(J), DPDD(J), DPDE(J))
```

where D and E are the density and energy provided to the routine

P is the pressure computed in ESA

C is sound speed from ESA

DPDD =  $\partial P / \partial \rho$  from ESA

DPDE =  $\partial P / \partial E$  from ESA.

The subroutine ESA is constructed in two parts: one for initializing, the other for computing pressure. The pressure computations are further subdivided into portions for compressed and expanded states.

A nomenclature list is provided for the subroutine. Following this is a listing of the subroutine.

# NOMENCLATURE OF INPUT AND PRINCIPAL VARIABLES IN ESA

B, ( $b_0, b_1, b_2, b_3$ )	Coefficients of the density expansion
EQSTC, EQSTD, EQSTS	Coefficients in the Hugoniot expansion, dyne/cm <sup>2</sup>
EQSTG, ( $\Gamma$ )	Grüneisen ratio
E1, E2, E3, ( $E_1, E_2, E_3$ )	Internal energies at data points on the expansion E-P-V surface, erg/g
F1, F2, ( $F_1, F_2$ )	Coefficients of the nonlinear energy term for compressed states, g <sup>2</sup> /dyne/cm <sup>4</sup>
F3	$(2F_1 - F_2)/\rho_{so}$
F4	$(F_2 - F_1)/\rho_{so}^2$
G1, ( $\Gamma_1$ )	Second term in the expansion for Grüneisen ratio
G2	$\Gamma - \Gamma_1$
G3	$\Gamma_1/\rho_{so}$
P1, P2, P3, ( $P_1, P_2, P_3$ )	Pressures at data points on the expansion E-P-V surface, dyne/cm <sup>2</sup>
RHOS, ( $\rho_{so}$ )	Initial solid density
R1, R2, R3, ( $\rho_1, \rho_2, \rho_3$ )	Densities at data points on the expansion E-P-V surface, g/cm <sup>3</sup>

# SUBROUTINE ESA

```

C      SUBROUTINE ESA(NCALL,IN,M,C,D,F,P,UPDR,UPDE)
C
C      ROUTINE COMPUTES PRESSURE FROM SIMPLE TWO-PHASE EQUATION OF STATE.
C      ESA HAS TWO PARTS, CORRESPONDING TO READING AND COMPUTING
C
C      HEAD INPUT (NCALL=0). CALL IS FROM GENHAT.
C      INPUT = NCALL, IN, M, MATERIAL PROPERTY CARDS
C      OUTPUT = PRINTS CARD IMAGES, ORGANIZES DATA INTO ARRAYS
C
C      COMPUTE PRESSURE (NCALL=1) CALL IS FROM HSTRESS USUALLY.
C      INPUT = NCALL, M, C, D, F
C      OUTPUT = C, P, UPDE
C
C      NAMED COMMON
C      REAL MU, MUH
C      COMMON /EUS/  EQSTA(6),EQSTC(6),EQSTD(6),EQSTE(6),EQSTG(6),
1  EQSTH(6),EQSTN(6),EQSTS(6),EQSTV(6),CZU(6),CWU(6),CZ(6)
C      COMMON /MELT/ EMELT(6,5),SPH(6)
C      COMMON /RHU/  RHU(6),RHOS(6)
C      COMMON /TSH/  TSH(6,30),EAMAT(6,20),TENS(6,3)
C      COMMON /Y/   Y(6),YADD(6),MU(6),MUM,YADUM
C
C      DIMENSION M(4,6),F1(6),F2(6),F3(6),F4(6),G1(6),G2(6),G3(6)
C      DATA IDU/1M /
C
C      IF (NCALL.EQ. 1) GO TO 200
C      *****
C      READ INPUT DATA AND INITIALIZE ARRAYS
C      *****
C      READ (IN,1100) A1,G1(M),F1(M),F2(M),P1,H1,E1
C      WRITE (6,1100) A1,G1(M),F1(M),F2(M),P1,H1,E1
C      WRITE (6,1121) IDU,IN
C      READ (IN,1100) A1,P2,F2,E2,P3,H3,E3
C      WRITE (6,1100) A1,P2,H2,E2,P3,H3,E3
C      WRITE (6,1121) IDU,IN
C      INITIALIZE COEFFICIENTS IN EXPANSION EQUATION
C      RU=RHOS(M)
C      F3(M)=(2.*F1(M)-F2(M))/RU
C      F4(M)=(F2(M)-F1(M))/RU/RU
C      G2(M)=EQSTG(M)-G1(M)      $      G3(M)=G1(M)/RU
C      INITIALIZE -B- ARRAY
C      AU=EQSTC(M)/RU
C      A1=P1-H1*F1*(G2(M)+H1*G3(M))-H1*E1*F1*(F3(M)+H1*F4(M))
C      A2=P2-H2*F2*(G2(M)+H2*G3(M))-R2*E2*F2*(F3(M)+H2*F4(M))
C      A3=P3-H3*F3*(G2(M)+H3*G3(M))-R3*E3*F3*(F3(M)+H3*F4(M))
C      REDEFINE A TO INCLUDE DENOMINATORS
C      RU=RHOS(M)
C      D01=R0-H1      $      D02=R0-H2      $      D03=R0-H3      $      D12=H1-H2
C      D13=R1-H3      $      D23=H2-H3
C      A0=A0/(D01*D02*D03)      $      A1= A1/(D01*D01*D12*D13)
C      A2=-A2/(D02*D02*D12*D23)      $      A3= A3/(D03*D03*D13*D23)
C      B(1,M)=-A0*H1*H2*R3-H0*A1*R2*R3-R0*R1*A2*R3-H0*H1*R2*A3
C      B(2,M)=H0*H1*(A2+A3)+H0*R2*(A1+A3)+H0*R3*(A1+A2)
1  +R1*H2*(A0+A3)+R1*R3*(A0+A2)+R2*R3*(A0+A1)
C      B(3,M)=-R0*(A1+A2+A3)-R1*(A0+A2+A3)-R2*(A0+A1+A3)-R3*(A0+A1+A2)
C      B(4,M)=A0+A1+A2+A3
C      RETURN

```


# SUBROUTINE ESA (Concluded)

C *****	*****	ESA	52
C	CALCULATION OF PRESSURE AND SOUND SPEED	ESA	53
C *****	*****	ESA	54
200	IF (D .LT. RHOS(M)) GO TO 300	ESA	55
C		ESA	56
C	*** COMPRESSION EQUATION OF STATE	ESA	57
	U=(U-RHOS(M))/RHOS(M)	ESA	58
	PH=U*(EUSTC(M)+U*(EUSTD(M)+U*EQSTS(M)))	ESA	59
	GG1=EQSTG(M)+U*G1(M)	ESA	60
	GF=1.-0.5*U*GG1	ESA	61
	FF=F1(M)+U*F2(M)	ESA	62
	P = PH*GF + (GG1*D + FF*E)*E	ESA	63
	DPDH = ((EQSTC(M)+U*(2.*EUSTD(M)+U*3.*EQSTS(M)))*GF	ESA	64
1	-PH*(0.5*EQSTG(M)+U*G1(M)) + (G1(M)*D + F2(M)*E)*E)/RHOS(M)	ESA	65
2	+GG1*E	ESA	66
	DPDE = GG1*U + 2.*FF*E	ESA	67
	GO TO 350	ESA	68
C		ESA	69
C	*** EXPANSION EQUATION OF STATE	ESA	70
300	GG3=D*(G2(M)+D*G3(M))	ESA	71
	FF =D*(F3(M)+D*F4(M))	ESA	72
	BTERMS=b(1,M)+D*(R(2,M)+U*(B(3,M)+D*H(4,M)))	ESA	73
	P = (D-RHOS(M))*BTERMS + (GG3 + FF*E)*E	ESA	74
	DPDH = (G2(M)+2.*D*G3(M) + (F3(M)+ 2.*D*F4(M))*E)*E	ESA	75
1	+BTERMS + (D-RHOS(M))*(H(2,M)+U*(2.*B(3,M)+U*3.*H(4,M)))	ESA	76
	DPDE = GG3 + 2.*FF*E	ESA	77
350	CSQ = U*DPH + P*DPDE/D**2	ESA	78
	IF (CSQ .GT. 0.) C=SQRT(CSQ)	ESA	79
	RETURN	ESA	80
1100	FORMAT (A10,7F10.3)	ESA	81
1121	FORMAT (1H,79X,5H IND=A2,5H IN=I2,* -ESA-*)	ESA	82
	END ESA	ESA	83



## REFERENCES

1. L. Seaman and R. K. Linde, "Distended Material Model Development, Vol. I: Experiments and Theory for the Model," AFWL-TR-68-143, Stanford Research Institute, Menlo Park, California, May 1969.
2. A. Holt, A. Kusubov, M. Carroll, and B. Hord, "Stress-Wave Propagation in Distended Asbestos Phenolic," UCRL-51120, Lawrence Livermore Laboratory, Livermore, California, September 3, 1971.
3. M. M. Carroll, and A. C. Holt, "Static and Dynamic Pore-Collapse Relations for Ductile Porous Materials," J. Appl. Phys., Vol. 43, No. 4 pp. 1626-1636, April 1972.
4. M. M. Carroll and A. C. Holt, "Steady Waves in Ductile Porous Solids," Journal Applied Physics, Vol. 44, No. 10, p. 4388, October 1973.
5. W. Herrmann, "Constitutive Equation for the Dynamic Compaction of Ductile Porous Materials," Journal Applied Physics, Vol. 40, No. 6, p. 2490, May 1969.
6. R. J. Lawrence and D. S. Mason, "WONDY IV--A Computer Program for One-Dimensional Wave Propagation with Rezoning," Sandia Laboratories Report SC-RR-810284, Albuquerque, New Mexico, August 1971.
7. B. M. Butcher, "Numerical Techniques for One-Dimensional Rate-Dependent Porous Material Compaction Calculations," SC-RR-710112, Sandia Laboratories, Albuquerque, New Mexico, April 1971.
8. L. Seaman, T. W. Barbee, and D.R. Curran, "Dynamic Fracture Criteria of Homogeneous Materials," AFWL-TR-71-156, Stanford Research Institute, Menlo Park, California, December 1971.
9. R. N. Brodie and J. E. Hormuth, "The PUFF 66 and P PUFF 66 Computer Programs," Research and Technology Division, Air Force Weapons Laboratory, Kirtland Air Force Base, New Mexico, May 1966.
10. L. K. Goodwin, L. A. Johnson, and R. S. Wright, "An Equation of State of Metals," DASA-2286, Aeronutronic Division of Philco-Ford Corporation, Newport Beach, California, April 1969.
11. H. E. Read and R. A. Cecil, "A Rate-Dependent Constitutive Model for Shock-Loaded S-200 Beryllium," DNA 2845F, Systems, Science and Software, La Jolla, California, February 1972.
12. L. Seaman and J. T. Rosenberg, "Characterization of Homogeneous Materials in Compression and Tension," for Air Force Weapons Laboratory, Final Report AFWL-TR-73-15, Stanford Research Institute, January 1973.

13. C. Zener, "Elasticity and Anelasticity of Metals," University of Chicago Press, Chicago, Illinois, 1948.
14. R. G. McQueen, S. P. Marsh, J. W. Taylor, J. N. Fritz, and W. J. Carter, "The Equation of State of Solids from Shock Wave Studies," in High Velocity Impact Phenomena, edited by Ray Kinslow, Academic Press, New York, 1970, pp. 294-417.
15. E. B. Royce, "GRAY, a Three-Phase Equation of State for Metals," UCRL-51121, Lawrence Livermore Laboratory, September 3, 1971.
16. S. L. Thompson, "Improvements in the CHART D Radiation-Hydrodynamic Code I: Analytic Equations of State," SC-RR-70-28, Sandia Laboratory, Albuquerque, New Mexico, January 1970.
17. Robert J. Naumann, "Equation of State for Porous Metals Under Strong Shock Compression," Journal Applied Physics Vol. 42, No. 12, pp. 4945, 1971.
18. Ya. B. Zel'dovich and Yu. P. Raizer, Physics of Shock Waves and High Temperature Hydrodynamic Phenomena, Vol. II, Academic Press, New York and London, 1967, p. 786.
19. H. Read, private communication.
20. 
21. M. Carroll and A. C. Holt, "Suggested Modification of the P- $\alpha$  Model for Porous Materials," J. Appl. Phys., Vol. 42, p. 759, February 1972.
22. J. K. MacKenzie, "The Elastic Constants of a Solid Containing Spherical Holes," Proceedings of the Physical Society, Section B, Vol. 63, p. 2, 1950.
23. N. Warren, "Theoretical Calculations of the Compressibility of Porous Media," Journal of Geophysical Research, Vol. 78, No. 2, p. 352, January 10, 1973.
24. W. Herrmann, "Constitutive Equations for Compaction of Porous Materials," Symposium on Applied Mechanics Aspects of Nuclear Effects in Materials, ASME Winter Annual Meeting, November 28-December 3, 1971, Washington, D.C.
25. C.A. Berg, "The Motion of Cracks in Plane Viscous Deformation," Proceedings Fourth U.S. National Congress Applied Mechanics, Vol. 2, p. 885, 1962.
26. H. Poritsky, "The Collapse or Growth of a Spherical Bubble or Cavity in a Viscous Fluid," Proceedings of the First U.S. National Congress of Applied Mechanics, ASME, New York, 1952, p. 813.

27. M. Carroll, private communication.
28. A. Mazzella, J. Shea, and T. Stefansky, "Dynamic Response of Porous Materials to Electron Beam Deposition," PIFR-216, Physics International Company, San Leandro, California, February 1972.
29. R. L. Coble and W. D. Kingery, "Effect of Porosity on Physical Properties of Sintered Alumina," Journal of the American Ceramic Society, Vol. 39, No. 11 p. 377, November 1956.
30. F. R. Tuler and B. M. Butcher, "A Criterion for the Time Dependence of Dynamic Fracture," International Journal of Fracture Mechanics, Vol. 4, p. 431, 1968.
31. Lynn Seaman, "SRI PUFF 3 Computer Code for Stress Wave Propagation," Technical Report No. AFWL-TR-70-51, Air Force Weapons Laboratory, Kirtland Air Force Base, New Mexico, September 1970.
32. L. Seaman, R. F. Williams, J. T. Rosenberg, D. C. Erlich, R. K. Linde, "Classification of Materials by Shock Properties," Technical Report No. AFWL-TR-69-96, Air Force Weapons Laboratory, Kirtland Air Force Base, New Mexico, November 1969.
32. D. A. Shockey, L. Seaman, and D. R. Curran, "Dynamic Fracture of Beryllium Under Plate Impact and Correlation with Electron Beam and Underground Test Results," Final Report (Advance Copy) AFWL-TR-73-12, Air Force Weapons Laboratory, Kirtland Air Force Base, New Mexico, January 1973.
34. D. C. Drucker and W. Prager, "Soil Mechanics and Plasticity Analysis or Limit Design," Quarterly of Applied Mathematics, Vol. 10, p. 157, 1952.